Effect of self healing and continuous hydration on the mechanical properties of cyclically loaded early age concrete

A case study of early age cyclic loading on a concrete bridge deck

Manank Vipulkumar Shah

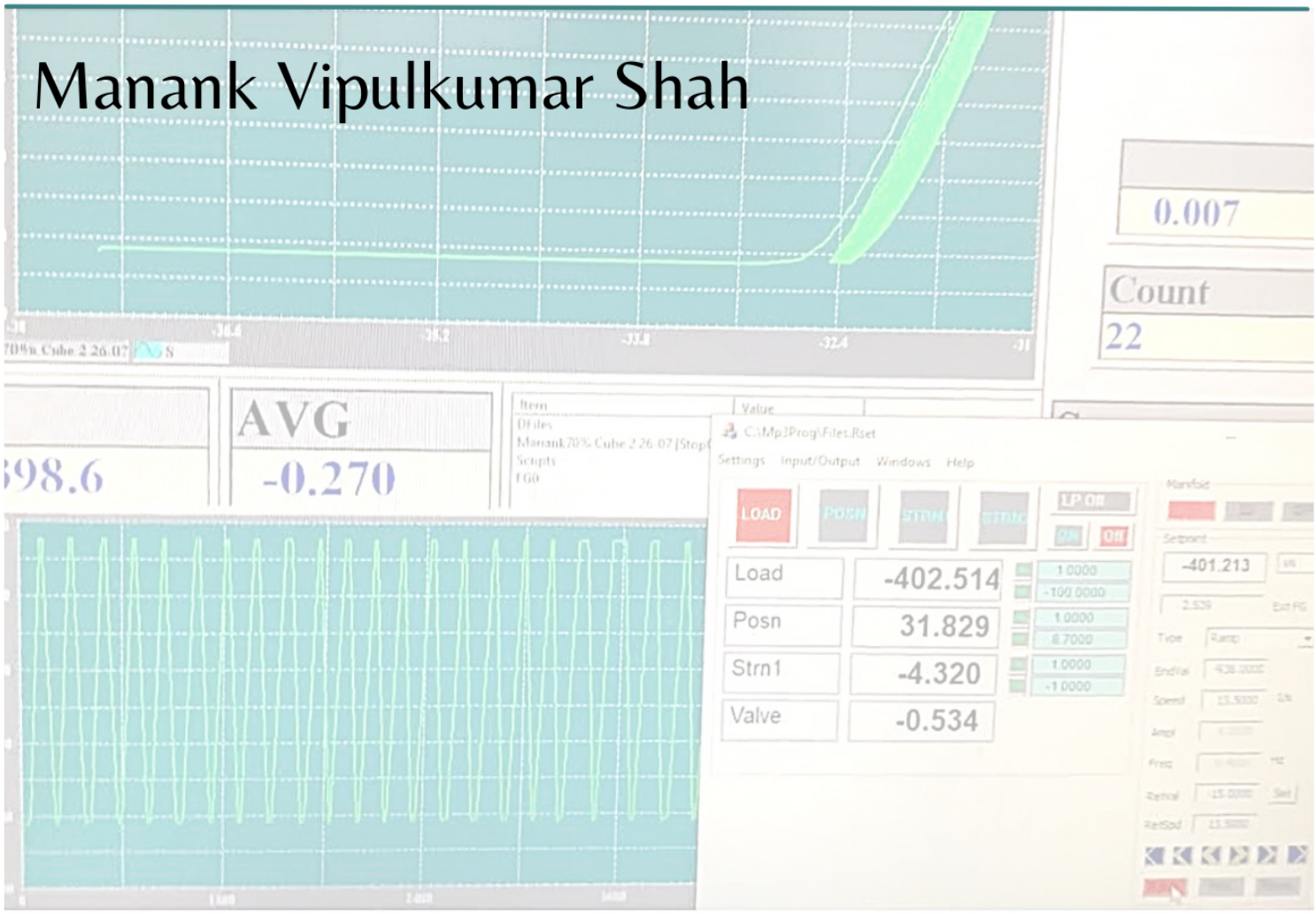

TU Delft

NOBLEO
bouw & infra

Effect of self healing and continuous hydration on the mechanical properties of cyclically loaded early age concrete

A case study of early age cyclic loading on concrete bridge deck

Masters Graduation Thesis

for the partial fulfilment of the
Master of Science in Civil Engineering and Geo-Sciences
at Delft University of Technology

by

Manank Vipulkumar Shah

An electronic version of this thesis is available at http://repository.tudelft.nl/.

This page was intentionally left blank.

Thesis Committee

Committee Chair:
Dr. Guang Ye
Department of Materials, Mechanics, Management & Design (3Md)

Daily Supervisor:
Dr. Hua Dong
Department of Materials, Mechanics, Management & Design (3Md)

Committee member:
Dr. Yuguang Yang
Department of Concrete Structures
Yuguang.Yang@tudelft.nl

Committee member:
Mr. Matthijs Somhorst
Operational Director - Nobleo Bouw & Infra

Masters Student:
Manank Vipulkumar Shah (5036283)
Track: Structural Engineering
Specialization: Concrete Structures
MSc Civil Engineering and Geo-Sciences

Preface

This Master thesis is performed at Delft University of Technology during the academic year of 2020-21. The basis for this thesis stemmed from the idea of effect of cyclic loading on early age concrete. It has been a great opportunity and experience to be able to work on this research. I would like to acknowledge and appreciate the financial support by Nobleo Bouw & Infra for this research work. I sincerely thank my daily supervisor Dr.Hua Dong for his continuous support throughout , my chair Dr. Guang Ye and my committee members Dr. Yuguang Yang, Mr. Matthijs Somhorst, MSc., for their patient advice and consistent guidance during the course of this thesis. I would also like to acknowledge the help of respected Lab technicians for their effort for conducting experiments at TU Delft. I could not have achieved my current level of success without a strong support group. First of all, my parents, who supported me with love and inspired me to dream bigger every single day. Lastly, my friends who helped me and kept me motivated throughout. Thank you all for your unwavering support.

Delft, December 2021

Summary

This research work in the form of this master thesis was inspired by a real engineering problem posted by Nobleo Bouw & Infra. During a restrengthening project of a culvert bridge, the new construction was needed to be opened for normal traffic just after 7 days of casting of a new bridge deck. In order to follow the timeline, the asphalting machinery was imposed after 3 days age of curing. Asphalting machinery was the source of cyclic loading on early age concrete. It was ensured that between the 3^{rd} day and the 7^{th} day after the cyclic loading, no other loading was applied on the bridge deck. Due to the fact that the first loading was applied on the 3^{rd} day, the fatigue strength of the concrete was compromised. 49.63% of higher fatigue strength could be achieved if the loading was applied on the 7^{th} day instead, provided that the cyclic loading applied on the 3^{rd} day would not cause any micro cracking, reducing the compressive strength of the concrete. It was also to be determined if the further strength development in concrete would be affected because of the application of cyclic loading.

A customised mix design which provided a compressive strength of 30 MPa on the 3^{rd} day was used in the practice. Firstly, it was important to find out what exact compressive stress would have been imposed on the 3^{rd} day age of concrete. Hence in association with the structural engineer, a conservative choice was made with a load level of 56% of the compressive strength of concrete at t= 3 days. It was determined that 30 load cycles would have been applied through the asphalting machinery. Loading frequency and loading time was also computed. Hence experiments were designed in order to determine whether this kind of cyclic loading could affect the mechanical properties or further strength development of concrete.

Coda Wave Interferometry (CWI) technique was used to detect the occurrence of micro cracking inside concrete. CWI utilizes the later part of a signal (coda) to retrieve information regarding the medium. The Co-relationship Coefficient (CC factor) was calculated for each loading cycle to comment on the starting of damage occurrence in concrete. Also wave speed analysis was performed and compared with the CC factor analysis. Cyclic loading was performed on 3 concrete cubes and after the application of loading, compressive strength was computed in order to assess the damage caused in concrete due to the cyclic loading. Axial Strain analysis was performed for all the concrete cubes.The final phase of the experimentation was to comment on the further strength development of concrete, where concrete cubes were cyclically loaded and strength is checked due to further hydration by comparison of strength development for unloaded concrete.

It was determined through the experiments that 56% loading, on 3^{rd} day age, for 30 load cycles was not enough cause any micro cracking inside concrete. There was no indication from CWI and wave speed analysis regarding the micro cracking inside concrete. Also, no reduction in the compressive strength was observed as compared to the unloaded samples. The next step was to increase the cyclic load level till the micro cracking and reduction in the mechanical strength of concrete is observed. During the course of these experiments, the loading age of concrete was fixed to 7 days and the loading frequency was increased to 13.5 KN/s. During these experiments, the number of load cycles applied to concrete cubes has been limited to 30 load cycles.

The cyclic loading level of 56%, 60%, 65%, 70% and 75% of the compressive strength was applied for 30 load cycles for the investigation in this thesis. Till 65% cyclic loading, no reduction in the mechanical properties is observed. 4.1% and 6.8% of reduction in the compressive strength of concrete was recorded when the loading level was increased to 70% and 75% of the compressive strength respectively. There was a clear indication from CC factors recording and wave analysis as the value of CC factor recorded

was less than 0.65. Also 6% reduction in the wave speed was recorded in case of 70% loading. It was at last concluded that CC factor is more sensitive to the moment of cracking and wave speed reduction is a good indicator of the progressive failure in concrete due to cyclic loading.

As the mechanism of autogenous self healing mechanism is possible in early age concrete, self healing potential of surface micro cracks is investigated under the fog curing conditions. Various self healing products were observed through the portable microscope and it was recorded that self healing is possible for the micro cracks less than 0.1 mm. It was also concluded that, even though, self healing potential is observed in concrete, strength recovery due to the self healing is not possible. The study is concluded by giving the final conclusions, recommendations and resemblance of this research work with the engineering practice.

Contents

List of Figures

List of Tables

1

Background and Motivation

Concrete as a construction material is the second highest used substance in the world after water. Concrete is prone to cracking under the influence of the loading occurring due to the static, dynamic and cyclic loading. At a certain number of load cycles in terms of vehicular loading, reduction of Young's modulus and Dynamic Elastic modulus along with the degradation of the mechanical properties like Compressive strength of the concrete is observed [35]. Moreover the effect of loading on the early age concrete and the development of micro cracks affects the Serviceability Limit State theory for the crack width control. If the crack width criterion is exceeded, the cracks provide the easy access to harmful agents like Sulphates, Carbonates and Chloride. Introduction of these agents in concrete can induce the corrosion of steel in concrete which can significantly affect the service life of the structures.[42]

A common place solution to the aforementioned problem is the man -made repair of the structures [4]. But in the past decade, lot of research is directed towards the self healing of the cracks in concrete. Due to the occurrence of cracking, the transport the material from any place to the crack becomes possible and thus through the process of reaction and precipitation, it is possible to heal the cracks. [4]. Moreover Haoliang and Guang detected the self healing potential of micro cracks in the cement paste due to continuous hydration at an early age. [15].

Through the self healing of micro cracks in concrete, it is possible to substantially reduce the cost of maintenance and repair which in turn enhances the service life of the structure [4]

1.1. Introduction

The route of a national highway was constructed in North-West of Holland consisting of many regions from Heerhugowaard till Enkhuizen. The project at hand was renovating and strengthening of a small bridge originally constructed in the year 1932. Due to the concerns on the structural safety and in order to achieve sufficient strength, the top deck of the bridge was replaced with ready mix concrete construction.

Due to the time constraints, the bridge consisting the new deck was opened to traffic just after 7 days of the construction.[rep] Heavy cyclic loading in terms of road constructing machinery was applied on newly constructed deck on just 3rd day after the construction[rep]. If the fatigue strength is calculated based on 3rd day load (time of application of first loading) than 49% reduction in fatigue strength was observed if the fatigue strength would have been calculated based on 7th day loading.

In NEN-EN-1992-1-1, formula (6.76) is , which defines the design value of the fatigue strength of the concrete.

$$f_{cd,fat} = k_1 \beta_{cc}(t_0) f_{cd}(1 - f_{ck}/250) \tag{1.1}$$

f_{cd} in the formula 1.1 represents design compressive strength of concrete. f_{ck} in the formula 1.1 represents the characteristic compressive strength of concrete. Value of k_1 is suggested to be 0.85. The β_{cc} in the formula 1.1 has been computed according to the first cyclic loading applied to finished concrete

at the age of 3 days. It is important to assess if the loading applied on the 3rd day to the concrete that can causes any any changes in the structural medium, in terms of micro-cracks, that could affect the mechanical strength properties of concrete.

Due to the micro cracking caused due to the cyclic loading the durability of the structure is affected in terms of chloride ingress. Due to the presence if un-hydrated cement particles in early age concrete, it is possible that the concrete heals itself and closure of the micro cracks occurs which causes the improvement in the service life of the structure.

Some researchers [31][34][32] replace part of the cement by fly ash or blast furnace slag which are respectively pozzolanic and latent hydraulic materials. As high amounts of these binders remain un-hydrated even at the later age, autogenous healing due to ongoing hydration is promoted. [materials]. Also it has been concluded that healing of the crack can then take place very easily in Blast Furnace Slag Concrete because the early age strength is low and a lot of hydration of the cement has to take place over time providing a potential to self heal the cracks. [34]. The maximum crack width that can be healed by autogenous healing varied and differed substantially among research made by various authors, i.e., 5 to 10 μm [17], 100 μm [29], 200 μm [9], 205 μm [1] and 300 μm [6].
Hilloulin et al. studied the mechanical strength recovery in mortar specimens made with limestone portland cement cracked at different ages due to autogeneous self healing process. Their results showed that specimens cracked at the age of 24 h achieved higher strength recovery in comparison to that of similar specimens cracked at the age of 72 h or later. According to Hilloulin et al.66, the lack of remaining un-hydrated products in specimens cracked at the age of 72 h or later was the main reason for reducing strength recovery in these specimens.

There are several Ultrasonic Pulse measuring techniques which are used for the purpose of Structural health monitiring and to assess damage in concrete structures. Among them, CWI (coda-wave interferometry) is a method which was initially designed for geoscience evaluations and has been recently been used to evaluate concrete structures. Multiple wave scattering through a media is used by CWI to assess small changes in the medium by altering the wave velocity [38].

1.2. Scope

The major objective of this research work is to investigate what cyclic loading level could cause damage in concrete. Effect of early age cyclic loading on the mechanical properties of the concrete is also to be investigated in the research work. A custom mix design concrete which provided compressive strength of 30 MPa at the age of 3rd day was used. Cyclic load level of 56% of compressive strength has been applied for 30 load cycles. The next objective is to assess the extent of damage caused due to cyclic loading in terms of crack width analysis for different cyclic loading levels. It is also to be investigated if the self healing phenomenon is possible for the micro cracks that are formed due to the cyclic loading. Investigation is to be carried out to determine the self healing potential under the fog curing conditions. Lastly, to comment on the long term performance of the cyclically loaded concrete, strength development of concrete after cyclic loading has to be analysed.

CODA Wave Interferometry technique is used to detect changes in structural medium in terms of micro cracking caused due to application of cyclic loading. It is to be investigated if the CWI can detect a moment of cyclic loading which causes microcracks inside concrete. Ultrasonic Pulse Velocity (UPV) measurement was also adopted and compared with the CC factor analysis for the different loading levels.

1.3. Research Hypothesis and Background

It is established by researchers that early age flexural loading on immature concrete have resulted in cracking, excessive immediate and long term deflections and failures in concrete structures [Gardner, 1985; Hindo and Bergstrom, 1985;Parsons and Naik, 1985; Fu et aL, 1986]
C.G. Carayanis etal. concluded that the early age cyclic loading significantly influences the behaviour and the overall capacity of the joints after the concrete curing period [19].

The background of this research work can be studied from the literature review. However from the literature, the damage caused due to the early age cyclic loading in terms of the micro cracking is apparent. It was hypothesized that in early age concrete, the autogenous self healing is possible under the fog curing conditions and hence the self healing potential is to be investigated under fog curing conditions.

1.4. Research Questions and Objectives

The objective of this project is to investigate if the cyclic load level incurred due to asphalting machinery can cause the occurrence of micro cracks in concrete. Then the next task is to investigate what cyclic load level can affect the mechanical properties of the concrete. Hence a series of experiments has been conducted to determine the stress level of cyclic loading which can cause reduction in mechanical properties of concrete. The research question to be answered in this thesis are formulated and stated below:

1. "Is the imposed cyclic load with prescribed load cycles can cause the micro cracks on the surface of the early age concrete cubes?"

2. "Is there any decrement in the mechanical property such as the compressive strength of early age concrete due to the application of early age cyclic loading ?"

3. "Is the autogeneous self healing phenomenon possible under fog curing conditions to the micro cracks formed during early age loading on concrete?"

4. "Is the strength development in concrete affected due to the further hydration after early age cyclic loading?"

1.5. Thesis Outline

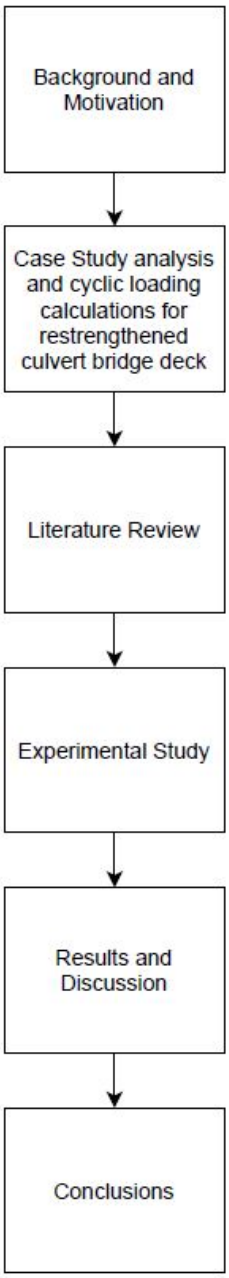

Figure 1.1: Outline of thesis research

2

Case Study analysis and cyclic loading calculations for restrengthened culvert bridge deck

2.1. Repair and Strengthening of bridge deck

This section of the literature review focuses on the information on restrengthening of the bridge deck. Information of quality assessment which led to the renovation of the bridge has been discussed. Secondly in association with the road contractor, information of the asphalting vehicles and load cases which ultimately contributed to the early age cyclic loading has been discussed.

2.1.1. Introduction

The original culvert bridge consists of two parts. The oldest part was built in 1932 and comprises of a U-shaped reinforced concrete box with a hinged reinforced concrete slab. The part from 1932 is a widening and deepening of an older floodgate in brick masonry construction. This lock has been partly removed (red highlighted slab in fig 2.1). In 1969 the culvert bridge was widened with a reinforced concrete tube. In the figure 2.1 shows a schematic cross-section of the box culvert bridge. In the year 2018, the renovation of the top deck of the culvert bridge was done.

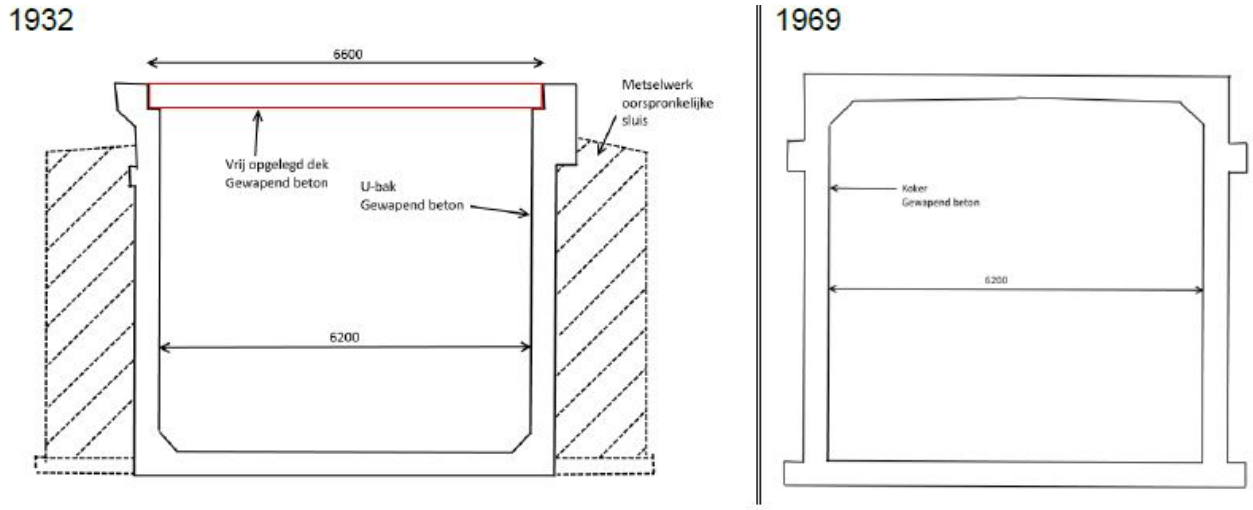

Figure 2.1: Cross-section diagram for culvert bridge (Credit: Nobleo Bouw & Infra)

The part from 1932 is founded on wooden piles and the part from 1969 was constructed on concrete piles. In both the constructions, the main reinforcement in the deck was designed parallel to the direction of travel. The transverse reinforcement was designed at an angle of 54 degrees to it (Parallel to watercourse and walls).

The route of the culvert bridge covers a total road length of approximately 40 kilometers and runs through the municipalities of northern part of the Netherlands. The route currently consists of the provincial roads which are important connecting roads to major highways, one being part of the A7 national road. The route operates at the regional level and is an important opening function which can connect two major cities Alkmaar to Zwolle in the near future.

Traffic on this route has increased significantly over the past decade, as a result reduced road safety, congested roads, delays and nuisance from cut-through traffic. The safety, quality of life and accessibility in the vicinity of the culvert bridge was perceived as insufficient by the parties involved. It is expected that this will deteriorate further without measures. This has three reasons: growing activity in the region, increasing importance of east-west traffic and increasing population. To improve this unattractive situation, the existing route needs to be upgraded.

Objectives for the restrengthening and repair of the bridge deck are:
1. increasing road safety;
2. improving the quality of life;
3. improving accessibility;
4. facilitate the growth of the number of inhabitants, the regional economy and employment

The upgrading of the culvert bridge aims to improve road safety and quality of life improve by terminating traffic and allowing it to flow better. The current road network has insufficient capacity due to the growth of traffic and the growth of housing numbers in the region to handle traffic in a safe way. By ensuring a good through connection the (cut-through) traffic in the cores will decrease, which contributes to the quality of life and safety. As a result of better traffic flow, the effects will be of traffic on air quality. Upgrading the culvert bridge will improve accessibility to the North Holland regions and would simulate economic development in the region.

The culvert bridge consists of two (not structurally connected) parts. The oldest part was built in 1932 and concerns a U-shaped reinforced concrete box with a hinged supported reinforced concrete slab. The part from 1932 is a widening and deepening of an older floodgate brickwork. In 1969 the culvert bridge was widened with a reinforced concrete tube.

2.1.2. Quality assessment for the existing construction (1932)

The investigation which was performed in order to assess the quality of the construction was twofold. On the one hand, a verification calculation was performed. The purpose of the verification calculation was to determine whether the culvert bridge, in the future situation, for a period of 40 years, with the legally required safety level can be maintained.

On the other hand, the culvert bridge was inspected more closely. This was because the visual inspection carried out by quality assessment company, a (large) number of damage scenarios were identified. The purpose of the inspection is to determine whether a renovation can extend the residual lifespan by at least 50 years and what measures should be taken for this.

From the verification calculations based on the design of construction used in 1932, it was clear that the concrete is not of sufficient strength for future and hence it failed the verification calculations of Concrete under compression or shear and Concrete without shear reinforcement. Also from the results of visual inspection and core testing of concrete, it was clear that the concrete quality failed in carbonation and chloride impact testing. Hence the decision was made based on 2 fold research that it was essential to repair and restrengthen the culvert bridge.

As the culvert bridge was located at a crucial location on the national highway, as per the government regulations, the culvert bridge should be ready to use for the traffic after 7 days of construction. It means that traffic can be redirected and diversion of the traffic is only allowed for 7 days. Time was critical factor in the process of construction as the new concrete casting was cast-insitu. Hence a custom made concrete was used to provide high strength at early age of construction. On the 3^{rd} day after the casting of concrete, asphalting vehicles were placed on concrete surface which provided the source of cyclic loading on the concrete surface.

Because of the early age cyclic loading, the final fatigue strength as was calculated from formula 1.1 of the concrete has been compromised. The $\beta_{cc}(t)$ factor which was calculated from the formula 3.3, used in the computation of the fatigue strength is a constant and it depends on the time when the concrete is first loaded. Hence if the first load is applied on concrete on 3^{rd} day after casting, the fatigue strength needs to be calculated based on the $\beta_{cc}(t)$ factor computed for that particular age. If the concrete is not loaded after 3^{rd} day till 7^{th} day (when the bridge is opened for general traffic), it is not known if there is any reduction in strength due to cyclic loading. Also further strength development after cyclic loading is interesting factor to analyse. If there is no further change in loaded and unloaded concrete than it is possible that $\beta_{cc}(t)$ used in fatigue strength formula is conservative and needs further investigation.

2.1.3. Geometry and Schematizing

Dimensions of existing construction (deck 1932)(Credit: Nobleo Bouw & Infra)

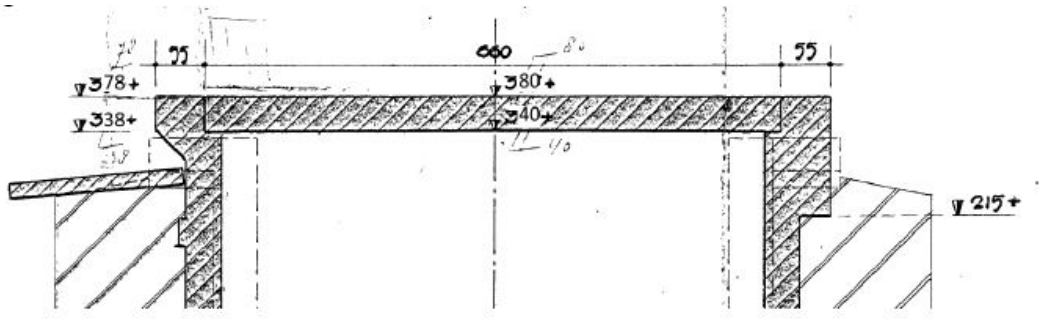

Figure 2.2: Cross-section of an existing construction part 1932(Credit: Nobleo Bouw & Infra)

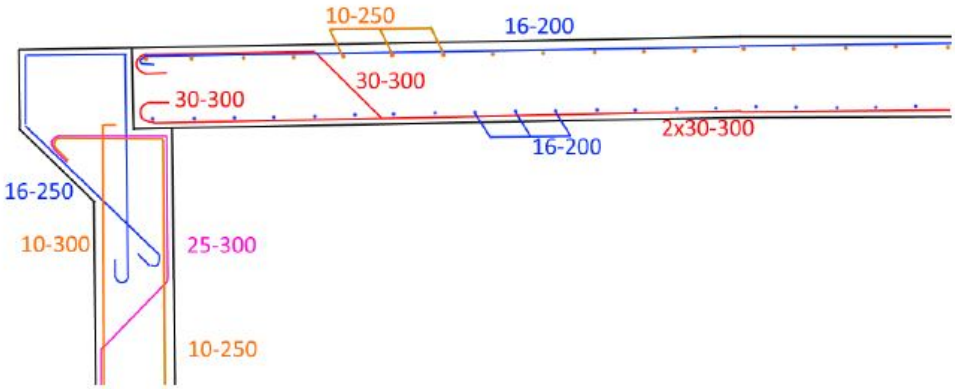

Figure 2.3: Reinforcement details from existing bridge deck of 1932

It was reported that the span perpendicular center to center dimension from support to support is 6.2 meters. The cross section view of the construction from 1932 is visualised in the figure 2.2. The reinforcement details involving the edge beam is visualised in the figure 2.3. The crossing angle was approximately 54 degrees and thickness of the existing deck is 0.4 meters. The crossing angle can be visualised from the figure 2.6.

Detailing for the re-strengthened bridge deck (2018)

The designing of the newly constructed bridge deck was made on SCIA Engineers design software. The spacing available in the northeast corner of the deck, at the time of designing, was minimal. 250 mm of space was made available for the reinforcement by an adjustment in the lateral cant. Because of the available thickness in the already built up structure, the thickness of the bridge deck needs to be varied. From a deck thickness of 250 mm, the deck thickness increases to 450 mm. An edge beam was installed on northern side of the deck. The edge beam has a thickness of 500 mm and a width of 470 mm. As the edge beam was used on the edge of the deck, A guide rail was mounted on the edge beam. It was computed from the SCIA Engineers engineers report that maximum bending moment was generated on the edge beam. This bending moment constitutes a major part of the total bending moment that is used to compute net compressive stress that would incur on early age concrete.

A separate model was drawn up for the schematization of the deck on the existing construction as can be seen from figure 2.4 . In the project, an isotropic plate was used with a stiffener at the edge in the form of a thicker plate as can be seen from figure 2.4 . The slope of the plate was incorporated in the model.The plan view of the new restrengthened culvert bridge can be seen from the figure 2.5. The thickness of the plate increases from 250 mm to 450 mm. The edge beam is 480mm high. This can be clearly visualised from the figure 2.6. No eccentricities were modeled. As a result, the stiffness

of the edge beam in particular is somewhat underestimated. The average element size used is 200 mm. Mindlin Reisner elements were used in the study.

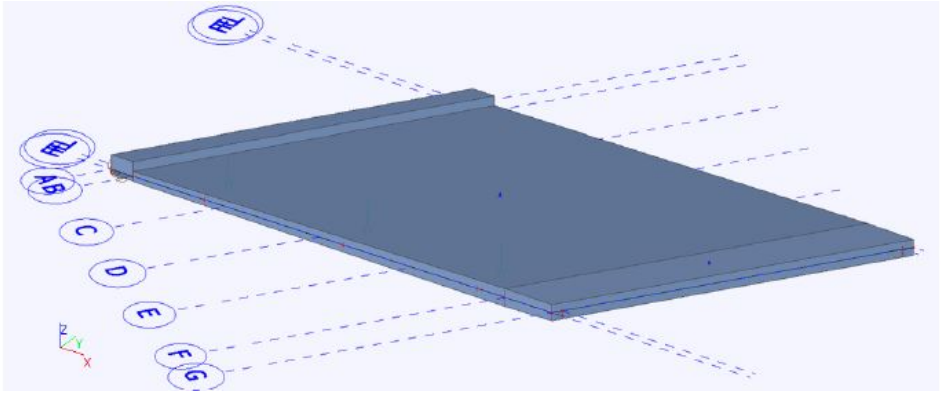

Figure 2.4: Isometric view of the re-strengthened reinforcing calculation model

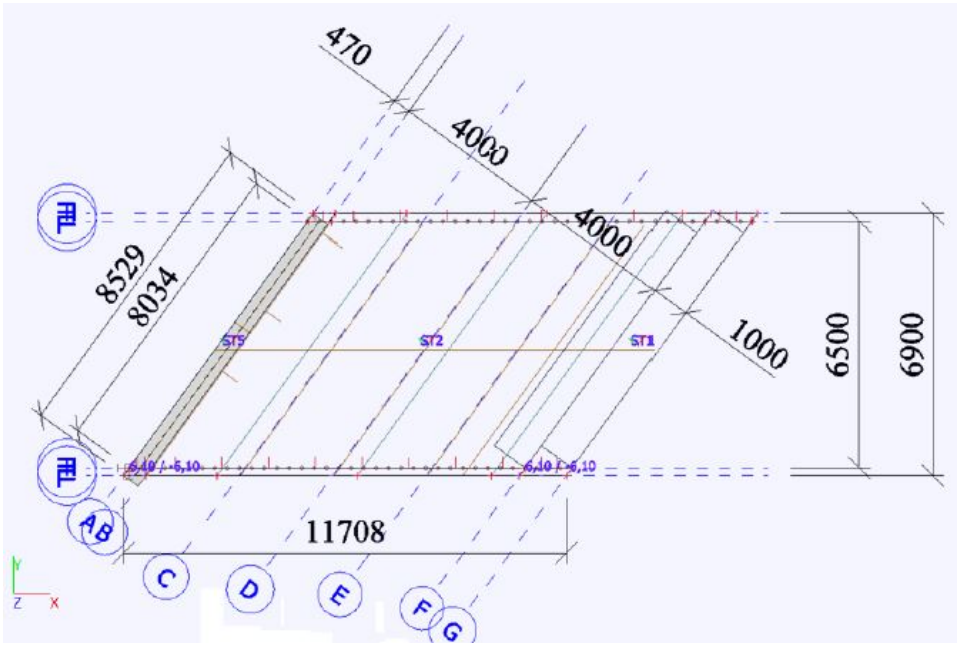

Figure 2.5: Plan view of the re-strengthened reinforcing calculation model

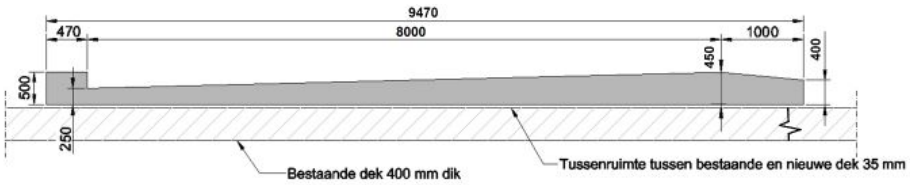

Figure 2.6: Section view of the re-strengthened reinforcing bridge deck with varying thickness(Credit: Nobleo Bouw & Infra)

2.2. Asphalting and loading cases for the bridge deck.

This section focuses on the discussion of the asphalt machinery that was used in the engineering practice in order to decide what exact compressive stress would have acted to the finished concrete on 3^{rd} day after the casting. In order to be on the conservative side, all the possible load combinations were taken into account which shall be discussed in this part. To compute the number of load cycles that would be required in order to compact the asphalt, 'Wals Index' of the loading vehicles was computed to determine which loading vehicle would have worst impact on the concrete surface.

Detailing for asphalting on the bridge deck

The information on the asphalt layers used for the restrengthening of the bridge was derived from the company report. Also the information on used asphalting machinery was reported. But the information on how many load cycles would the asphalt machinery incur on concrete surface was not mentioned. Hence through the discussion with the road designer, those data is computed. Also it was specifically mentioned in the project report that no 2 asphalting machinery is present together on the fresh concrete for the rolling process. The total height of asphalt used during the renovation project was 145-155 mm.

Three different layers of asphalt material was used which is mentioned below.

- 45 mm ZOAB 11 NB
- 70-80 mm AC 22 TL-C PMB
- 30 mm Microflex

The above mentioned asphalt layers are mentioned in order of how they are applied in the original engineering condition, the top layer being ZOAB and bottom layer being Microflex layer. The application of ZOAB is necessary to counteract the risk of detachment from the asphalt on the concrete deck. The basic principle is that the asphalt surfacing is applied after the deck has undergone only limited surfacing. If paved at a later stage, the excess moisture will be able to escape sufficiently, so that no problems are expected with the adhesion of the asphalt to the concrete, and the 45 mm ZOAB can be dispensed with.

Description of asphalting and cyclic loading

As discussed in the section for detailing of asphalt, approximately 150 mm asphalt layering has been applied in three layers. Due to the time constraints during the construction activity, the bridge deck needs to be open for traffic at the age of 7^{th} day after the concreting of the deck. To achieve this objective, on the 3^{rd} day after the concreting, asphalting process needs to be executed. Hence, on the 3^{rd} day after the casting of concrete on the bridge deck, asphalting vehicles were present on the bridge deck. This vehicles are the source of early age cyclic loading on the concrete bridge deck. Vehicles used for the project are discussed in detail in the section below. Number of loading cycles and the loading time has been defined on the advise of contractor and is based on the thickness the asphalt layer which has been discussed in detail in the upcoming section.

The estimation and selection of the loading and frequency of load for the laboratory experiments are orchestrated based on the 'Wals Index' value for each vehicle. The asphalt vehicle with highest Wals Index was selected based on the fact that higher the Wals Index, higher the damage on the concrete deck. In order to apply the cyclic loading on the 3^{rd} day after concreting, minimum concrete quality of C30/37 needs to be achieved before the application of vehicular cyclic loading on the bridge deck. The overall concrete strength quality used for the project is C55/67 at the age of 28 days. The strength development curve for the concrete strength provides the inputs and basis for the mix design used for the laboratory work.
In association with the road designer information on how the asphalting process causes stress to grains which in turn is transferred to concrete surface was discussed. The process of asphalting is a dynamic process in terms of the cyclic loading as well as the frequency of the loading which can be deduced from the thickness and type of materials used for asphalting.

During the first phase of rolling, the process of re-arrangement of the grains in the asphalt mixture

takes place. The weight of the roller ensures compression of the the grain skeleton, reducing the volume of the asphalt and its density increases. The hot bitumen ensures that the grains pass through each other well can slide easily on the surface.
In the second phase of the rolling, the density increases further. By cooling, the asphalt entraps the air present in the asphalt, the bitumen also shrinks sometimes and as a result, the mortar becomes stiffer, causing the asphalt to settle and it behaves somewhat resiliently.
In the third phase (final phase) of the rolling, the asphalt has cooled down to such an extent that further compression of the grain skeleton (with heavy roller) is possible again.

Well-compacted asphalt is more resistant to weather influences and traffic loads so it has higher service life as compared to the loosely compacted asphalt. Because rolling is the last operation in the whole process of road construction, the quality of the road is greatly affected by the way of rolling final product. High demands are therefore placed on this rolling itself; craftsmanship of the rolling machine operator is therefore indispensable.

2.2.1. Asphalt machines and 'Wals Index'

The figures below demonstrates the type of vehicles in use which results in the early age cyclic loading on the bridge deck. Static Drierolwals, as the name indicates, has 3 rollers with two on the backside and one on the front side of the vehicle. Tandemwals contains 2 rollers, one on the front and one on the back of the vehicle. The number of cycles along with the time taken for for each vehicle were approximated through the advise of the road contractor depending on the thickness of each asphalt layer. This information is concised in the table **??**.

Asphalt machinery detailing

A higher weight has a greater compaction effect. The size of the roll is ultimately decisive for the pressure transferred to the asphalt surface. Figure 2.9 depicts the asphalting machinery used for the compaction of approximately 150 mm of three asphalt layers discussed under the section of Detailing for asphalting. Figure 2.9 (a) is the Static Drierol machinery which was used in the restrengthening project for the compaction of approximately 75 mm thick layer of AC 22 TL-C PMB. Figure 2.9 (b) is the Tandemwals machinery which has been operational for the compaction of 30mm Microflex asphalt layer and 45mm ZOAB 11 layer.

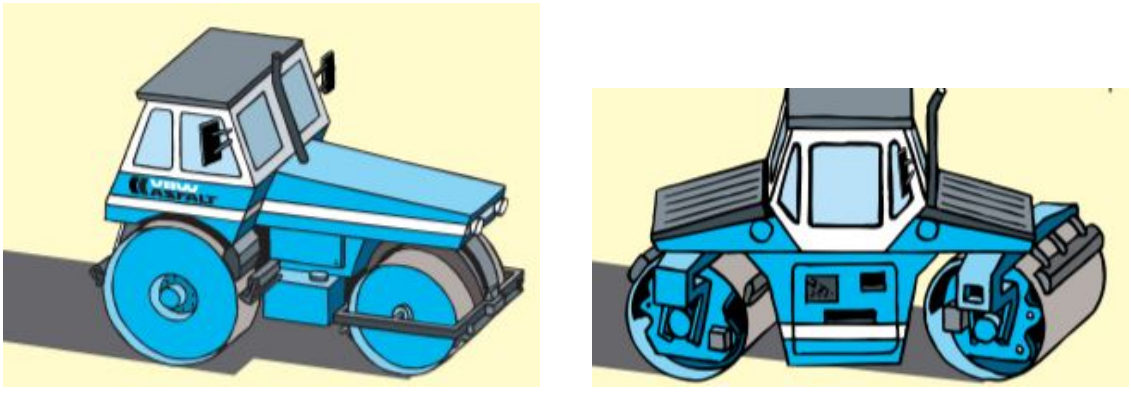

(a) **(b)**

Figure 2.7: Asphalting vehicles for cyclic loading. (a) Static Drierolwals (8-15 tonnes) . (b) Tandemwals (1-18 tonnes).

Table 2.1: Detailing on cyclic loading, frequency and time.

Detailing on cyclic loading, frequency and time.			
Asphalt Layers	**Machinery used**	**Number of load cycles**	**Time of loading**
30 mm Microflex	Tandem wals	10 X	2 hours
70-80 mm of AC 22 TLC PMB	Static Drierolwals	30 X	5 hours
45mm ZOAB 11	Tandemwals	5 X	1 hour

Table 2.1 depicts the detailing about the frequency, time and machinery used for individual asphalt layers. This vehicular loading on the asphalt surface is the source of cyclic loading on the young concrete surface. To imitate the cyclic loading conditions by the asphalting machinery in the laboratory, it is imperative to deduce which of this asphalting machinery would have the worst impact on the concrete in terms of the cyclic loading. 'X' in the table 2.1 represents the number of times the cyclic loading needs to be applied to the concrete. More information about dimensions of rolls of the asphalting machinery is demonstrated in the table 2.2.

Table 2.2: Detailing and dimensions of the asphalt machinery .

Detailing and dimensions of the asphalt machinery .				
Type of machinery	Roll	Diameter (D) (mts)	Length (L)(mts)	Load (P)(KN)
Static drieroll	Front roll Rear roll	1.25 1.55	1.1 1.1	40 60
Tandemwals	Front and rear roll	1.31	1.75	51.5

Wal's Index calculation

Wal's index is an impact indicator of a machine on the any surface. It is a tool to differentiate which asphalting machinery would give the most impact/loading to the early age concrete surface. The estimation and selection of the loading and frequency of load for the laboratory experiments are orchestrated based on the 'Wals Index' value for each vehicle. The asphalt vehicle with highest Wals Index was selected based on the fact that higher the Wals Index, higher the damage to the concrete deck. Wal's index can be calculated as can be seen from figure 2.8.

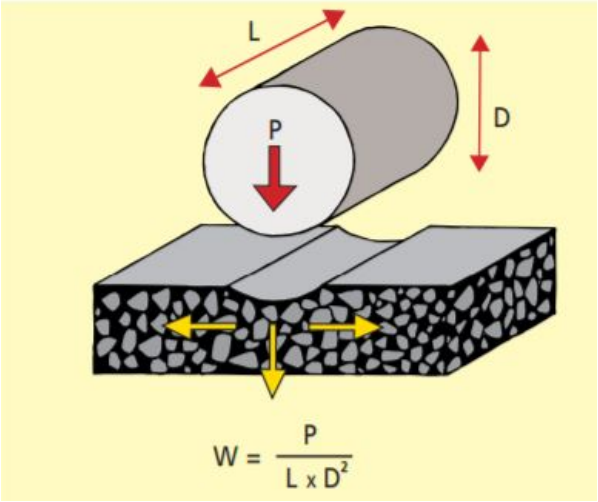

Figure 2.8: Wals Index

For the calculation of Wal's index **'W'**, **'P'** indicates load of the roller in KN, **'L'** indicates width of the roller in meters and **'D'** indicates the diameter of the roller in meters.

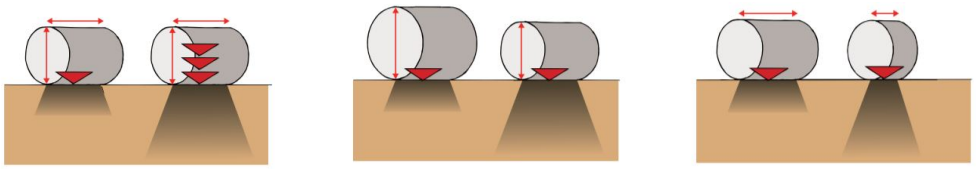

(a) Same roll diameters **(b)** Varying roll diameters **(c)** Narrower roll

Figure 2.9: Effect of roll size on the contact pressure

With the same roller diameter, the roll width has the important role in deciding the contact pressure. It is important to note that with the higher weight of the roll, the greater is the compacting capacity. The size of the roll which ultimately determines the pressure transferred to the asphalt surface. At the same roll diameter and roll width has the roll with the highest weight a bigger compacting power. This phenomenon can be visualised in the figure 2.9a .
A smaller roll diameter (at same roller weight and roll width) means a greater contact pressure and thus a greater compaction capacity. This phenomenon can be visualised in the figure 2.9b.
A narrower roll (at the same roll weight and roll diameter) means a bigger one contact pressure and therefore a greater compacting power.This phenomenon can be visualised in the 2.9c.

Wals index of Static drieroll and Tandem wals

Based on the information available in table for Detailing and dimensions of asphalt machinery, Wal's index for the asphalting machinery is computed. 'P', 'L', 'D' are the parameters as discussed in the figure 2.8.

$$\text{Wal's index for Static Drieroll} = W = \frac{P}{L \times D^2} = \frac{40}{1.1 \times 1.25^2} = \mathbf{23.2.}$$

$$\text{Wal's index for Tandemwals} = W = \frac{P}{L \times D^2} = \frac{51.5}{1.75 \times 1.31^2} = \mathbf{17.14.}$$

Due to the fact that Static Drieroll has higher Wal's Index value compared to the Tandemwals, selection of the loading and frequency of the cyclic load for the laboratory experiments are orchestrated based on the 'Wals Index'. The Static Drieroll has highest WalsIndex among the asphalt machinery used and hence it is selected based on the fact that higher the Wals Index, higher the damage to the concrete deck. It was mentioned in the project report that asphalting process for each asphalting layer is mutually exclusive, meaning that no 2 asphalting vehicles would work together for the asphalting process.

Hence to be on the conservative side, selection of the asphalt vehicle which provides worst impact loading on concrete has been selected. Hence cyclic loading with **30X** cycles for the span of **5 hours** is applied on early age concrete of age 3 days to assess the damage in terms of micro-cracks development inside the concrete. 'X' being the number of load cycles that needs to be applied to the concrete cubes.

2.2.2. Loads and Loading combinations considered for the bridge

In this part of the report, the load cases that have been considered. Information on all the load cases that contributed to the total compressive stresses acting on the early age concrete has been mentioned in detail. Some of the exact values are available for each loading case but some values were not available in the report. But all the load cases which are considered is reported in this section. At the end of this section, the net compressive stress that acts on early age concrete is computed.

Self weight of concrete

The dead weight was automatically determined by means of the geometry entered in SCIA engineer. The mass of the concrete material is 2500 kN/m^3. The entered gravitational acceleration is 10 m/s^2. Hence the self weight of the concrete is calculated as: 2500*10 = 25000 N/m^3 = 25 kN/m^3.

Live load

The live load on the deck consists of asphalt and the guide rail for the bridge.

- Guide rail: 1 kN/m on the raised deck edge
- Asphalt: 150 mm at 23 kN/m^3 = 3.5 kN/m^2

Traffic Loading

The traffic load in accordance with Load Model 1 (NEN-EN 1991-2 article 4.3.2) was applied. Calculations were made with two lanes with a width of 3.0 meters and one lane with a width of 2.75 meters. The old construction (part from 1969) was continued, allowing a three-lane layout. Three load classifications were examined for the SCIA engineers calculations.

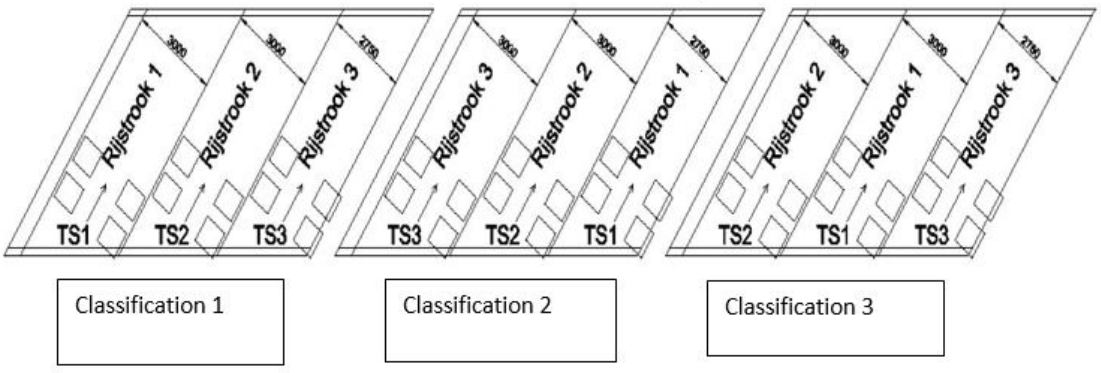

Figure 2.10: Applied traffic loading classification (report)

The following traffic loading have been introduced in accordance with Load Model 1 (NEN-EN 1991-2 article 4.3.2)

- Uniformly distributed load for lane 1: Q_{1k} = 9 kN/m^2

- Uniformly distributed load lane 2 : $Q_{2k} = 2.5$ kN/m^2
- Uniformly distributed load remaining area: $Q_{rk} = 2.5$ kN/m^2
- Axle load 1 (TS1): 2*Q_{1k} = 2*300 = 600 kN
- Axle load 2 (TS2): 2*Q_{2k} = 2*200 = 400 kN
- Axle load 3 (TS3): 2*Q_{3k} = 2*100 = 200 kN

In accordance with NEN-EN 1991-2 art. 2.2 (4) the traffic load can be reduced on the basis of a residual life of 40 years. The reduction factor is:

$$\psi = \frac{\ln\left(n_{\text{obs}} \cdot t\right)^{0,45}}{\ln\left(n_{\text{obs}} \cdot T\right)} = \frac{\ln(2.000.000 \cdot 40)^{0,45}}{\ln(2.000.000 \cdot 100)} = 0,978$$

Conservatively, this reduction was not included in the calculations for the SCIA engineers.

Braking Load
The braking load on the deck was considered separately in connection with the rigidity of the imposed deck. The brake load can be calculated:

$$Q_{lk} = 0,1{}^*9{}^*3{}^*6,4/\cos\left(54^\circ\right) + 360 = 377\text{KN}$$

The inclination of the bridge deck is 54 degrees. In order to check whether the deck is stable, the situation is considered in which lane 1 (most heavily loaded lane) is located most northerly or most southerly corners.

Vertical compressive vehicular loading
The vertical tyre pressure acting on the concrete surface has been computed based on machinery applied on the asphalt surface as shown in the figure 2.11.

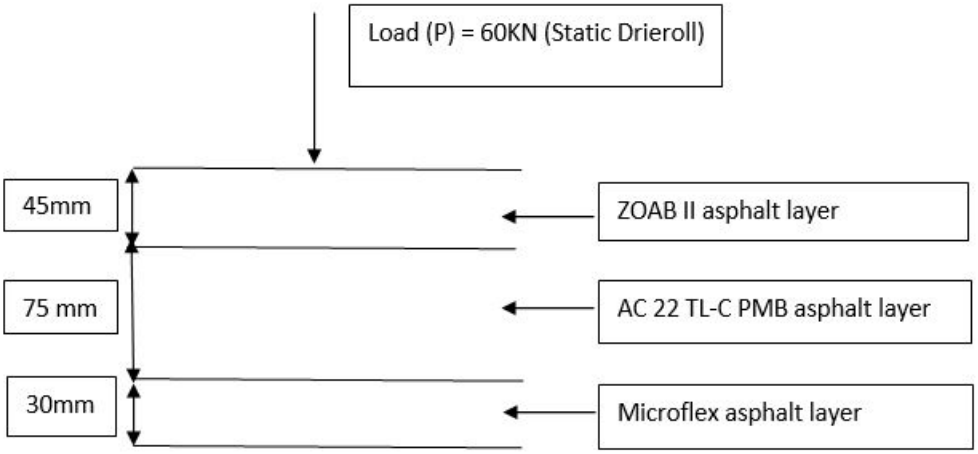

Figure 2.11: Asphalt layers and Vertical vehicular loading schematizing (figure not to scale)

Fatigue Loading
The new deck was tested for fatigue load. This is based on load model 1 (NEN-EN-1991-2 article 4.6.2) or load model 4b (NEN-EN-1991-2 article 4.6.5). The load during execution was considered negligible for fatigue. A dynamic factor is taken into account when determining the fatigue loading in SCIA Engineers software. The design of the fatigue loading has been made based on the number of load cycles of $N_{obs} = 0.5 * 10^6$.

The β_{cc} in the formula 1.1 has been computed according to the first cyclic loading applied to finished concrete at the age of 3 days. From 3^{rd} day till 7^{th} day, no other loading was applied on the bridge deck. If the fatigue strength has been calculated based on first loading applied on the 3^{rd} day, the net fatigue strength achieved is very low as compared to the first loading applied on the 7^{th} day age of concrete. Hence it is important to assess if the cyclic loading applied on the 3^{rd} day age of concrete affects mechanical strength of concrete and if the further strength development after the cyclic loading is affected.

Untreated Load Cases:
The following load cases have not been considered for the SCIA engineers calculations:
• **Soil load**:
No soil loading was applied to the slab for the SCIA engineers calculations.
• **Additional load due to settlement**:
The plate was placed (more or less weight neutral) on an existing construction. In addition, the plate was statically determinate, so settlements would not directly lead to forces in the construction.
• **Shrinkage and creep**:
The dimensions of the construction are limited. In addition, it is a statically determinate deck. Shrinkage and creep were not considered relevant for this phase.
• **Centrifugal load**:
The road axis was parallel to the axis of the structure. Hence there was no centrifugal load applied.
• **Pedestrian tax**:
Pedestrian tax was not assessed as normative hence it was neglected from the calculations.
• **Wind load**:
Wind load was neglected, given the limited dimensions of the construction.

Tyre pressure and calculation of maximum compressive stress
The Average contact pressure to be achieved by the asphalting vehicle on the concrete surface is about 70 psi which converts to **0.48 MPa**. This is the vertical compressive stress occurring on the first asphalt layer as can be seen from 2.11. As the first layer of concrete is beneath the 3 asphalt layers, the effective compressive stress due to tyre pressure would be lesser than the actual value. To be on the conservative side, the value of 0.48 MPa was chosen as the tyre contact pressure.

The tyre pressure is minimal as compared to the loading which is caused due to load cases as discussed in the section above. In order to take into account additional loads due to bending moments and loading due to the load cases as described above, load sheet can be referred from the figure 7.2. Addition of vertical tyre pressure along with the compressive stresses caused due to all the loading cases, gives a net compressive stress of **16.9 MPa**. Aforementioned, the concrete compressive strength at the age of 3^{rd} day is 30 MPa. Hence the achieved loading is about 56% load of the compressive strength of concrete.

Hence this is an important input for the laboratory work. One of the first task at the laboratory is to assess if 56 percent loading (Ref. 7.2) for 30 load cycles and time of loading being 5 hours (Ref. 2.1) can cause any micro cracking or reduction in mechanical properties of concrete.

3

Literature Review

The state of the art is sub-divided into 3 sections. The first section focuses on the effect on the mechanical properties of the concrete by the application of the cyclic loading. The second section illustrates the autogeneous self healing potential of cracks in concrete. Also strength recovery due to autogeneous self healing has been studied in the literature. The final section illustrates CODA Wave Interferometry technique and the co-relationship between the literature studied and research performed along with the probable practical applications of the research.

3.1. Effects of cyclic loading on the mechanical properties of early age concrete

Hence after the computation of net loading, it is important to study how does the cyclic loading affects the mechanical properties of the early age concrete. Hence in this section, damage mechanism of the concrete subject to cyclic loading at an early age has been discussed.

Due to the fact that structures are becoming more slender, the traffic volume is increasing, the axle loads are larger, and the traffic speed limits are higher; the interest of fatigue in concrete structures has increased during the last few years. Concrete fatigue is mainly a problem of offshore structures, railway sleepers and bridges because these types of structures are often exposed to repeated loading. With increased axle loads, the original condition for the bridges has changed and many existing bridges are nowadays required to carry larger loads than what they where originally designed for [24].

Fatigue is a phenomena in which a material loses its original strength due to cyclic stress and the development of consecutive damage. The load amplitude and number of load cycles, as well as the stress intensity, are all important factors in concrete fatigue. Even if the highest stress exerted is less than the material's usual strength bearing capacity, still concrete structure can fail due to the fatigue phenomenon.

In general, it has been observed that the fatigue damage propagation process involves the following stages: (1) crack nucleation, (2) short crack growth, (3) long crack growth, and (4) final fracture. Based on the assessment of load cycles applied in the case of uniaxial compression, in the first stage of damage, there is measurable drop in the axial stiffness during the first a few cycles (Region I), which is followed by a region of gradual, almost linear change (Region II). The linear rate of de-crease in Region II suggests that the damage accrues at a constant rate in the material in this stage.This is subsequently followed by a large and rapid decrease in stiffness prior to failure (Region III). Hence it is important to assess that for the different loading levels, for fixed number of load cycles, concrete reaches in which aforementioned damage regions. The damage regions can be visualised from the figure 3.1

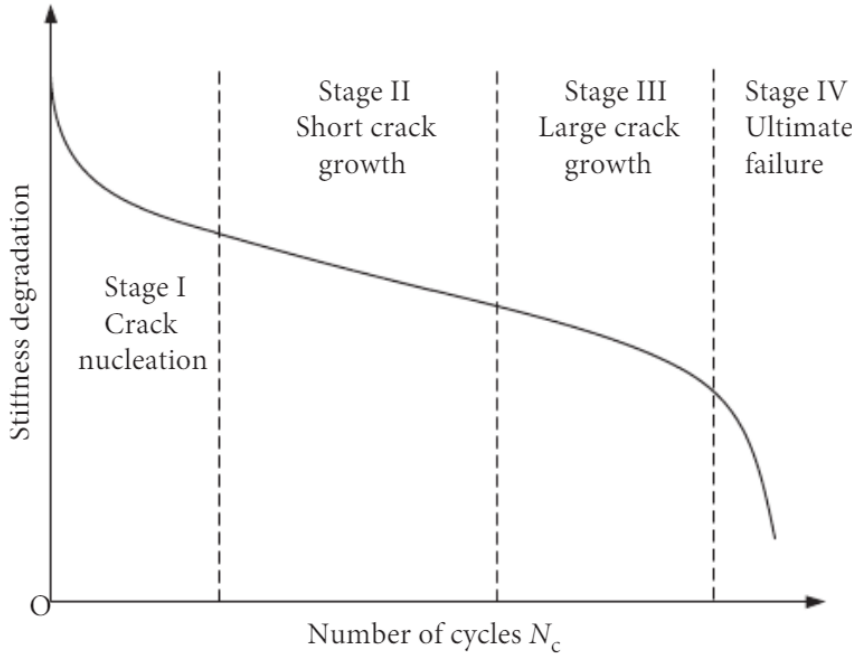

Figure 3.1: Fatigue damage phases (adapted from [12])

Fracture in a confined section of a structure exposed to cyclic loads can be used to characterize and diagnose fatigue failure in a structure. When a structure fails due to cyclic loads, it is considered to have reached the end of its fatigue life. Fatigue loading can take two different forms, each with its own set of failure characteristics. Low-cycle fatigue and High-cycle fatigue are two types of fatigue that is studied in the literature. The load is applied at high stress levels for a relatively small number of cycles in low-cycle fatigue analysis (typically less than 10^4) , whereas the load is applied at lower stress levels for a large number of cycles in high-cycle fatigue study. This research work is based on the Low-cycle cyclic loading analysis on concrete cubes.

In comparison to steel, fatigue in concrete is usually detected at a much later stage. Concrete is a non-homogeneous material, and several factors influence its fatigue resistance, including moisture content, cement/water ratio, and load effects such as load frequency and maximum load level. Air bubbles and micro-cracks emerge during the hardening process. Thermal strain, which is produced by temperature fluctuations, causes the micro-cracks to develop. The fatigue process begins when micro-cracks propagate, and it is a gradual process. The propagation of micro-cracks is quite slow at the start of the stress application. As loading continues the micro-cracks will proceed propagate and lead to macro-cracks, which may grow further. The macro-cracks determine the remaining fatigue life caused by stress until failure occurs.[24]

The influence of cyclic loading imposed at an early stage of the concrete curing period on the capacity of beam-column T-connections the age of 28 days was experimentally studied by C. G. Karayanis and C. E. Chalioris. From the experimental results of 20 specimens which were first tested at an early stage and then retested at the age of 28 days, the following concluding remarks have been drawn from the study: The early age cyclic loading significantly influences the behaviour and the overall capacity of the joints after the concrete curing period. The concrete age at which the early age loading takes place is an important parameter for the final capacity of the elements. Specimens subjected to a very early age loading (12 or 24 hours after casting) in the second test, at the age of 28 days, exhibited peak load values, loading stiffness and energy absorption capability higher than the ones of the specimens subjected to the first loading at the age of 2 or 7 days. This may be attributed to the formation process of the damage which in the case of very early age loading continues for a time period after the loading , the partial recovery of the caused damage is observed. [19]

It is possible that an overestimation of the fatigue life could occur if a fatigue model is developed and designed using a higher frequency of loading compared to that of the real structure is used in an analysis or design. Investigations that were conducted on the influence of loading frequency by Graf and Brenner, suggests that the number of cycles which leads to failure of concrete specimens decrease as the frequency of loading decreases. For higher fatigue stress levels, the assessment of concrete damage depends on the fatigue cycles and on the duration of the cyclic loading where creep effects become significant, leading to a reduction in the fatigue life.

On the contrary, Takhar et al., based on statistical analysis, concluded that there was no significant difference between tests conducted at a loading frequency of 20 cycles per minute and 60 cycles per minute for stress levels of 0.8 and 0.9 (fractions of average compressive strength) [40].

It has also been reported in the literature that the loading level used in fatigue loading influences the fatigue life. However, the influence is more prominent at maximum stress levels equal to or greater than 0.8, or at maximum stress levels that result in failure at cycles less than or equal to 1000 [16].

Static failure of a plain concrete specimen contains the following several stages, Before loading, there exist initial defects and microcracks on the interface between matrix and aggregate, which distribute randomly. In the initial loading stage, stress concentration takes place at the tip of interface cracks, which causes cracks to propagate along the weakest direction on the interface. These microcracks only propagate mesoscopically with increasing loading, but no macrocracks form, In the last loading stage, where the load is added to its ultimate value, cracks propagate rapidly so that at least a macrocrack through the specimen forms. At this time, the specimen fails [14].

When the applied stress level is less than the concrete's fatigue strength, the initial cracks that exists on the interface between matrix and aggregate of the specimen are stable and do not propagate, so the applied stress level can be regarded as a critical parameter for determining whether the cracks propagate or not [14].

When the cyclic loading stress level continues to rise and exceeds the fatigue strength, the fractures will mesoscopically propagate, causing the relative displacement caused on the interface to induce a drop in elastic modulus. The elastic modulus of concrete decreases linearly as the cycle number of stress increases.

EN 1992-1-1: Eurocode 2: Design of concrete structures, specifies the fatigue verification formula for concrete under compression as follows:

$$f_{\mathrm{cd,fat}} = k_1 \beta_{cc}\left(t_0\right) f_{\mathrm{cd}} \left(1 - \frac{f_{\mathrm{ck}}}{250}\right) \tag{3.1}$$

where:

$$f_{ctm}(t) = \beta_{cc}(t) \cdot f_{cm} \tag{3.2}$$

$\beta_{cc}(t_0)$is a coefficient for concrete strength at first load application.
t_0 is the time of the start of the cyclic loading on concrete in days.

Also the CEB-fib Model Code 2010 suggests a way to predict the strength and stiffness by correlating the compressive strength of concrete at different ages to the mean compressive strength at the age of 28th day. Also the strength depends on cement strength class used for the study:

$$\beta_{cc}(t) = \exp\left\{ s \cdot \left[1 - \left(\frac{28}{t} \right)^{0.5} \right] \right\} \tag{3.3}$$

where:

$f_{\mathrm{cm}}(t)$ is the mean concrete compressive strength at an age of t days.
f_{cm} is the mean compressive strength at 28 days.
$\beta_{cc}(t)$ is a coefficient which depends on the age of the concrete t.
t is the age of the concrete in days.
s is a coefficient which depends on the type of cement:
$= 0,20$ for cement of strength Classes CEM $42,5$R, CEM $52,5$ N and CEM$52,5$R (Class R)
$= 0,25$ for cement of strength Classes CEM $32,5$R, CEM $42,5$ N (Class N)
$= 0,38$ for cement of strength Classes CEM $32,5$ N (Class S)

In Model Code 1990, Model Code 2010, and EN $1992-2$ β_{cc} factor is prescribed as the strength increase over time. As this factor depends on the time of first loading, it is therefore also found relevant to study this factor further and to evaluate in more details if strength development is affected over time which can be considered for concrete fatigue design.

3.2. Self healing potential of micro-cracks in early age concrete

Cracks that can be caused due to shrinkage or due to the application of external loading like cyclic loading are unavoidable in concrete structures. Durability of structure is highly affected due to the ingress of harmful like chlorides and sulphates inside the concrete. It accelerates the corrosion process of steel rebars which eventually reduces the service life of the structure. It is possible to repair or heal the accessible surface cracks through manual repair but it requires much material and manpower. The micro cracks which are difficult to find, will continue to grow and increase in crack width due to the continuous loading. Hence it is desirable if concrete develops self healing capability to self heal both the surface and internal micro cracks in the concrete.[41]

There are many techniques through which self-healing phenomenon in the concrete can be assessed. For

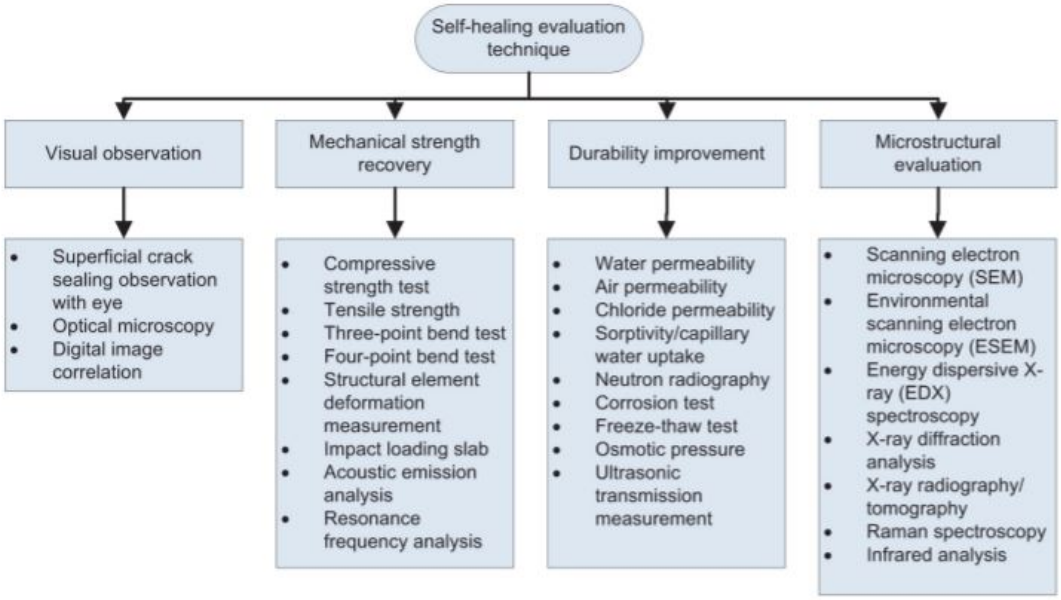

Figure 3.2: Techniques for Self-healing performance in concrete, adapted from [26]

example by using visual observation, mechanical strength recovery, permeability, durability improvement and microstructural evaluation which can be seen from the figure 3.2. Main factors contributing in evaluating the self-healing are: crack sealing, visualisation and the identification of healing compounds causing it, the improvement of the durability performance and the recovery of mechanical strength properties [26].

From the literature it is evident that there are principally two sorts of self-healing mechanisms possible in concrete: autogenic and autonomic self healing processes [41]. Autogenic self-healing, also known as Autogeneous self-healing, is an inherent material healing property in which the self-healing process begins with the generic elements already existing inside chemical composition of concrete. Due to the rehydration of unhydrated cement particles remaining on the surface of the cracks is the cause for cementitious materials have self-repairing or self-healing properties. Autonomic self-healing, on the other hand, entails the utilization of materials that aren't typically found in concrete. [41]

The hydration of unhydrated cement that remains in the matrix is one of the key mechanisms of autogenic self-healing. However, the amount of healing compounds produced in this manner is restricted. As a result, autogenic self-healing is effective in cracks with a width of 50–150 μm [22]. Because of the high percentage of unhydrated cement and other factors such as compression stress[34], autogenic self-healing capability is better at a young age. Application of wet-dry cycles on concrete can increase the healing performance[45]. The use of fibres to limit crack opening and the usage of superplasticizer

in engineered cementitious composites (ECC) to minimize the w/c ratio can also promote autogenic healing performance. [45].

In contrast to autogenous healing, autonomic self-healing in concrete demands the release of the healing agent from reserved encapsulation or a continuous vascular network. Various researchers used several different healing agents in order to inculcate autonomic self-healing in concrete. Some researchers used epoxy resins, alkali-silica solutions [21][8], expansive minerals [27][2], and bacteria-based microorganisms [18][28].

3.2.1. Autogenous self-healing of cement and concrete

Lauer and Slate envisioned autogenous self-healing in cement in the twentieth century, and the notion was subsequently researched and established by many scholars. The basic mechanism in autogenous self-healing of matured concrete is the crystallization of calcium carbonate within the fracture. [10] Eqs.(1)–(3) show the reactions involved in calcium carbonate deposition (3).

$$H_2O + CO_2 \leftrightarrow H_2CO_3 \leftrightarrow H^+ + HCO_3{}^- \leftrightarrow 2H^+ + CO_3^{2-} \tag{3.4}$$

$$Ca^{2+} + CO_3^{2-} \leftrightarrow CaCO_3\,(pH_{WATER} > 8) \tag{3.5}$$

$$Ca^{2+} + HCO_3^- \leftrightarrow CaCO_3 + H^+\,(7.5 < pH_{water} < 8) \tag{3.6}$$

In those reactions, CO_2 dissolved in water from the air, and the calcium ion Ca^{2+} is derived from concrete, as can be seen from the Eq.3.4. As cement powders make contact with water, a chain of reaction called the hydration process starts. Such reaction will convert clinkers contained in the cement powder into cement matrix, which consists of calcium silica hydrate (CSH), calcium hydroxide (CH), and gypsum(3.5,3.6).

Different researchers [30] have proposed the following reasons for autogenous self-healing: (i) further reaction of the unhydrated cement, (ii) expansion of the concrete in the crack flanks, (iii) crystallisation of calcium carbonate, (iv) closing of the cracks by fine particles in the water, and (v) closing of the cracks by spilling off loose concrete particles resulting from the cracking. Figure 3.3 shows a schematic representation of this five-step concept.

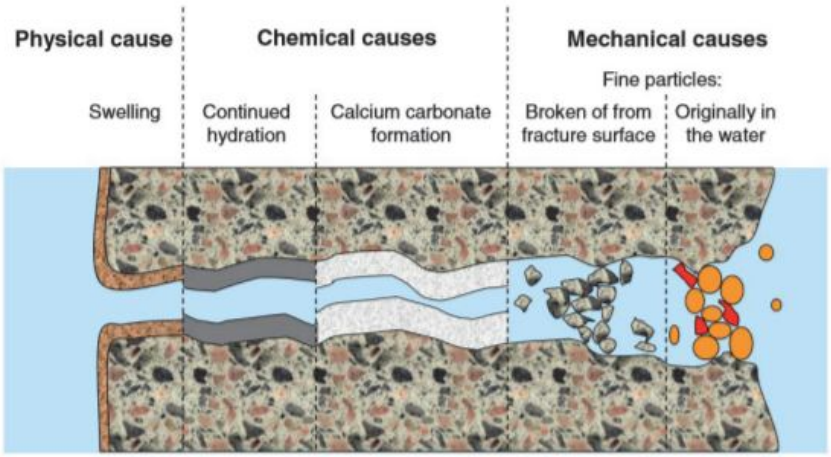

Figure 3.3: A model of five steps taking place within three processes, physical, chemical and mechanical(Reproduced from [34])

Existing condition influence in autogenous self-healing
Autogenous self-healing in concrete is influenced by its age, internal stress, and curing conditions. Due to autogenous healing, concrete heals quickly at an early age. Under 0.1, 1 and 2 Mpa compressive pressures, concrete prisms with cracks up to 50 μm were autogenously repaired [34]. (Figure 3.4a). The propelled compressive stress makes contact with the crack face. As a result, concrete specimens that were cured under any amount of compressive stress healed far better than specimens that were not compressed (Figure 3.4b).

Only a small fraction of compression is required to keep the crack faces in contact. Water-soaked samples regained their strength during the curing process. It turned out that only in the case the specimens were stored under water during the healing period recovery of strength is possible. In the case of storing the specimens in an environment of 95% or 60% RH almost no increase in strength was observed. In the case of 95% RH the specimens were even stored for a period of 3 months. Also in that case no crack healing was observed [34].

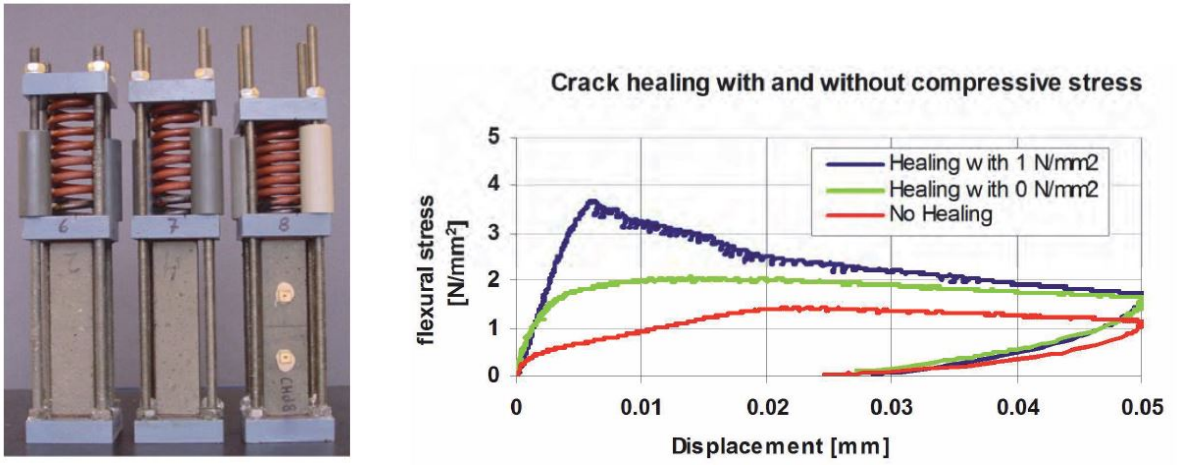

(a) (b)

Figure 3.4: Effect of existing conditions on self healing . (a) Load application on prisms . (b) Stress vs Displacement comparison after healing for loaded and unloaded samples (adopted from [34])

3.2.2. Effect of curing conditions on the self-healing capacity

It is important to note that chemical composition of concrete mixture and curing conditions has great influence over the self healing capacity of the micro-cracks in concrete. B. Šavija and E. Schlangen researched about the Autogeneous healing and chloride ingress in cracked concrete at Delft University of Technology, the Netherlands. The effect of autogeneous healing on chloride infiltration in cracked concrete was investigated in an experimental investigation. Two concrete compositions (Portland cement and blast furnace slag), two healing regimes (submerged and fog chamber), two cracking ages (14 and 28 days), and different crack widths were considered as criteria in the research.

Furthermore in their research, it appeared that resistance of small cracks to chloride ingress has improved not only when cured under water, as expected [17], but also when specimens were cured in the fog room. This suggests that autogeneous crack healing could occur in real structures in humid climates, rather than just under submerged situations [33].

In the study performed at Delft University of Technology, the recovery of resistance to chloride ingress has been studied as a parameter to evaulate the self healing capacity in the concrete. From the results, there was no substantial difference between specimens cured in the fog room and those cured under water. Both specimens cracked at 14 days and those cracked at 28 days appear to be in this category. In terms of chloride transport, it appears that curing in the fog room provides a sufficiently wet environment for crack healing process. As a result, there is no need to cure for a long period of time under

water. This could have some practical implications: in locations with high relative humidity and a lot of rain, like the Netherlands, minor fractures may repair without the need for contractor involvement [33].

It was indicates that the strength recovery in the cement based specimens was essentially produced by delayed hydration and pozzolanic reactions, rather than by precipitation and crystallisation of $CaCO_3$ in the healed cracks. In a previous study, Ferrara et al.63 investigated mechanical properties recovery of concrete incorporating crystalline admixtures. They found that the mechanical recovery was attributed to further hydration reactions rather than to conversion of $Ca(OH)_2$ into $CaCO_3$. Upon cracking, such products become exposed to outdoor moisture and/or water, which could not otherwise penetrate the quite impervious and compact skin of an undamaged specimen, and undergo delayed hydration reactions which produce C-S-H crystals sealing and healing the cracks. Hence it is necessary to investigate the strength recovery which is caused due to further hydration and if the self healing mechanism possible under the fog curing conditions.

3.2.3. Self-healing by further hydration and effect on the mechanical properties

The unhydrated cement particles on the fracture surfaces begin to dissolve once they come into touch with water, as seen in Figure 3.5. The silicate begins to diffuse out of anhydrates shortly after Ca2+ ions begin to diffuse out [44]. As a result, the concentrations of various ions in the crack solution steadily rise. Further hydration products are produced in the crack solution once the ion concentrations surpass the equilibrium conditions for precipitation. Because there is sufficient of CSH on the crack surfaces once the crack forms, the induction period of hydration does not occur throughout the subsequent hydration processes [37].

Further hydration slows down and becomes more diffusion-controlled when additional hydration products are generated at the unhydrated cement surfaces in the crack [5]. Some of the ions are utilized to create the inner products during this time, while others may diffuse into the crack solution. As a result, the formation of healing products in the crack continues, though at a reduced rate [15]. For self

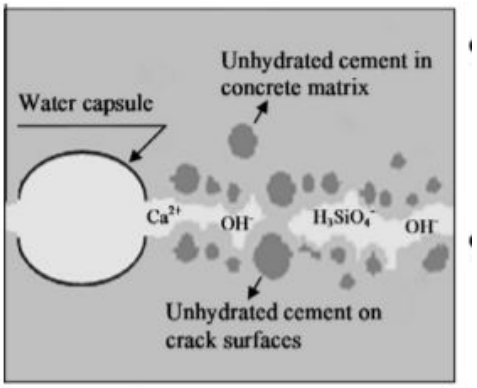

Figure 3.5: Schematic diagram of the mechanism of further hydration: further hydration of unhydrated cement on crack surfaces(adapted from [15])

healing potential under saturated condition,the amount of hydration products in the crack increases dramatically during the first 20 h. After 20 h, the speed of self-healing of the crack starts to slow down. The reason is that the transport of ions to and from the surface of the unhydrated cement particle is getting more and more difficult as further hydration products are formed around the unhydrated cement. From the modeling results, it can be learned that after 20 h of further hydration about 30 percent of the crack's volume is healed when the width of crack is 10 μ under saturation condition[15].

Mechanical properties regain was observed in the literature. The results show that very good mechanical regains can be obtained within 2 weeks, both in terms of stiffness and bending strength for

relatively small cracks with a width of less than 10μm when they are created before 72 h. Thus, concrete structures subjected to premature cracking can heal with mechanical regains while immersed into water [39].

Several researchers studied the strength recovery due to self-healing and effect of existing conditions on the strength recovery due to self healing. Firstly, the influence of cracking age on strength recovery was studied. It was concluded that a clear decrease in strength recovery was observed with increasing age of the specimen when making the first crack. Also influence of crack width on the self healing capacity was studied. A larger crack mouth opening will result in a longer crack which has propagated further into the specimen. The load that can be carried at a larger crack opening will be smaller. There was quite some scatter in the plot but there seems to be no influence of crack opening on the strength recovery due to self healing [34].

3.3. Ultrasonic data monitoring with CODA Wave Interferometry technique

Monitoring of concrete structures is of a great importance to cope with the concern of ageing infrastructure in many countries [20]. Structural health monitoring systems provide valuable insight into the condition of a structure, enabling planners to make better decisions regarding maintenance, and help to ensure the safety of a structure's inhabitants.

Unfortunately, there has been a lack of mainstream adoption of structural health monitoring systems due to two problems. For starters, systems are costly to install, with prices rising at a quicker pace than a linear rate as systems grow in size. Second, in terms of cost savings to structural owners, the benefits now received from a permanently installed structural monitoring system are difficult to quantify. Clearly, if monitoring system installation costs can be reduced while system capabilities are expanded to incorporate robust structural damage identification, health monitoring systems will become more widely used. [20]

The Non-Destructive Testing (NDT) approach is the most advanced quality assurance testing available, allowing for the evaluation of structure quality and condition without causing damage to the original structure. Ground penetrating radar, laser testing technique , DIC , and FOS are only a few of the NDT technologies that have been developed and employed in the manufacturing industry and civil engineering for decades. Many of these techniques can be utilized for long-term SHM.

For decades, ultrasonic transmission measurements have been employed to monitor concrete sub-subjects, largely on a laboratory scale. The most common application is estimating concrete strength from wave velocities, as defined in European standards [code]. Ultrasonic transmission is also used to test concrete samples for freeze-thaw resistance [3]. They have recently been effectively used in concrete fatigue testing [7]. The most common method of data evaluation is to calculate the time of flight and velocity. [23]

Unfortunately, the sensitivity of this technique is limited, as distances between transmitter and receiver are short (and so is transit time) and quite low frequencies (25–150 kHz) must be used due to the inherent scattering properties of concrete [23].

The CWI approach has also been successfully deployed on real structures and large-scale specimens in outdoor contexts. Traditional NDT tools are often utilized on the structure's surface, with just a shallow penetration depth. A new embedded US transducer was created to focus more on changes inside the structure. Early stage single crack detection was investigated utilizing a combination of CWI and FOS approaches using novel embedded US transducers.

It is necessary to examine the propagation and scatter of ultrasonic waves in concrete in order to determine the CWI's effective usage capability. More importantly, it's noteworthy to study how they relate to physical and mechanical property parameters of concrete, such as stress concentration and the occurrence of micro cracking in concrete.[master thesis]

3.3.1. Ultrasonic Wave Propagation and Scattering in concrete

Elastic waves propagate through concrete in the same way that they do in the earth, which means that they are partially reflected and partly transmitted at junctions where mass density and/or stiffness change. [11]. P-waves (longitudinal or compressional waves), which are polarized in the direction of propagation, and S-waves (transverse or shear waves), which are polarized perpendicular to the direction of propagation, are the two forms of body waves which propogates in any medium.

The different sizes of heterogeneities contained in concrete lead to different levels of scattering and attenuation with varying frequency [25]. Hence, four different regimes of scattering in concrete are proposed; modal-analysis regime, simple-scattering regime, multiplescattering regime, and attenuation regime. The regimes are governed by the wavelength of the signal with respect to the dimension of the heterogeneities, as well as the size of the overall structure [thesis]

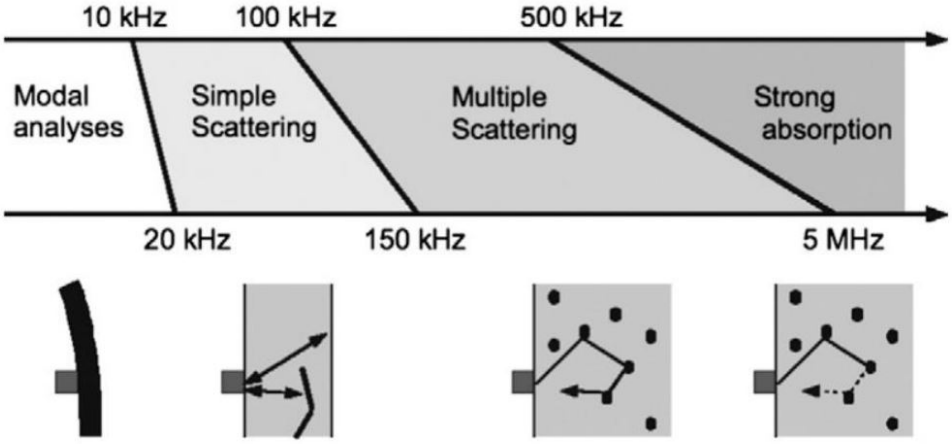

Figure 3.6: Various regimes of signal scattering in concrete (adapted from [25])

The wavelength of the signal is around 20 cm at lower frequencies, often below 20 kHz, with a typical P-wave speed in concrete of around 4000m/s, which is roughly comparable with the macroscopic dimension of the structure. At higher frequencies, even if the wavelength is much lower than the actual size of the structure, signal scattering is expected due to the concrete's relatively bigger heterogeneity.

The signals are more sensitive to subtle changes of medium as their frequency increases. However, energy absorption will also increase at higher frequencies. Therefore, it is important to choose a signal frequency such that a usable signal-to-noise ratio in the coda can be obtained, while retaining sensitivity to subtle changes in medium. [thesis]

It's reasonable to assume a fall in wavespeed when microcracking occurs. Furthermore, due to wave attenuation, microcracks may cause the waveform to vary [17], [18]. As a result, the creation of microcracking could produce a change in wave velocity and waveform in a specimen with the same stress before and after treatment. Hence this technique is used in order to detect any changes in the structural medium or detect any micro cracking because of the cyclic loading in concrete.

3.3.2. CODA Wave Interferometry (CWI)

CWI is a technique which utilizes the later part of a signal (coda) to retrieve information regarding the medium. The coda of the signal often provides more clues regarding what is happening in the medium, since this part of the signal had travelled longer distance compared to the first arrival of the signal. The technique is used to detect changes in the propagation medium by detecting wavespeed change through cross-correlation between two signals where there is virtually no difference in the first arrivals of both.

As multiply scattered waves travel much longer than direct or single reflected ones (Figure 3.7), they are much more sensitive to weak perturbations of the medium.

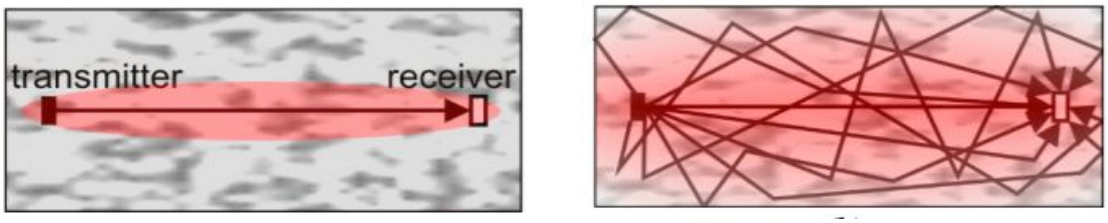

(a) (b)

Figure 3.7: Principle of ultrasonic transmission measurements, propagation paths, and areas of influence (red) . (a)) Direct wave (time of flight); (b)) multiple scattering (coda)(adapted from [43]

The aforementioned two signals should propagate across the medium, one through the reference (untreated) medium and the other through the treated (temperature changes, moisture content changes, compressive or tensile stresses) medium. While the treatment will change the wave propagation and scattering between the two signals, it is important to note that wave scattering is more stable than particle scattering [43], as seen in Figure 3.8.

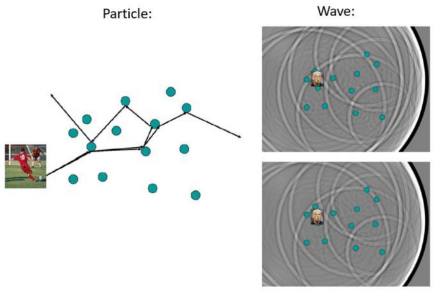

Figure 3.8: While particle will scatter differently due to minor changes in initial conditions, wave propagation is more stable with minor changes in initial conditions. Adopted from [43]

There are two distinct approaches to compare CODA for the purpose of using CWI: one is to break the two signals into numerous time windows and then compare the signals inside the corresponding windows, thereby removing the lag to comprehend the change in velocity, which is known as the Doublet Technique.

The second way is to stretch the time axis for the entire signal and compare it to the original reference signal, with the amount of stretching determining the change in velocity. This is known as the Stretching Technique.
In this research work, stretching technique will be utilized to comprehend the CODA wave results.

Stretching technique and Cross Co-relation factor (CC factor)
For the analyses of wave form by this method, the difference in wave speed is computed by comparison of the reference signal with the 'stretched' signal by cross-correlating both signals. The time axis of the signal to be compared with the reference should be extended to entirely fit the reference signal, with the degree of stretching defined by the velocity change in the medium relative to the reference medium [13] The principle used by this technique is demonstrated in Figure 3.9
In order to stretch the signal for computation with the reference signal, the steps below must be followed. The first step is to change the time axis by multiplying by $1+\tau$ factor. The quantity of time axis that needs to be compressed or extended is represented by τ for the computation.

$$\mathrm{t}' = t(1+\tau) \tag{3.7}$$

The following step is to establish a spatial link between wave speed and time stretching. Since the original signal and the stretched signal have the same spatial distance, this relationship can be developed. This means that a minor increase in the transit time results in a small drop in the wave speed.

$$\frac{dt}{t} = -\frac{dV}{V} \tag{3.8}$$

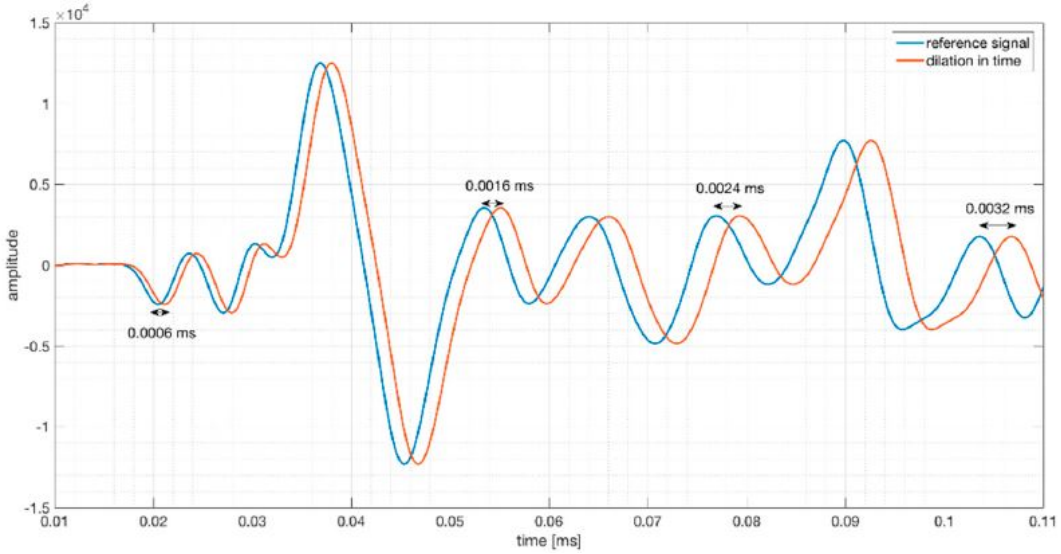

Figure 3.9: Time Stretching Technique (adapted from [13])

$$t' = t(1-\epsilon); \epsilon = \frac{dV}{V} \tag{3.9}$$

Where t' represents the stretched time axis, ϵ represents Time axis stretching factor to velocity, relative change of wave velocity or dV/V, t is Time or time axis.

After the computation of the relationship between the stretching time and wave speed, it is important to assess the relationship between the original signal and the stretched signal.In order to compare both signal, cross- correlation between them needs to be calculated.

$$CC = \frac{\int_0^T h'[t']\, h[t] dt}{\sqrt{\int_0^T h'^2[t']\, dt \cdot \int_0^T h^2[t] dt}} \tag{3.10}$$

The above formula is used to calculate the Cross-Correlation factor (CC factor).Where in the formula, h' is the stretched signal, h is the reference signal, and T is the window length. It is important to note for interpretation of the cross-correlation factor, CC = 1 means perfect correlation between two signals, while CC = -1 means perfect anti-correlation between two signals.

In the PHd thesis titled 'Coda-Wave Monitoring of Continuously Evolving Material Properties' presented at Delft university of technology, shows in detail how CC factor computation can be related to damage is discussed. When Unconfined Compressive Strength (UCS) testing was performed with the CWI, it was observed that increasing axial strain within the elastic limit, very high CC values (close to 1) were recorded. At the onset of elastic phase, when plasticity is introduced, gradual slope towards 0.7 was recorded in CC factor plot. Hence the CC factor value of 0.7 could be set as an threshold value that could indicate the plastic deformation/damage in any material. Hence it is evident from the literature that reduction in CC factors was observed when plastic strain occurs in any material. Hence CC factor analysis could be an indicator of the micro-cracking in the concrete cubes. Hence CWI methodology is used to detect any change in the structural medium in concrete.

Research Gap

• It is evident from the literature how the fatigue loading on early age concrete affects the mechanical strength properties of concrete. But it is to be investigated what loading level can cause reduction in

the mechanical strength properties of concrete.
• Also it has be investigated if the CWI can give an indication of damage occurrence in concrete cubes due to early age cyclic loading.
• This research work also emphasis on what crack widths are expected to occur under a particular load level for 30 load cycles.
• Also emphasis has been made on the evaluation of mechanical strength of concrete after being loaded with cyclic loading, which was missing from the literature.

From the literature, self healing potential of cracks under fog curing conditions has been studied through the chloride penetration depth. It is still not clear, what crack widths can be healed under fog curing conditions which has been studied in this thesis. Strength development aspect due to further hydration has been studied after the application of the cyclic loading.

4

Experimental study

Experimental study has been performed to investigate the influence of cyclic loading on the early age concrete through micro cracking and self-healing phenomenon. Moreover, concrete strength development due to further hydration has been studied after the application of cyclic loading. This chapter gives detailed explanation on procedures followed during the design, casting, testing, and post-processing of the early age concrete cube specimens. The discussion and post processing of CWI results along with recommendations and summarised in the results and discussion section.

4.1. Research methodology

As discussed in earlier section, one of the most important task was to find cyclic loading stress level which would incur visible micro cracking on early age concrete surface with the help of damage indication from CWI analysis. The next task is to analyse the crackwidths occurrence at a particular load level and to investigate if the self healing potential of micro cracks is possible under the fog curing conditions. Lastly, further strength development in concrete, after the application of cyclic loading, has been analysed in fog curing conditions.

For each particular cyclic load level 3 cubes were cyclically loaded. Arrangement have been made by gluing the holders to attach surface attached sensors to the opposite concrete face as can be seen from the figure 4.3b. CODA wave recording along with the axial strain measurement for each load cycles for all the loading levels has been performed. 70% loading case has been selected to analyse the crack width and self healing potential of micro cracks formed due to cyclic loading. After the load cycles have been applied to the concrete cubes, a crack width measuring card will be used along with the portable microscope to assess and compare the crack widths before and after continuous hydration. Lastly, strength development in concrete due to continuous hydration after the application of cyclic loading has been analysed.

Choice of cyclic loading levels

From the literature and some calculations as discussed, it was evident that cyclic loading level applied on the concrete was 56% of the compressive strength of concrete, for 30 load cycles, acting on 3^{rd} day after casting of concrete (Ref. 2.1). Hence this loading level was considered as the starting load level to begin the experiments. Furthermore the loading level were increased from 56% to 60%, 65%, 70% and 75% of the compressive strength of concrete till the visible micro cracks were observed on the surface of concrete cubes. Maximum of 30 load cycles has been applied to the concrete specimens of 150 mm * 150 mm * 150 mm. Experiments with 56 percent load level were performed with 2 different loading frequency in order to successfully perform the experiments on 3 cubes and to check the if there is any effect of loading frequency on concrete cubes.

Choice of measurement techniques
In order to investigate the changes in structural medium in terms of initiation of micro cracking inside concrete cubes, as discussed earlier, CWI technology is used. 2 surface attached sensors were placed on the opposite end of the cubes in order to record and analyse CODA waves after each loading cycle. As discussed, after each loading cycle, real time CC factor has been computed for each loading cycle to assess the number of load cycles that causes damage to the concrete cube. CWI measurement in terms of CC factor and ϵ values has been recorded for each load cycle and the signal is stretched and compared with the adjacent previous load cycle for assessing the damage inside the concrete.

To verify the CWI results, axial strain analysis has been performed for each concrete cube. Computation of Incremental strain has been made in order to analyse what axial strain is incurred for a particular load cycle. Similarly, Cumulative strain is derived for each cube in order to examine total axial strain incurred as a result of application of 30 load cycles. The axial strain results will be analysed and compare with the CWI results. In order to check the increment in concrete strength due to self healing, cracked concrete cube at 70% loading level has been prepared and kept in the curing room for the age of 7 days. Also crack width analysis using portable microscope has been performed in order to check the effect of continuous hydration and self healing potential under fog curing conditions.

4.2. Materials and Mix design

For this study, as mentioned in the earlier section, special concrete which provides 3^{rd} day concrete grade of C30/37 (strength of approximately 30MPa). Surely, the self-healing potential and hydration products of the micro cracks would depend on the chemical composition of the materials used for the mix design. In this study it has been focussed on the self-healing potential of the micro cracks of this specific mix design.

4 trials mix designs were tried and tested to achieve the desired strength at specified loading age. Physical property of the concrete like slump of each mix design was calculated. Initial concrete mix designs had higher cement contents and hence resulting into higher concrete compressive strength than expected. After some adjustments in the chemical composition (change in the cementitious content) for the mix design, desired strength was achieved.

Table 4.1: Mix design of concrete used for the study.

Mix design of concrete used for the study.	
Ingredients	Dry Weight (Kg/m^3)
CEM IIIB	300
CEM I 52.5 R	100
Sand (0-4 mm)	807
Gravel (4-16 mm)	940
Water	183
Superplasticizer	2.4

Glenium 51 superplasticizer was used for this research study. The casting of concrete, mechanical properties testing and cyclic loading experiments were performed in standard laboratory conditions.

4.3. Cyclic loading and Compression testing setup

For the application and to control the cyclic loading of the specimens and to record displacements and strain of the specimens, an integrated loading apparatus and displacement-measurement module is used. Mentioned module consists of a personal computer which has load-control software as well as displacement- and load-measurement software installed, a hydraulic jack and a loading frame.
Depending on the experiment, the loading frame and hydraulic jack vary. For the cyclic loading, a 3000kN hydraulic jack is used, installed in a compressive loading cage (refer to figure below).

(a) **(b)**

Figure 4.1: Loading apparatus used for the study. (a) TONI bank machine for the application of cyclic loading . (b) Compression testing equipment.

4.4. CODA Wave Interferometry setup and implementation

Proceq Pundit PL-200 ultrasonic pulse velocity and wave analysis equipment were utilized for the generation and analyses of the CODA wave part of the signal. 2 surface attached sensors are attached to opposite surface on concrete cube as can be visualised from 4.3. The sensors are attached with the help of the glued holders on the concrete phase and are tightened through a bolt to the concrete surface. The wave analysis and computation of signal is performed through proceq setup as can be visualised from 4.2. The sampling frequency used for the study was 1 MHz. Coupulant paste was used between the sensor and concrete surface in order to remove the possible air entertainment between 2 surfaces.

Signal Processing strategy

The time axis of a signal should be extended and then cross-correlated with the reference signal to calculate the relative change of waveform through CWI. The entire signal is stretched to fit a certain window in this scenario, and the process is repeated for all of the recording's windows. While this process is computationally expensive because each signal is stretched multiple times, it provides better accuracy than windowing the signal first and then stretching it, because stretching a windowed signal will not yield good results due to a lack of information in the part where the signal is trimmed. The following processing procedure is used to process the signal in order to conduct CWI:.

- Importing the binary signal from the data logger into MATLAB.
- Assigning the reference signal and the target signal to be stretched.
- Assigning the range of wavespeed change (epsilon) for assessment.
- Assigning the first arrival of the signal.
- Assigning the center of the window based on the first arrival and recording span.
- Assigning the width of the windows.
- Signal stretching
- Stretching the signal time axis with respect to epsilon with Equation .

$$t' = t(1-\epsilon); \epsilon = \frac{dV}{V} \tag{4.1}$$

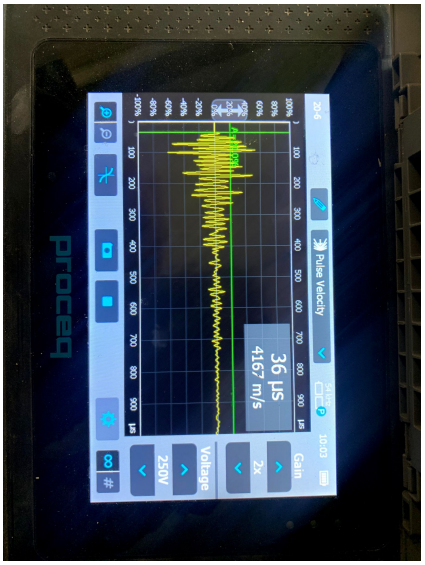

Figure 4.2: Proceq setup

Where t' represents the stretched time axis, ϵ represents Time axis stretching factor to velocity, relative change of wave velocity or dV/V, t is Time or time axis. -The CC factors for the stable Epsilon value has been calculated.
- The epsilon,CC values and waveform after stretching for each load cycle is stored.

During the stretching technique, the central frequency of the signal that is selected as. f = 50*10^3. The period of the wave is calculated through $p = 1/f$ and each window length selected for the computation is window length $g = 10^*$p which would be 200 microseconds. The matlab code to compute the signal stretching analysis was prepared by a PHd candidate at Delft university of technology. Also literature on the stretching technique and CC factor analysis was thoroughly studied before the laboratory work [43].

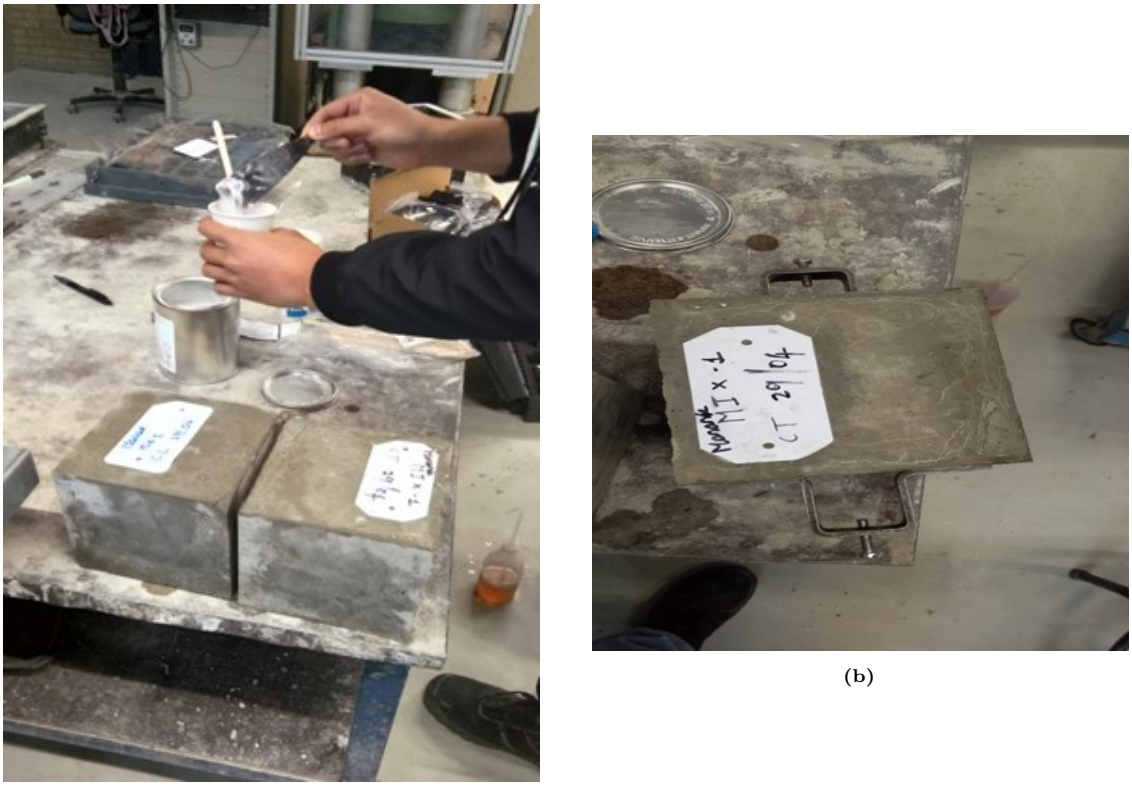

(a) (b)

Figure 4.3: CODA wave equipment setup. (a) Gluing process. (b) Gluing holders to attach sensors.

The recording of the CODA wave is performed at 2 points, one at the start of the loading cycle and one at the end of the loading cycle. The recording at the start of the load cycle is termed at Lower Stress analysis and furthermore will be referred as 'LS' and similarly the recording at the end of the load cycle is termed as Higher Stress and will be referred as 'HS'. The schematic diagram for recording of the CODA wave readings is visualised in the figure 4.4.

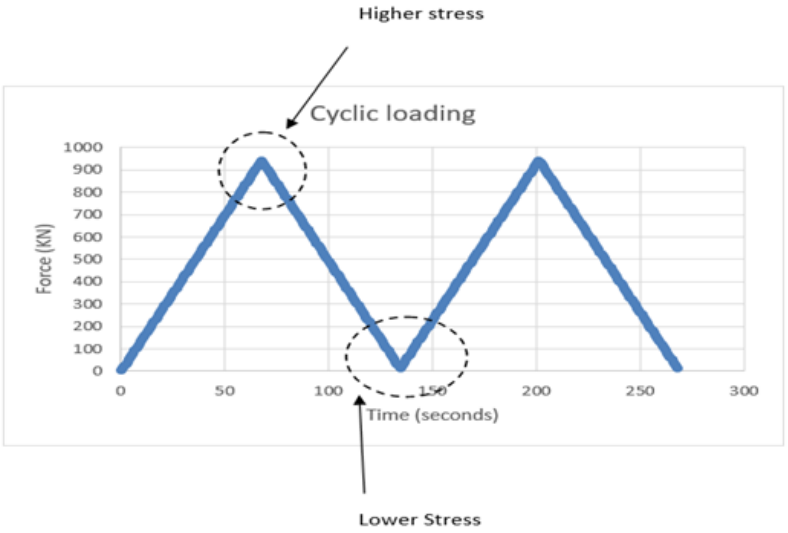

Figure 4.4: Schematic of points to record the CC factor

A portable microscope with the zoom capacity of 1000 X is used to analyse any micro cracks incurred

due to the cyclic loading. The microscope would be used to analyse the crackwidths caused due to cyclic loading and visualisation of any self healing products formed due to continuous hydration in concrete. For the visual inspection and measurement of the crackwidths, a crack width measuring card with the range of 0.05 mm till 3mm has been used for the study.

Figure 4.5: Portable microscope for the analysing of micro cracks

5

Results and Discussion

This section of results and discussion is divided into damage detection and assessment for different cyclic loading levels with the help of strain analysis and CODA wave interferometry. The effect of cyclic loading on the mechanical properties of concrete has been documented and discussed. A section on analysis of damage assessment through direct wave speed has been discussed. Next section focusses on the strength development aspect of the loaded and unloaded samples and effect of different. Furthermore, possibility of self-healing of microcracks due to continuous hydration has been discussed.

The compressive cyclic loading due to the compaction vehicle, computed from the literature is 56 percent loading of the compressive strength of the concrete. Also more importantly, from the strength development curve used in the real bridge design, the concrete strength gained at the of 3^{rd} day is 30MPa. Hence from the mix deign described previously, it is possible to achieve 3^{rd} day compressive strength of 30 MPa.

As discussed in previous chapter, the vehicle with maximum 'Wal's Index' was chosen as it would have most detrimental effect on concrete. Tandem Drierols was the machinery with the source of cyclic loading on early age concrete with 30 load cycles requiring to compact 3 layers of asphalt as discussed in the previous section. Co-relation factor (CC factor) has been computed at the ascend and descend of each cycle as visualized in the previous section. The reading at ascend of each cycle is termed as High Stress values (HS) and the readings at descend of each cycles is termed as Low Stress values (LS). CC factors were calculated at particular time windows with stable ϵ values. To validate the CWI results, axial strain analysis was performed for each concrete cube, for all the loading levels.

Compressive strength of 3 cubes were analysed at the age of 3^{rd} day. Compressive strength of the cubes was respectively: 32.43MPa, 31.25MPa, 31.77 MPa with the average strength of 31.81 MPa at the age of 3 days. The slump of the concrete achieved was 72 mm. After the casting of concrete cubes, the cubes were covered with the plastic sheets to avoid any cracking due to shrinkage. After 24 hours, the finished cubes shall be transferred to the fog curing room. This phenomenon can be seen in the figure 5.2.

(a) **(b)**

Figure 5.1: (a) Slump measurement of fresh casted concrete. (b) Slump Cone.

Figure 5.2: Finished casted concrete cubes

5.1. Understanding the monitoring techniques to evaluate damage of concrete

Major objective of this section is to discuss on the monitoring techniques that could determine damage in concrete cubes. As discussed in the section of monitoring techniques for damage detection in concrete, hysteresis curve analysis has been performed for each loading level to comment on occurrence on plastic deformation, if any, during the application of the cyclic loading. Hence this section focuses on analysis and comparison of the hysteresis curve for all the loading levels. The next objective is to verify and corroborate the result from the hysteresis curve analysis with the axial strain analysis. In the net step, the reduction and computation of the CC factor analysis and wave speed analysis is linked with the axial strain analysis.

5.1.1. Influence of cyclic loading on hysteresis curve analysis of concrete

The typical hysteresis loop of the concrete specimens under cyclic loading comprises the unloading curve and reloading curve which can be visualised from the figure 5.4. A full cycle of the stress–strain response is consisted of two distinct paths: unloading path and reloading path. The unloading path is curvilinear characterized by a progressively diminishing slope, until it intersects the strain axis. The reloading path is almost linear that starts from the strain axis and intersects the envelope curve. In case of non linearity there would be an occurrence of slip phenomenon on the strain axis which causes permanent plastic deformation to any structure.

Load = 56 % of the compressive strength, original load frequency

The loading rate, as discussed previously, was 5 hours of loading required for the application of load cycles. The calculation simplifies with 10 minutes required for each load cycle with the loading rate of about 1.36 KN/s.At the slower loading rate of 1.36 KN/s, it is possible to perform cyclic loading experiment on 2 concrete cubes. To check the influence of cyclic loading frequency on concrete cubes, the loading frequency has been changed to the standard loading rate of 13.5 KN/s for 30 load cycles. To have standardised results, the 7 days loading age of concrete has been selected. Firstly it is important to assess the case of 3 rd day age cyclic loading on concrete and compute the change in mechanical properties of concrete, if any.

Figure 5.3 shows schematic loading diagram for cyclic loading for 56 percentage loading which extends to 30 load cycles. Analysis of overall strain development along with Incremental strain has been performed to analyze the damage assessment per load cycle. Figure 5.4 demonstrates a typical hysteresis curve from one of the concrete cube with 56 percent loading.

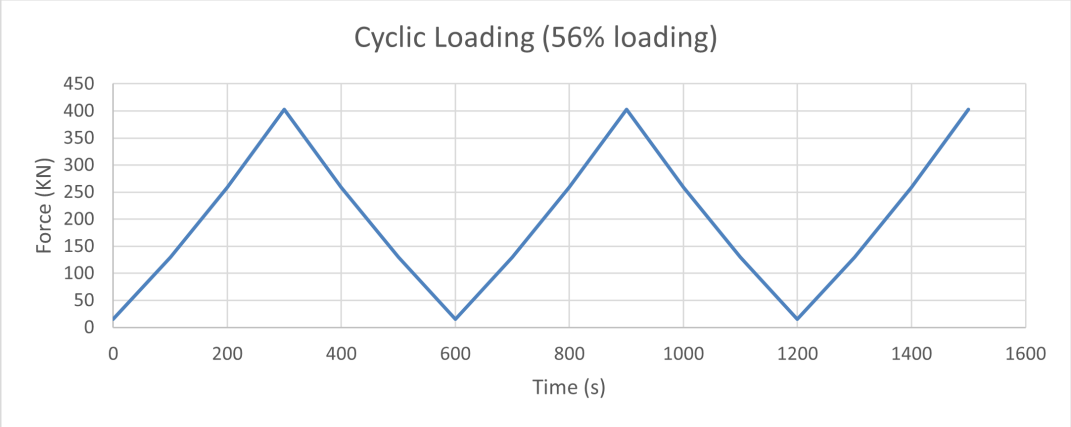

Figure 5.3: Realistic loading scheme for 56 percent loading

In the case of 56% loading, there was no non linearity seen as the reloading phase was linear in nature. Hence it can be asserted that for 30 load cycles at the aforementioned load level, there is no plastic

slip occurrence between the load cycles. Hence it was deduced that this loading level, no plastic strain occurrence was seen.

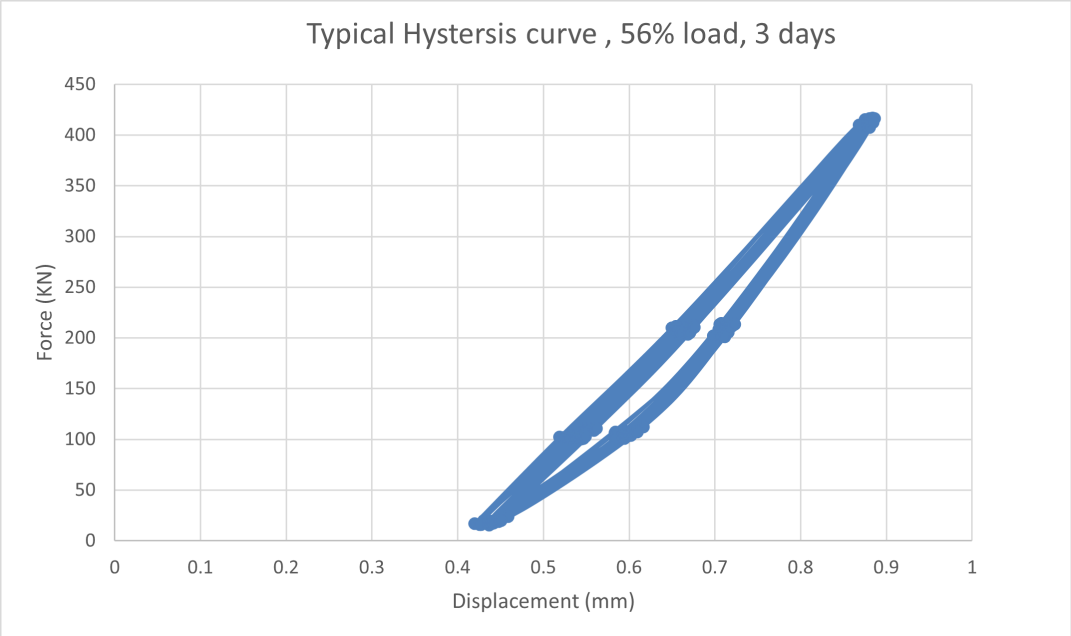

Figure 5.4: Schematic hysteresis curve for 56 percent loading

Load = 56 % of the compressive strength, enhanced load frequency
As discussed in the previous section, the cyclic loading frequency has been enhanced in order investigate if there is any influence of cyclic loading frequency on the mechanical properties of cyclically loaded concrete. Hence the loading frequency is enhanced to standard loading rate of 13.5 KN/s and the age of concrete for the testing of cyclic loading is set to 7 days. 30 load cycles has been applied to 3 concrete cubes. CODA wave recording was performed on 2 concrete cubes and the Strain analysis has been performed for 3 cubes.

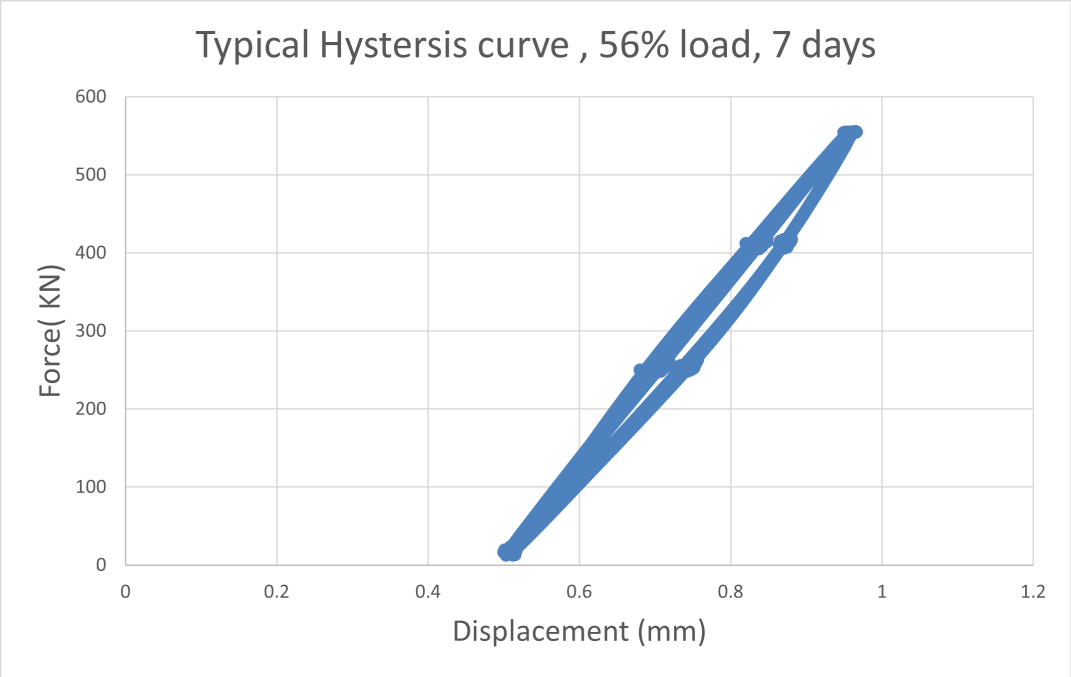

Figure 5.5: Schematic hysteresis curve for 56 percent loading, enhanced frequency

Figure 5.5 represents the hystersis for load level = 56% of the compressive strength for 30 load cycles. Also during the loading and reloading phase, it is sen that there is no slip occurrence as can be visualised from the figure. It can also be visualised that the Force vs Displacement line for the loading phase is completely linear. Hence it can be concluded that still the cyclic loading is in the elastic phase and there is no occurrence of plastic strain to the concrete cube. Hence the deformation and the strain occurrence is in the elastic regime.

Load = 60% of the compressive strength, enhanced load frequency.
In order to investigate the cyclic loading level that could cause cause the cracking phenomenon inside the concrete cubes, the load level has been enhanced to load = 60% of the compressive strength of the concrete. 8 concrete cubes were prepared in order to have detailed analysis of cyclic loading under the aforementioned loading.

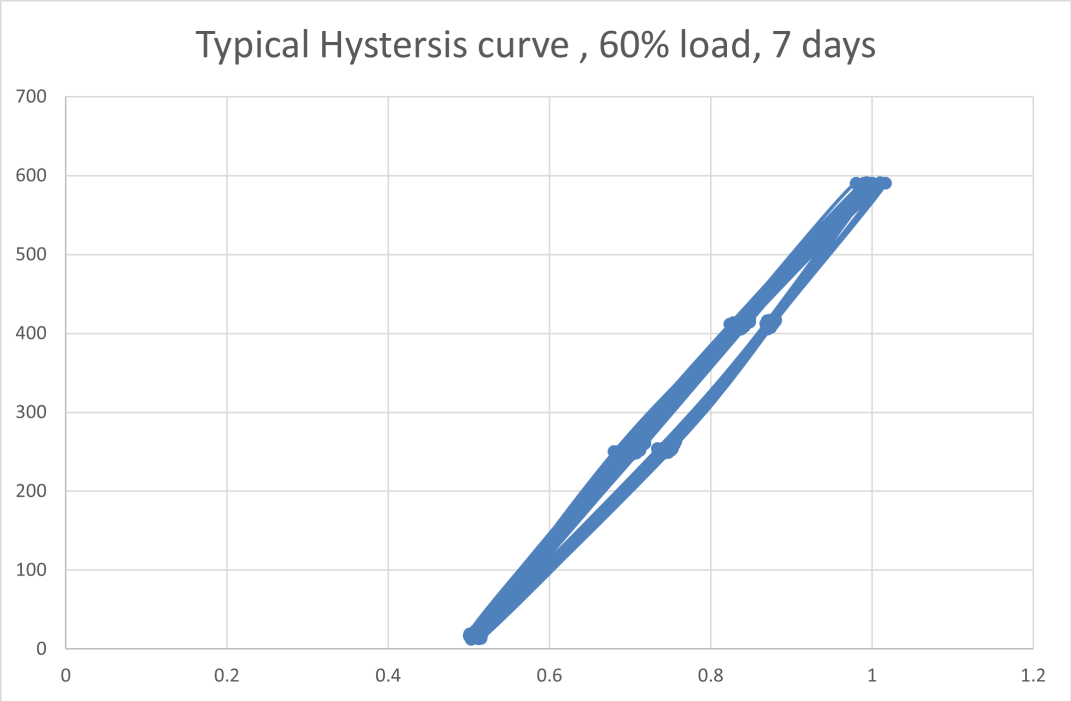

Figure 5.6: Schematic hysteresis curve for 60 percent loading

The nonlinearity is seen when the curve exceeds the previous envelope unloading strain, and becomes more apparent as accessing to the envelope curve. As it can be seen from the figure 5.6, the unloading scheme and the reloading scheme almost has the similar envelope for all the loading cycles. Hence it can be asserted that no non-linearity occurs at this particular loading level. Also no slip between the loading cycles was observed at the strain axis and hence there is no plastic deformation that occurs at this loading level.

Load = 65% of the compressive strength, enhanced load frequency.
In order to investigate the cyclic loading level that could instigate the cracking potential inside the concrete cubes, the load level of concrete has been enhanced to the load = 65% of the compressive strength for the application of 30 load cycles. The cyclic loading has been applied to 3 concrete in order to assess the reduction in the mechanical properties of concrete, if any. A total of 7 cubes were casted out of which first 3 cubes were used to find the average compressive strength of the concrete. After the computation of the average compressive strength, 65% of the load has been computed. After the CODA Wave interferometry setup of attaching sensors to the concrete cubes, the cyclic loading procedure has been performed.

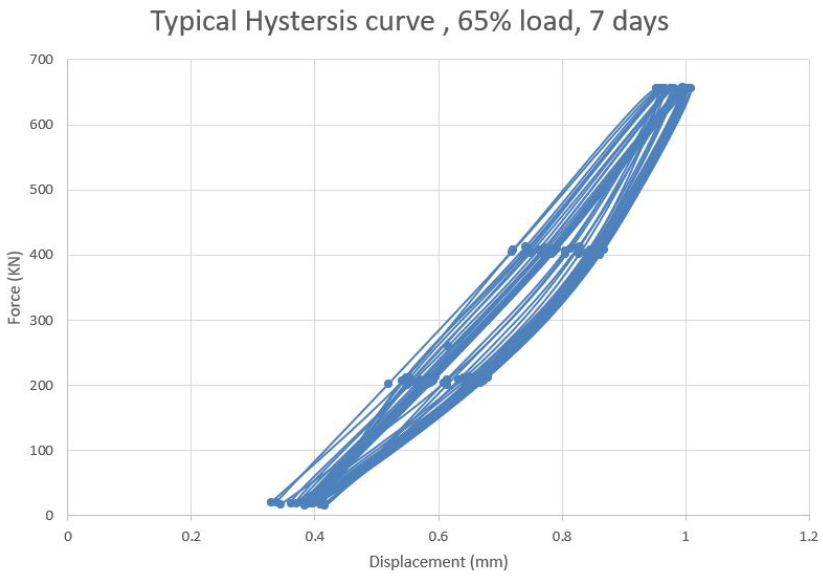

Figure 5.7: Schematic hysteresis curve for 65 percent loading

This loading case is bit interesting as there is some slip observed on the strain axis between the load cycles. This slip could be induced by some residual strain occurrence between the load cycles. This loading level with 30 load cycles could cause a fracture point which induces an irreversible strain in the concrete cube and hence not all the load cycles has very similar unloading strain and the width of the unloading strain is larger as compared to the previous case.

When the there is a difference between the unloading and reloading strain, it does not necessarily means the that the concrete has achieved complete non linear phase as the Force vs Displacement graph achieved for this loading case is almost a straight line. There could be the process initiation of micro-cracking at this particular load level. It was also indicated by the CC factor analysis which will be discussed in the next section.

Load = 70% of the compressive strength, enhanced load frequency.
Further increasing the load to 70% of the compressive strength of the concrete, in order to investigate if this loading can cause cracking for 30 load cycles. Figure 5.8 shows a schematic diagram of a typical hysteresis curve obtained in the case of loading = 70% of the compressive strength of concrete. A clear slip in the strain axis is visible as compared to the hysteresis curve for lower loading levels.

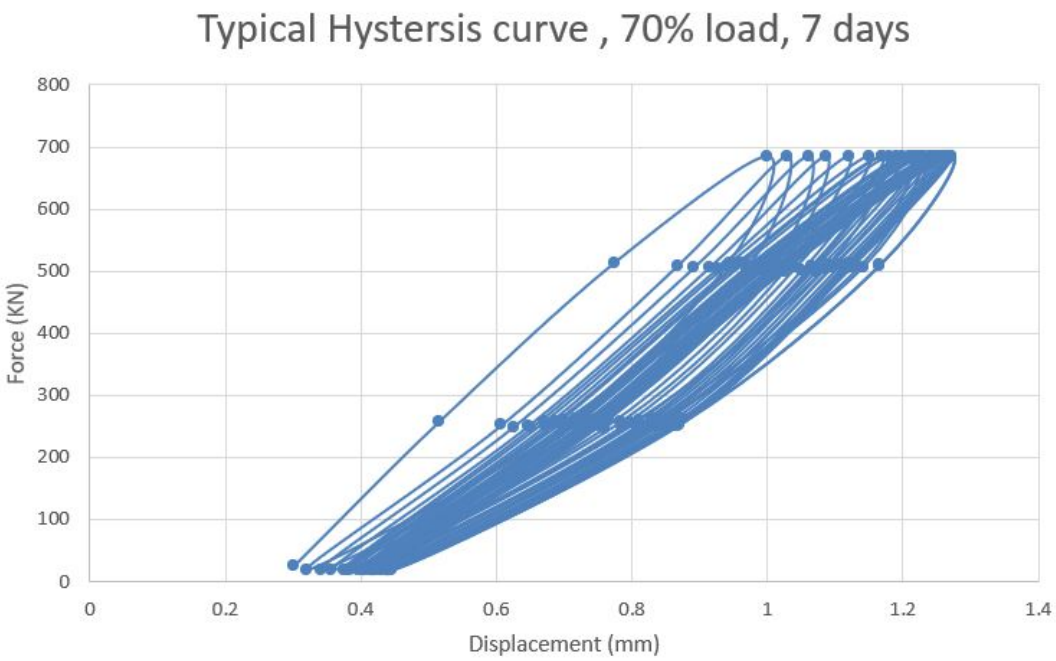

Figure 5.8: Schematic hysteresis curve for 70 percent loading

As it is visible from the figure 5.8, during the unloading phase, there is clear indication that the unloading part does not really overlap with the reloading part and hence there is occurrence of some plastic strain during the application of the load cycles. It is evident that first few load cycles with aforementioned loading level causes irreversible strain to the concrete which causes cracking to the concrete cubes. It was also observed that the Force vs Displacement line is not completely linear as in the previous case and hence it concluded that this loading level causes non linearity in concrete.

Load = 75% of the compressive strength, enhanced load frequency.

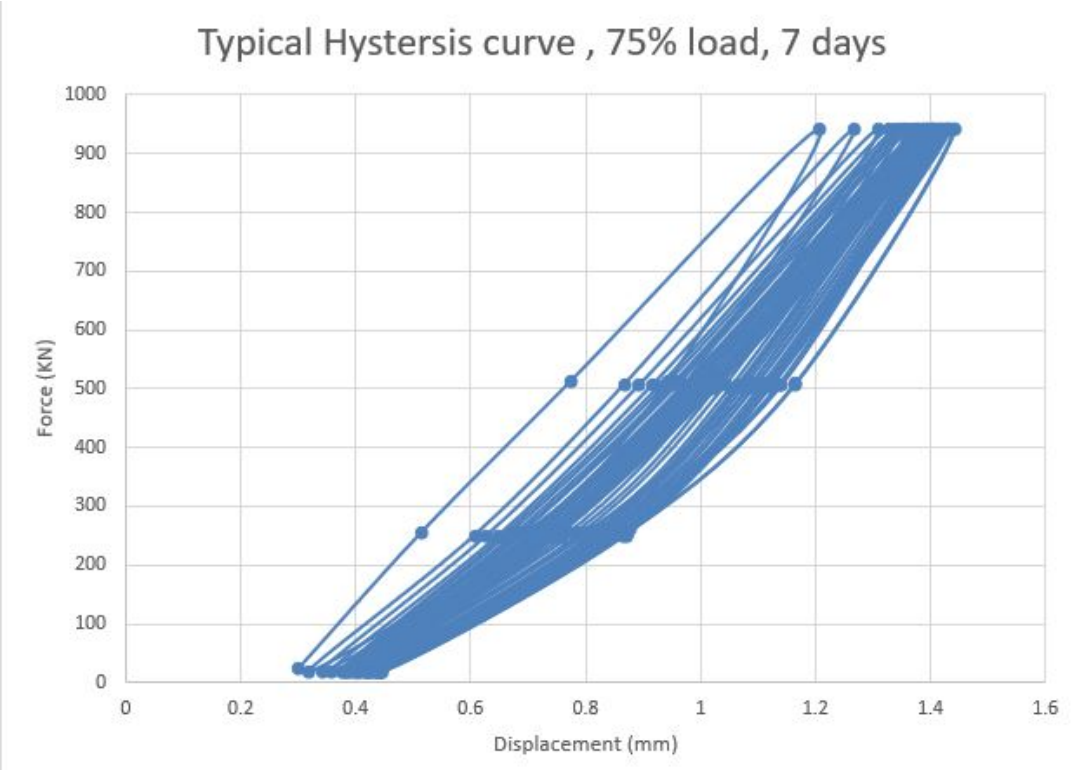

Figure 5.9: Schematic hysteresis curve for 75 percent loading

During the unloading phase, as shown in figure 5.9 of hysteresis curve, there is clear indication that the unloading component does not truly overlap with the reloading part, resulting in some plastic strain during the application of the load cycles. It is clear that the first few load cycles at the aforementioned loading intensity produce irreversible strain in the concrete, resulting in cube cracking. The Force vs Displacement line is also not totally linear, as it was in the prior case, leading to the conclusion that this loading level generates non-linearity in concrete.

Plastic strain is the residual axial strain of concrete on the unloading path when the stress is unloaded to the zero stress. The relation between plastic strain and envelope unloading strain is one of the significant cyclic aspects. Hence a clear relationship between the aforementioned 2 aspects can be established. The relationship was out of the scope of the thesis. Hence by the comparison of hysteresis curve for all the loading levels, it can be concluded that initiation of plastic strain starts to occur at 70% loading case as well as 75% loading case.

To verify and corroborate the finding in the hysteresis curve analysis, axial strain analysis needs to be performed. It would be interesting to see the how does the cumulative strain analysis would vary with the increase in the loading level. It is suspected that in the case of 65%, 70% and 75% loading, much higher cumulative strain would be achieved in comparison with the case of 56% and 60% loading. Also it would be interesting to see the what 'per cycle' strain (incremental strain) would be incurred and how would it vary with increase in the loading level. Hence to have further analysis on damage occurred to the concrete cubes per load cycle, 'Cumulative strain analysis' and 'Incremental Strain analysis' has been analysed for each concrete cube for all the loading cases.

5.1.2. Influence of cyclic loading on axial strain analysis of concrete

In order to have detailed analysis of the axial strain caused per load cycle, an analysis including the 'Incremental Strain' and 'Cumulative Strain' for all the loading levels. The strain measurement for all the loading level is performed during the unloading phase after each loading cycle. Incremental Strain in the context represents the axial strain caused per load cycle. Hence from the figure 5.10 and figure 5.11 it is evident how much strain in incurred in each load cycle.

Also the analysis of Cumulative Strain has been made which constitutes the total addition of all strains occurring at the end of 30 load cycles. The red line in the figure 5.10 and figure 5.11 represents the Cumulative Strain and the blue line represents the Incremental strain for the concrete cubes.

Load = 56% of the compressive strength, original load frequency.

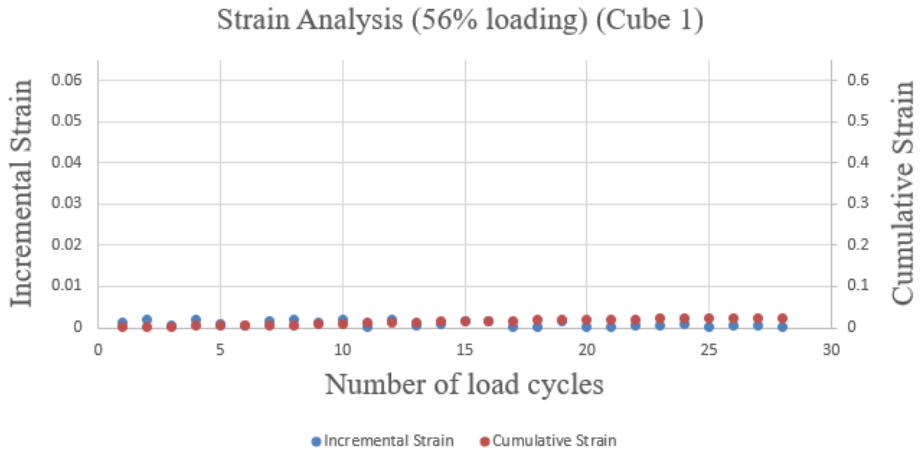

Figure 5.10: Strain analysis (56 percent load, cube 1)

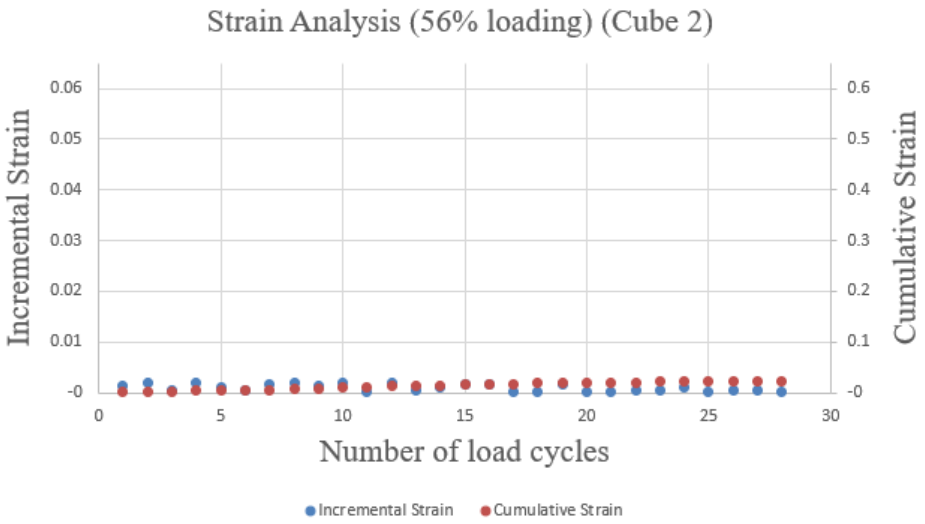

Figure 5.11: Strain analysis (56 percent load, cube 2)

Figure 5.10 demonstrates the strain analysis for Cube 1 with 56 percent loading and 30 load cycles. As mentioned earlier, Incremental strain represents the lateral strain occurrence per load cycle in the direction of the load. 0.002 is maximum strain incurred at 7^{th} cycle for cube 1 and at 8th load cycle for cube 2 . The red line represents the cumulative strain incurred cumulatively at the end of 30 load cycles which reaches to 0.019 and 0.023 for cube 1 and cube 2 respectively. This data is important to

compare strain development of concrete for different load level.

As it can be visualised from figure 5.10 that from load cycle 17 to 18 and from load cycle 24 to 25 the cumulative strain decreased a bit as compared to the previous cycle. This could be an error during to strain computation by the setup used to compute the axial strain because the magnitude of the strain caused is very low.

Load = 56% of the compressive strength, enhanced load frequency.
The results of Incremental strain and cumulative strain can be seen from the figure 5.12, 5.13, 5.14. It is evident that same loading, load =56% of the compressive strength of the concrete has been applied to the concrete for 30 load cycles at the age of 7 days in contrast to the loading applied to the concrete at the age of 3^{rd} day in previous section. The axial strain per load cycle and cumulative strain in the case of 7 day loading is higher than in the case of 3^{rd} day loading.

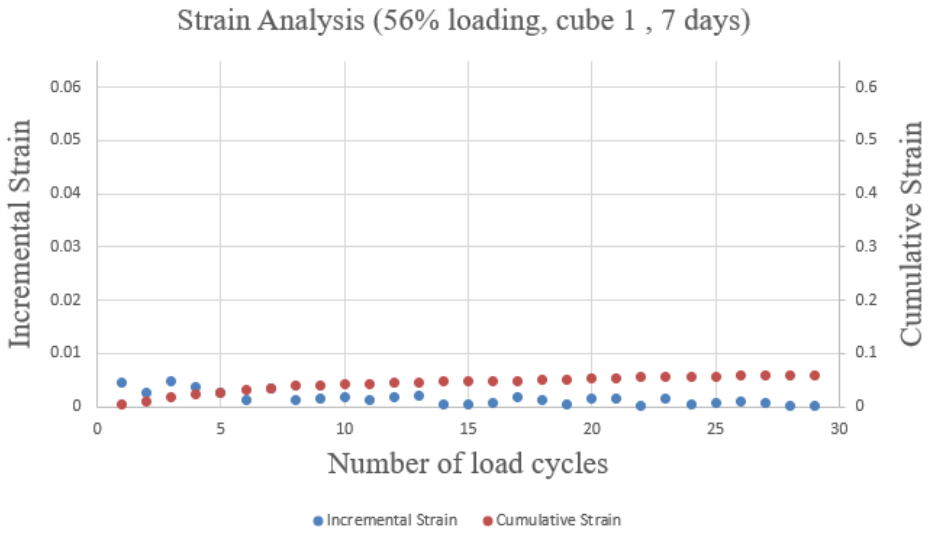

Figure 5.12: Strain analysis (56 percent load, cube 1)

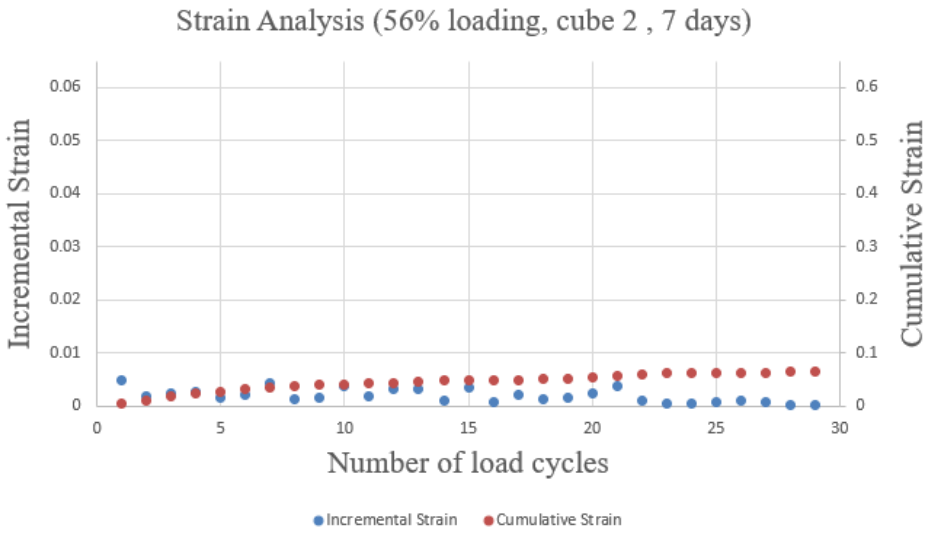

Figure 5.13: Strain analysis (56 percent load, cube 2)

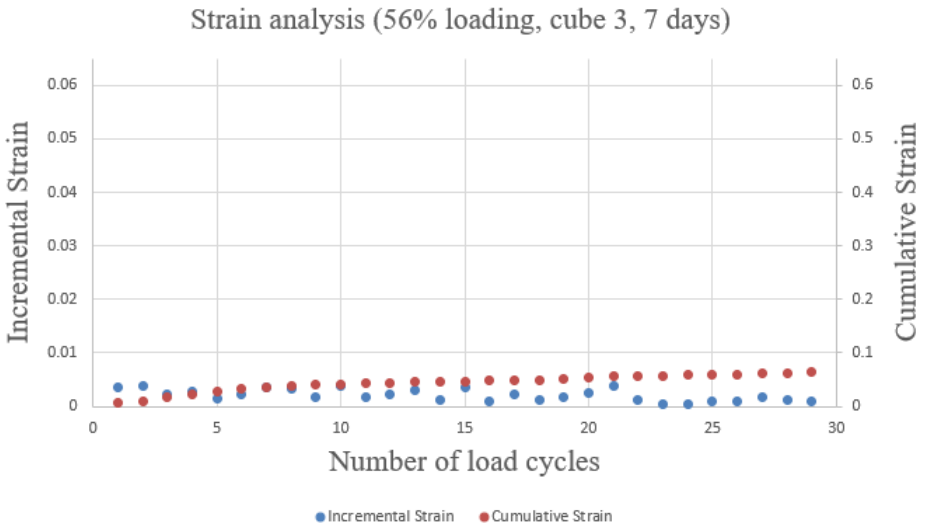

Figure 5.14: Strain analysis (56 percent load, cube 3)

It is evident from the figure 5.13 that maximum Incremental Strain incurred is 0.005 at the very first load cycle and the maximum cumulative strain occurrence is about 0.065 at end of 30 load cycles. This values are higher as compared to the maximum value of cumulative strain value of 0.023 and Incremental strain value of 0.002 incurred in case of 56% loading applied on 3^{rd} day as can be the figure 5.11.

The reasoning behind the increased strain for 7^{th} day loading can be traced back to the evolution of Young's modulus of the constituents in the concrete. Cement is the only constituent in concrete whose Young's modulus grow with the increase in time. But the Young's modulus of both fine aggregate as well as the coarse aggregate remains constant with the time.

The cyclic load is applied to the concrete cubes on the 3^{rd} day age of the concrete is about 18.4 MPa, which is 56% loading of the compressive strength of concrete. In contrast to that, the cyclic load applied to the concrete cubes on the 7^{th} day age of the concrete is about 24.7 MPa, which is 56% loading of the compressive strength of concrete. Hence the effective load incurred to the aggregates will be much larger on the 7^{th} day as compared to the 3^{rd} day and hence there is occurrence of some elastic deformation in the concrete. Still this strain is within the elastic regime and hence there is no plastic strain occurrence at this stage.

Load = 60% of the compressive strength, enhanced load frequency.
To analyse the occurrence of axial strain per loading cycles for all the different loading levels, analysis of Incremental strain and cumulative strain has been performed. Figure 5.15, 5.16, 5.17 shows the cumulative and Incremental strain analysis for the aforementioned loading at the age of 7 days. The figures are very similar with the strain analysis in the case of load =56% of compressive at the age of 7 day loading. The maximum cumulative strain incurred is 0.08 mm (fig 5.17) in contrast to the maximum cumulative strain of 0.065 mm achieved in the case of loading = 56% of the compressive strength of concrete (figure 5.13. Also the maximum Incremental strain occurred increased about 0.005 to 0.0078 by increasing the loading from 56% to 60% loading.

Also, it can be visualised that the first few load cycles generates a higher axial strain as compared to the later load cycles. In the case of 56% loading 5.13 , it can be visualised that similar amount of strain occurs in all the load cycles in contrast to the case of loading =60% of the compressive strength.

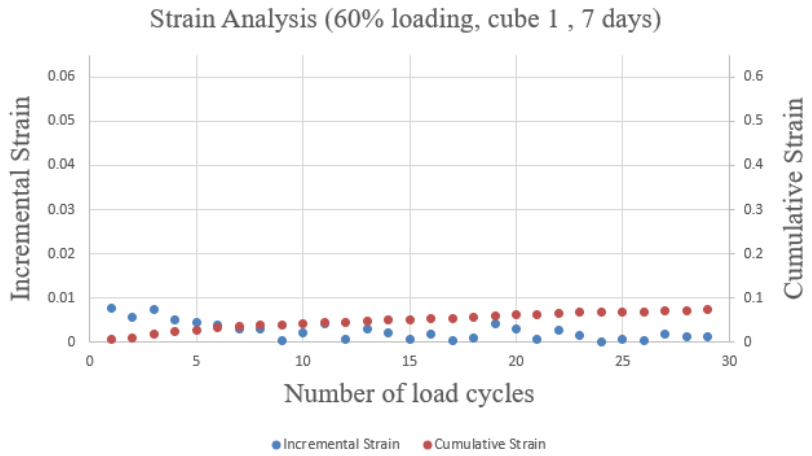

Figure 5.15: Strain analysis (60 percent load, cube 1)

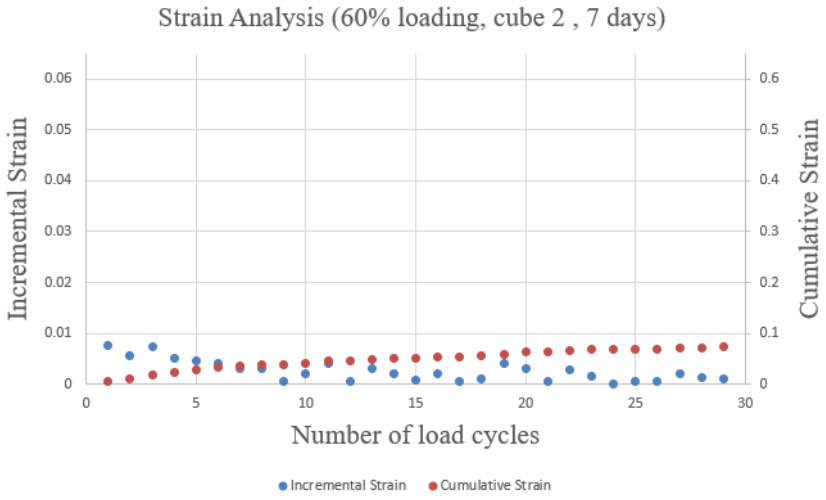

Figure 5.16: Strain analysis (60 percent load, cube 2)

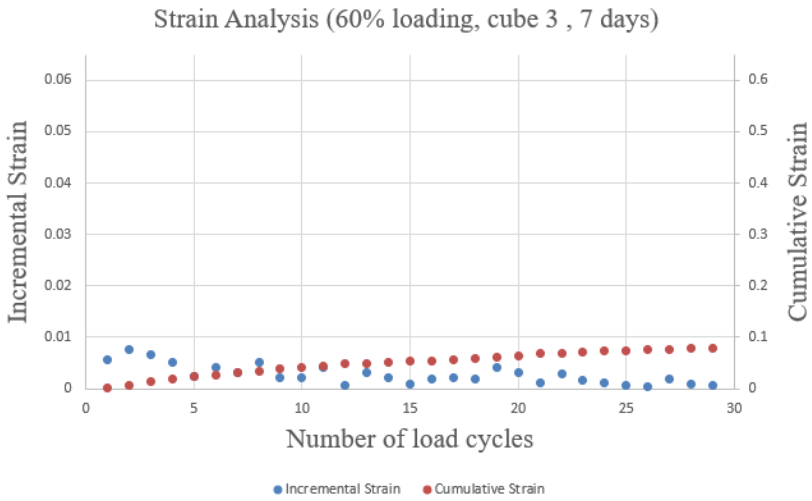

Figure 5.17: Strain analysis (60 percent load, cube 3)

Load = 65% of the compressive strength, enhanced load frequency.
It was observed that there is nonlinear increase in the Incremental Strain when the loading level increased from 56% load to 65% load. Also a stable increase, as expected, can be visualised in the cumulative strain. It is interesting to visualise from the figure 5.18 that the Incremental strain accumulated in the first 7 load cycles is equivalent to the strain caused from rest all other cycles combined.
The maximum Incremental strain incurred for 65% loading is 0.018 as compared 0.0075 achieved in the case of 60% loading. Also the cumulative strain incurred to an average of 0.1 which was almost 2 folds as compared to the cumulative strain incurred in the case of 56% loading.

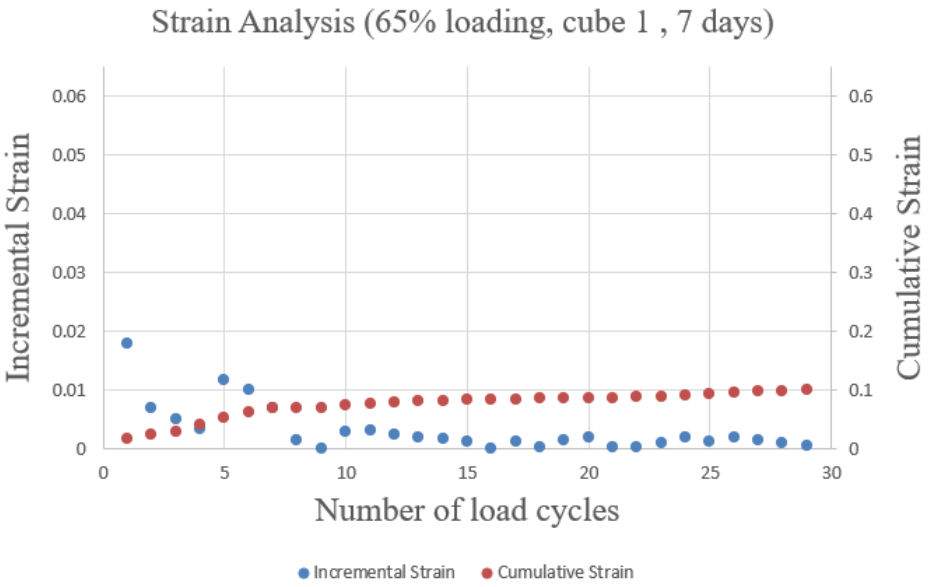

Figure 5.18: Strain analysis (65 percent load, cube 1)

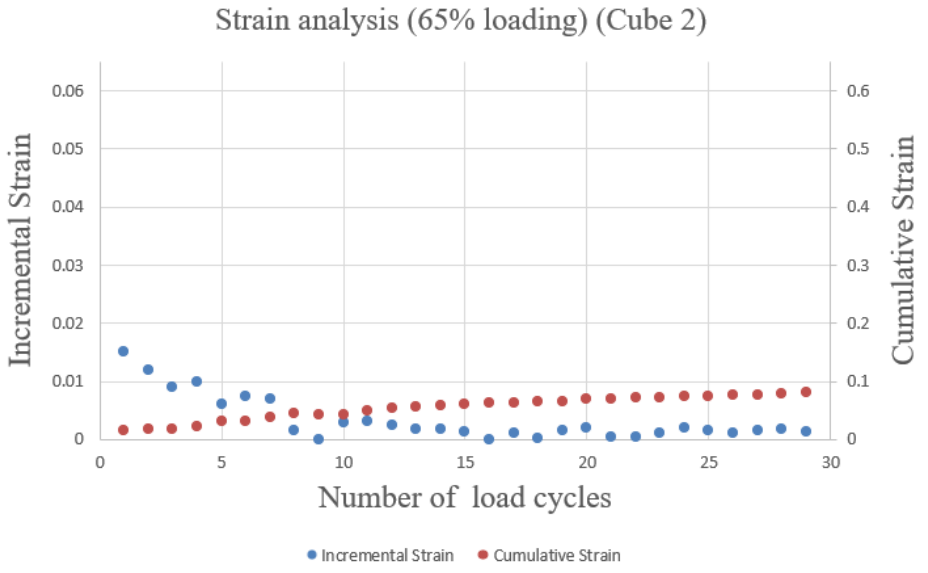

Figure 5.19: Strain analysis (65 percent load, cube 2)

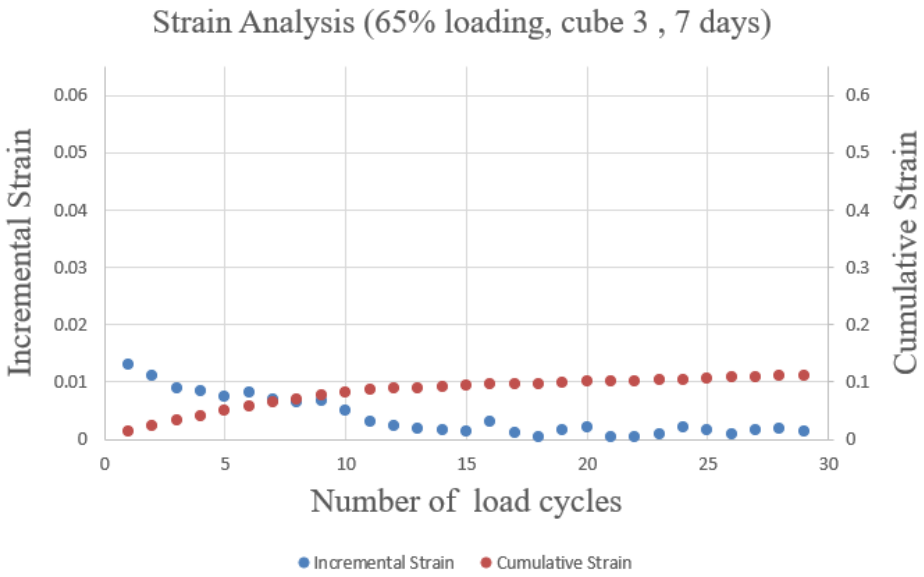

Figure 5.20: Strain analysis (65 percent load, cube 3)

Load = 70% of the compressive strength, enhanced load frequency.
It can be visualised from the figure 5.21,5.22,5.23 that the Incremental strain increases enormously as the loading level increases. The Incremental strain caused by this loading level is almost 10 folds as the Incremental strain caused in the case of 56% loading case.Also it is more evident that strain incurred to concrete is much more in the first few cycles is very large as compared to the strain occurrence in the later cycles. Also some variation is seen in the Incremental strain between the cubes of this same loading level. This can be attributed to the heterogeneous nature of the concrete.

The cumulative strain increases very rapidly as the loading level increases. By increasing the load level from 60 to 65%, the cumulative strain increased to about an average of 20% in contrast to about 57% increase from 65% to 70% of the load level. The maximum cumulative strain achieved is 0.3 which is strain where the concrete usually is in the cracked phase.

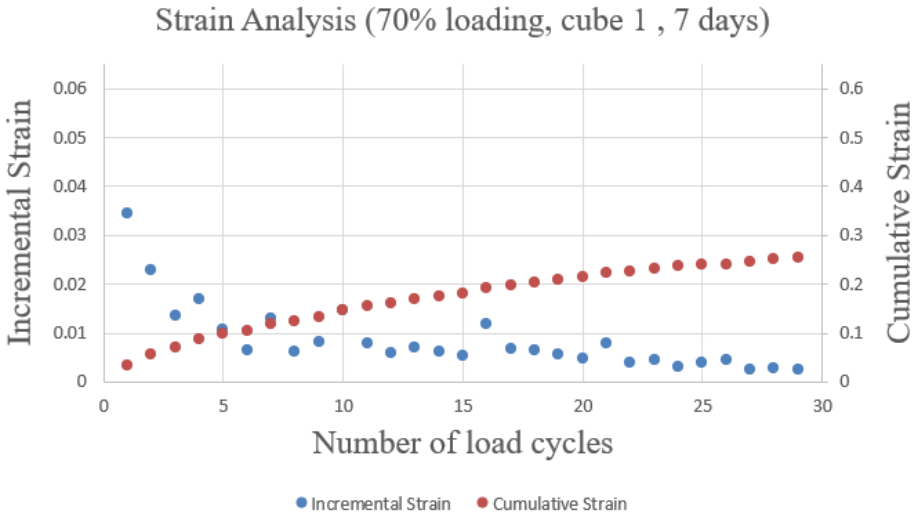

Figure 5.21: Strain analysis (70 percent load, cube 1)

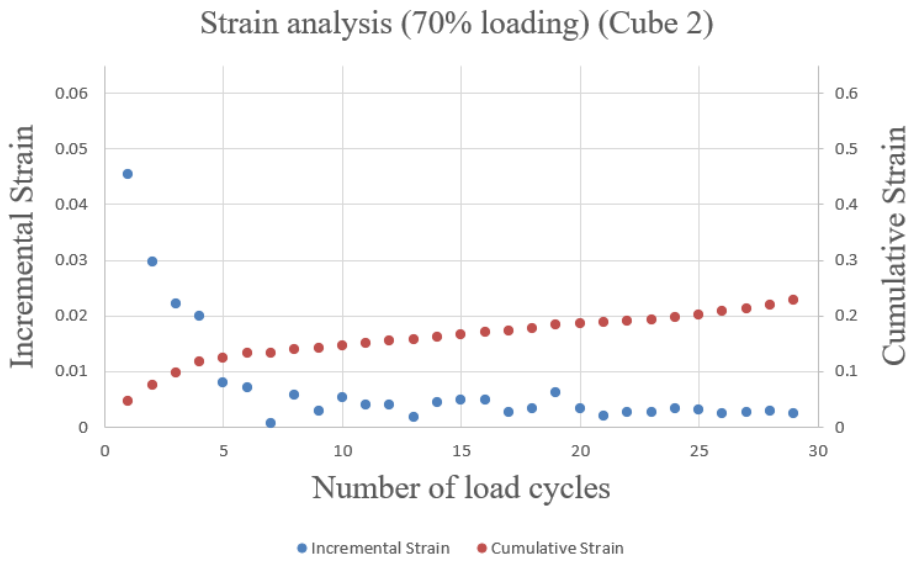

Figure 5.22: Strain analysis (70 percent load, cube 2)

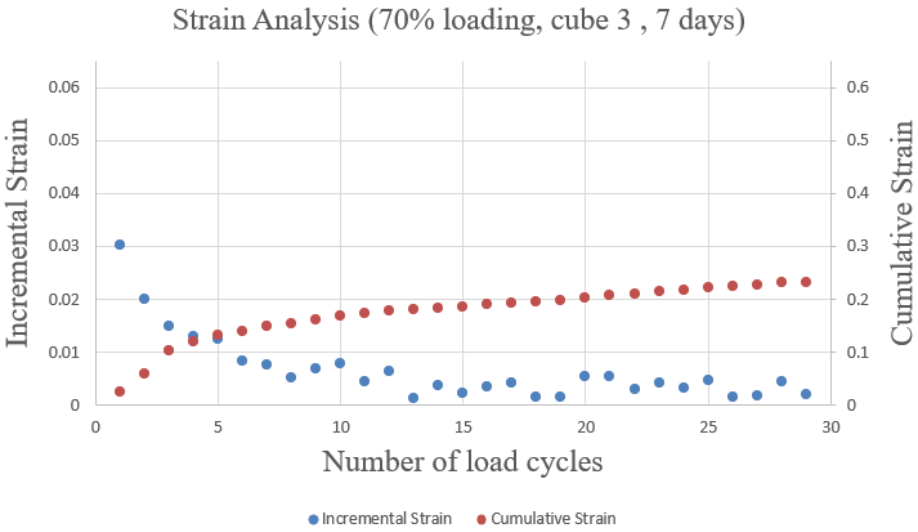

Figure 5.23: Strain analysis (70 percent load, cube 3)

It was also verified from the visual inspection that after the application of 30 load cycles, visual cracks were observed on the concrete cubes. Hence it is proved that at this loading level, achieved average cumulative strain of 0.25 causes cracking in concrete and reduction in the mechanical properties which will be discussed in the later section.

Also the average Incremental strain 0.05 was observed which is about 10 times the strain achieved in the case of 56% loading. This shows the extend of damage occurrence in the first few load cycles. It was also observed that with the increase in cyclic loading level, logarithmic increase in both cumulative strain and Incremental strain is observed.

Load = 75% of the compressive strength, enhanced load frequency.
Cyclic loading level has been further enhanced to see the variation in the crack width and it's effect on the mechanical properties of the concrete. Hence the loading level has been increased to 75% of the compressive strength of concrete. The incremental strain that is incurred to the concrete in just 1 st cycle is equal to the net cumulative strain achieved by the concrete cube in the case of 56% loading

case. It demonstrates the increase in extent of the damage with the increase in the cyclic load level. The visible cracks were observed at the end of 10 load cycles.

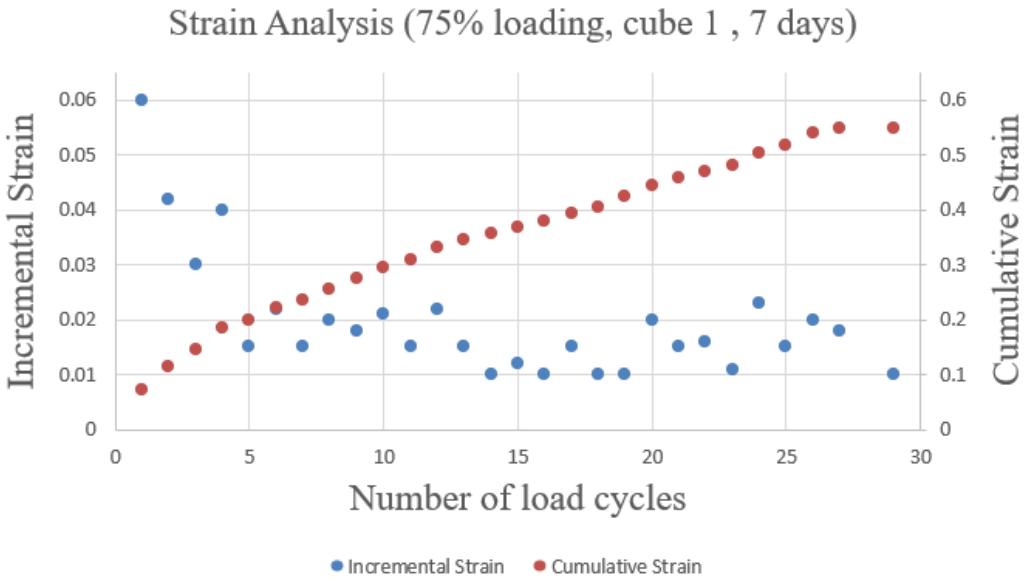

Figure 5.24: Strain analysis (75 percent load, cube 1)

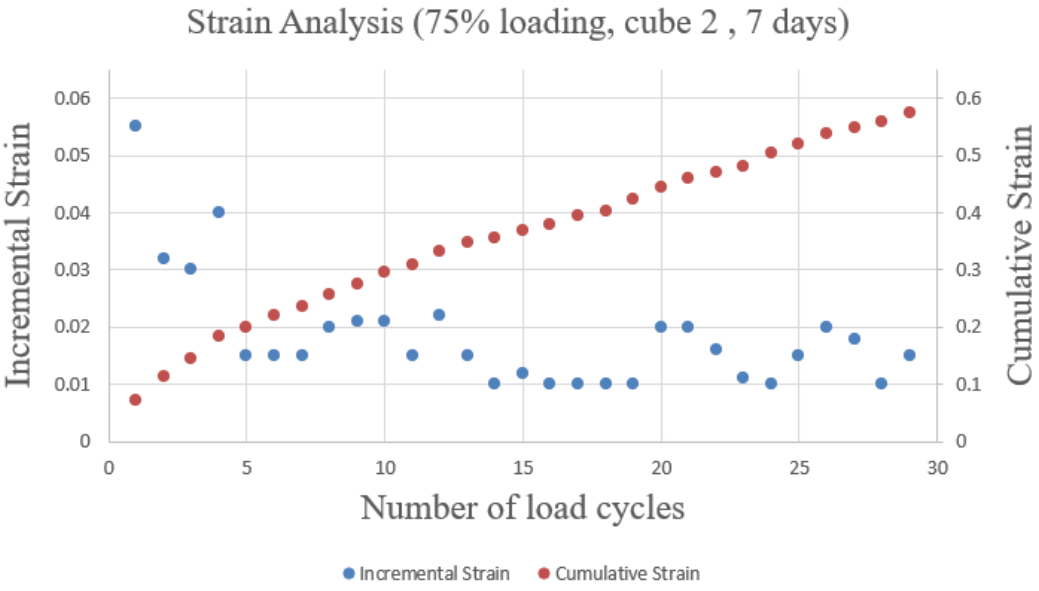

Figure 5.25: Strain analysis (75 percent load, cube 2)

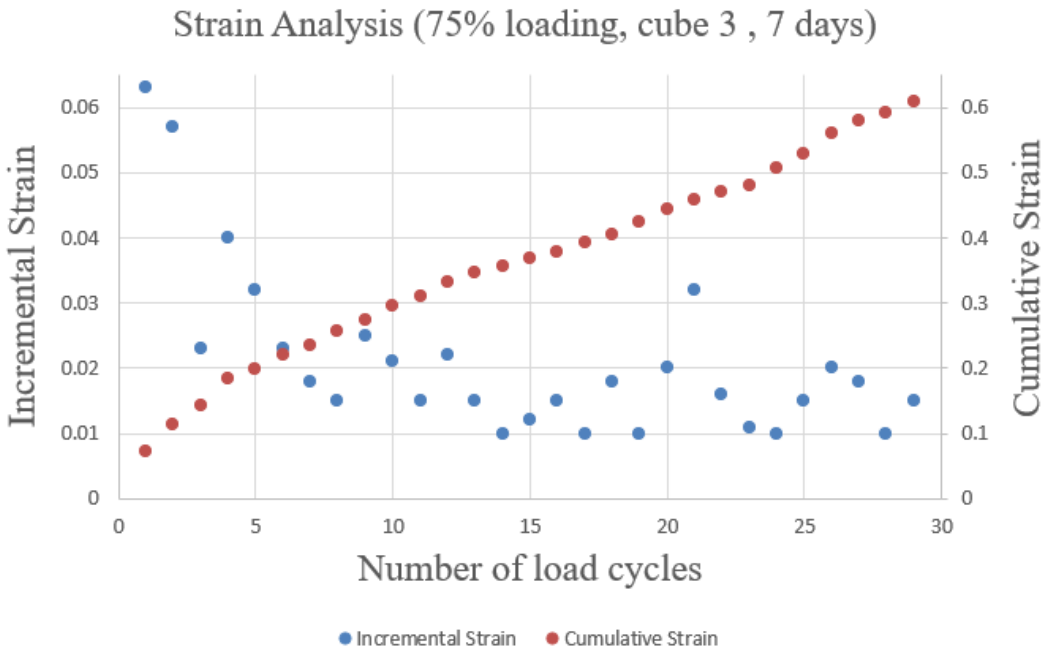

Figure 5.26: Strain analysis (75 percent load, cube 3)

It can be visualised from the figure 5.24 ,5.25,5.26 that for the case of Incremental strain increases enormously as the loading level increases. The Incremental strain caused by this loading level is almost 10 folds as the Incremental strain caused in the case of 56% loading case.Also it is more evident that strain incurred to concrete is much more in the first few cycles is very large as compared to the strain occurrence in the later cycles.

Also much high variation in the cumulative as well as the Incremental strain is observed. At this loading level, the concrete is in the cracked phase. it really depends on how the internal micro cracks develop and propagate inside a particular concrete cube under this loading level. If the cracks are connected, then that could cause much high axial strain as compared to when the cracks are not connected. Hence the variation in the axial strain is observed among the cubes loaded at the same loading level. This phenomenon can be attributed to the heterogeneous nature of concrete cubes. Under this loading level, visible micro-cracks are observed under the less than 10 load cycles.

5.1.3. Comparison and Discussion on Strain analysis for cyclic loading

A full cycle of the stress–strain response is consisted of two distinct paths: unloading path and reloading path. The unloading path is curvilinear characterized by a progressively diminishing slope, until it intersects the strain axis. The reloading path is almost linear that starts from the strain axis and intersects the envelope curve. The nonlinearity is seen when the curve exceeds the previous envelope unloading strain, and becomes more apparent as accessing to the envelope curve.

Significant degradation in elastic stiffness with increasing loading level can be observed for some of the the presented cyclic stress–strain curves. Till the 65% loading case, The initial unloading path is almost vertical with an abrupt stress drop for a small strain increment, however, at the 70% and 75% loading level, when accessing to the strain axis, the curvature of the unloading path turns larger. For the reloading path, remarkable deterioration in concrete strength can be observed in comparison with the envelope unloading stress at the same unloading strain, which is caused by crack propagation and damage accumulation. It is evident from the curves presented that plastic strain or irreversible strain occurs for the 70% and 75% loading case as it physical surface cracks were verified by visual inspection.

Figure 5.27 demonstrates the plot for incremental strain occurrence for the first load cycle. As it was determined from the stress analysis of concrete cubes that maximum axial strain is incurred during the application of first load cycles. Hence a data of of incurred incremental strain has been plotted in the figure 5.27. All the loading level are demonstrated in a single plot. Average values of Incremental Strain for 3 cubes has been computed for all the loading level. It can be seen that incremental strain incurred is 0.0043, 0.0069, 0.0153, 0.035, 0.059 for the loading levels 56%, 60%, 65%, 70% and 75% loading respectively. It is interesting to observe that incremental strain increases almost 10 folds when loading level is increased from 56% to 70%. Almost 68% increase in the incremental strain was observed when loading was increased from 70% to 75%.

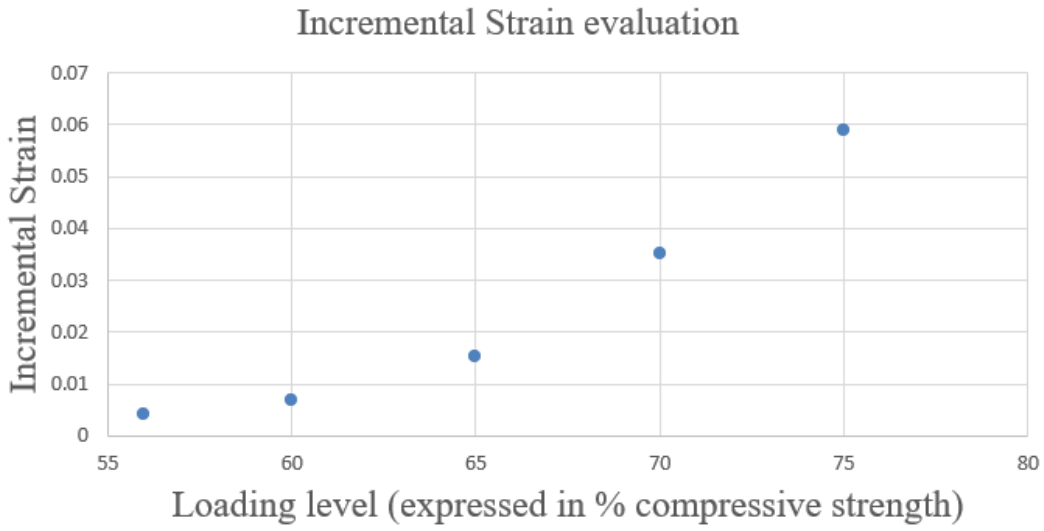

Figure 5.27: Incremental Strain occurrence for first load cycle

Based on the strain analysis, it was observed that maximum axial strain occurrence is in the first few load cycles. Hence the damage phase in cyclic loading can be divided into 2 phases which is discussed below.

Sharp damage increasing stage (initial load cycles)

At this stage, the concrete specimen reaches the maximum density, the micro cracks start to propagate and the damage initially increases, which induces a decrease in the elastic stiffness of concrete. After a certain loading level, in our case load = 65% of compressive strength of concrete, the damage evolves quickly in the form of alike a power function, with unstable propagation of the cracks. The reduction in

elastic stiffness of concrete is the faster. At this stage, the cracks inside the concrete specimens propagate promptly, with the crack width turning larger, which damages the instinct mechanical properties of concrete significantly.

Stable Damage Phase
After the application of first few loading cycle, the major damage almost has been evolved completely as can be visualised from the figure 5.21. The cyclic stress–strain curve is stable. At this stage, only the main macro cracks of concrete specimen propagate slowly. Hence it can be suggested that maximum damage occurs in the first few load cycles. In the case of 56%, 60% loading the difference in incremental strain for first 5 load cycles is less than 10% as compared to incremental strain incurred due to rest load cycles. Hence a clear distinction between the damage phases couldn't be made.

In the loading cases greater than 60% of the compressive strength, a clear distinction between the damage phases is observed.In case of 65% loading, the difference between the incremental strain caused due to first loading cycle and the maximum strain incurred from 10 to 30 load cycles is 83%. Difference of 87% and 61% was observed in the case of 70% and 75% loading. The reasoning that the decrease in difference was observed in the case of 75% loading is due to the fact that the load cycles in the range of 10-30 also causes higher incremental strain which causes more damage to the concrete cubes in terms of cracking.

Hence the performed load levels have been divided into 3 categories based on the strain analysis: loading = 56% and 60% has been divided into the un-cracked zones, loading = 65% could be a loading level which might instigate the micro cracking inside the concrete, loading = 70% and 75% has been divided into the cracked concrete phase. The verification of the results have been performed through the CC factor analysis, by computation of the mechanical properties and by visual inspection.

5.1.4. Influence of cyclic loading on CC factor analysis for concrete

In order to predict the moment or load cycle which causes change in the structural medium in terms of occurrence of micro cracking inside the concrete cubes, CODA wave interferometry analysis is used. The sensors are attached through the holders to the concrete surface and the waves are recorded. This can be visualised from the figure 5.28. As mentioned before, 2 readings have been recorded, one at the start of the cycle and one at the end of the cycle. After each load cycle, the real time CC value has been computed by stretching and comparing the signal from previous load cycle.

Figure 5.28: Attached sensors through the holders to the concrete cube

Computation of average CC factor

- After importing the binary signal into MATLAB, streching analysis has been performed.
- As mentioned 2 readings have been recorded, at ascend and descend of each loading cycle.
- Real time CC factor was computed by stretching the wave from adjacent previous load cycle with the current loading cycle.
- It is possible to get a plot of CC factor from the MATLAB for all the time windows. But it is important to covert a CC factor plot into average number. - Also the ϵ plot was visualised and for the time windows with stable ϵ values, the average CC factor was computed. The variation in stable ϵ values seemed to be varying for each loading case.
- The part of the CC factor plot, with stable ϵ time windows, was trimmed and saved as a new plot and from the option of 'data statistics' the mean value of CC factor was computed.

CC factor analysis for 56% loading, original loading frequency

CC factors were analyzed at the ascend and descend of each cycle. CC factor value of 0.7 has been kept as a threshold value to detect any changes in structural medium inside the concrete. CC factors calculated by stretching technique, uses the wave from the adjacent previous load cycle and through stretching and comparing with the wave of next adjacent load cycle, computes the CC factor. The computation of Epsilon values has been done. The CC factors are computed by averaging when the Epsilon values are stable at certain time windows. The wave and the time windows that has been recorded to compute the CC values are shown in the figure below.

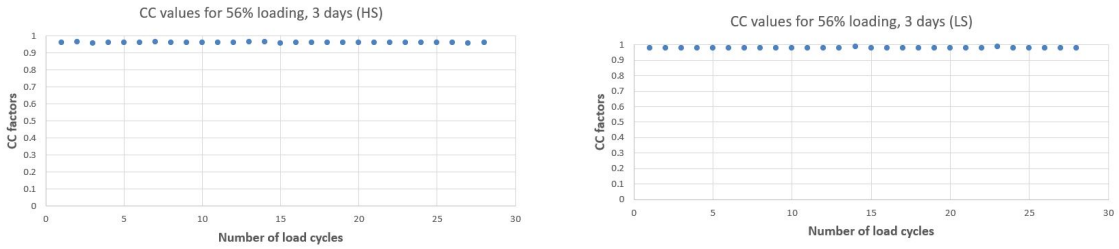

(a) **(b)**

Figure 5.29: Co-relationship Coefficient for 56 percent load. (a) HS values. (b) LS values.

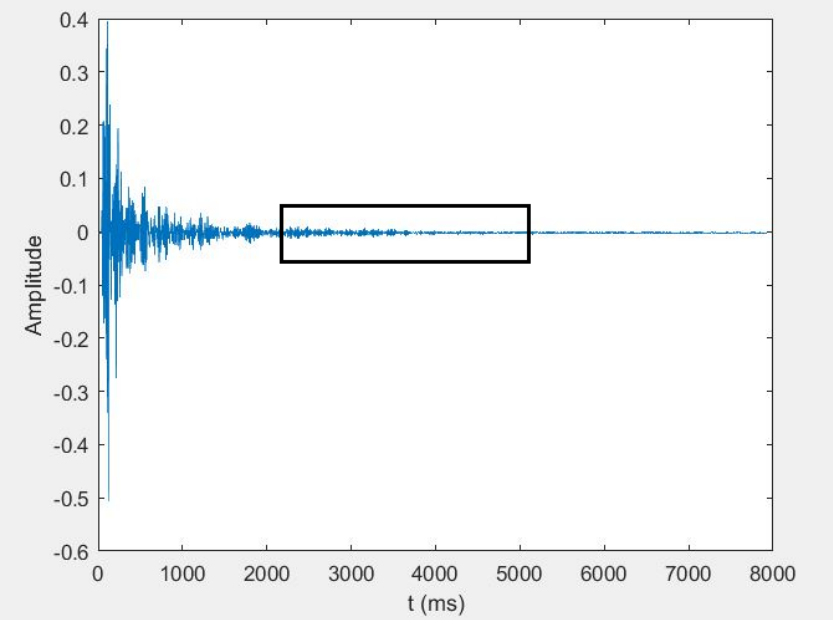

Figure 5.30: Recorded wave for the CC factor analysis of HS for cube 1.

The boxed area as can been seen from the figure 5.30 represents the part of the wave that has been selected calculated from the 0.8 ms correlation windows shown over a single waveform. At this part of the wave, the stable Epsilon values were observed. Average of all the CC values have been taken during this time window to calculate the net CC value. Each blue dot in the figure 5.29 demonstrates the CC factor computed for that particular load cycle. It was to be determined when the computed CC factor for any given load cycle should be less than 0.7, then it would demonstrate some change in the structural medium in the concrete cube.

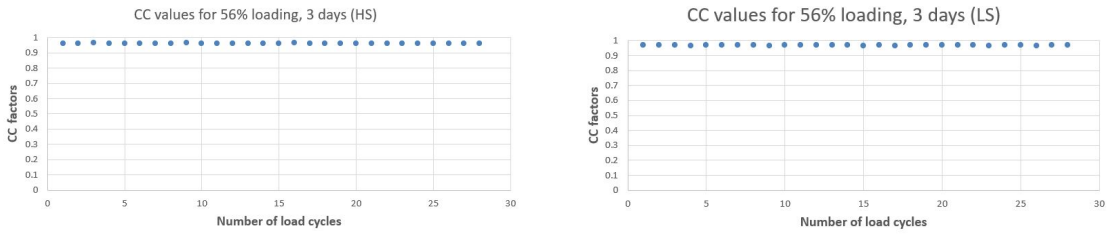

(a) **(b)**

Figure 5.31: Co-relationship Coefficient for 56 percent load. (a) HS values. (b) LS values.

It was observed by the computation for CC factor as can be seen from the figure 5.29, 5.31 that the computed CC factors were greater than 0.94. There was very little variation that was observed in the computed CC factors.The maximum variation of 0.4% was observed among the CC factors which is considered as minimal.Hence under this loading level, there was no variation in the CC factor was observed which could indicate cracking inside concrete cube. In this particular case, the Epsilon value was not found stable from particularly 55 ms till 80 ms time windows. So those time windows were avoided to compute the CC factors. Similar to this case, the amplitude of the wave decreases due to diminishing strength of the signal and hence the computed CC factors are very low at the very late time windows as can be seen from the figure 5.37. Those time windows should be avoided to compute the CC factors.

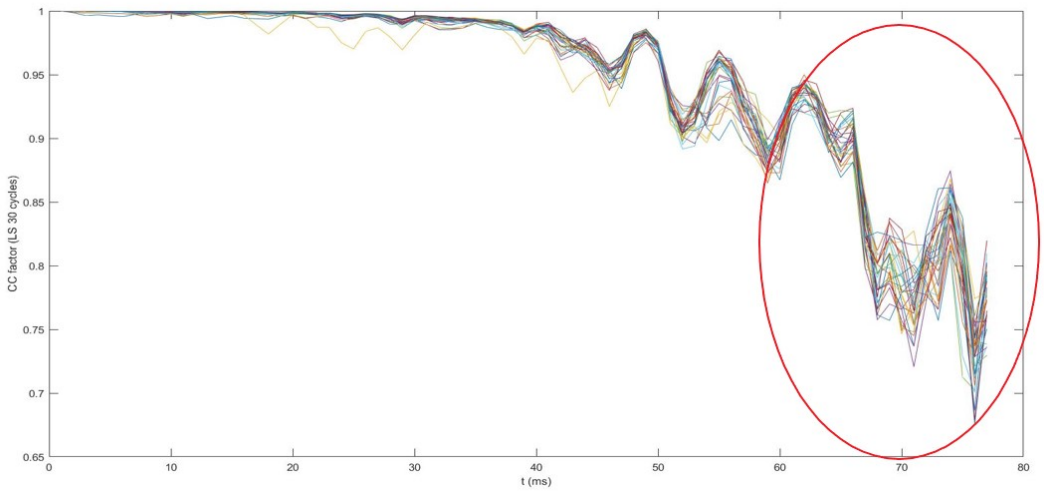

Figure 5.32: Weaker signal for later time windows

CC factor analysis for 56% loading, enhanced loading frequency

To analyse if change in loading frequency affects the internal micro-structure of concrete and if it is possible to analyse with CWI, the loading frequency has been increased to 13.5KN/s and 30 load cycles are applied to 3 concrete cubes. CWI analysis has been performed on 2 of the concrete cubes. Figure 5.33 represents the computed CC factor for the aforementioned loading and figure 5.34 represents the boxed section of the wave used to compute the CC factors.

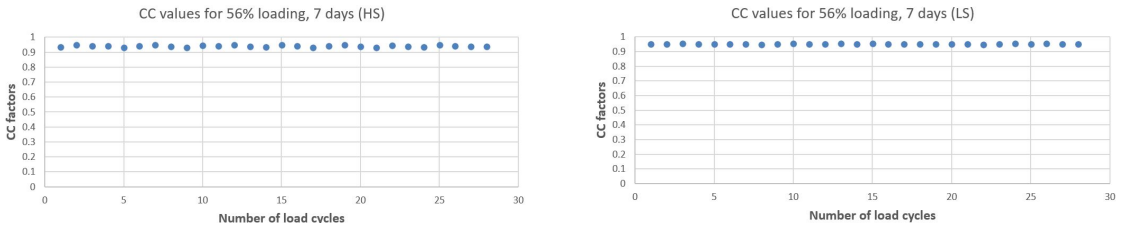

(a) **(b)**

Figure 5.33: Co-relationship Coefficient for 56 percent load,enhanced loading. (a) HS values. (b) LS values.

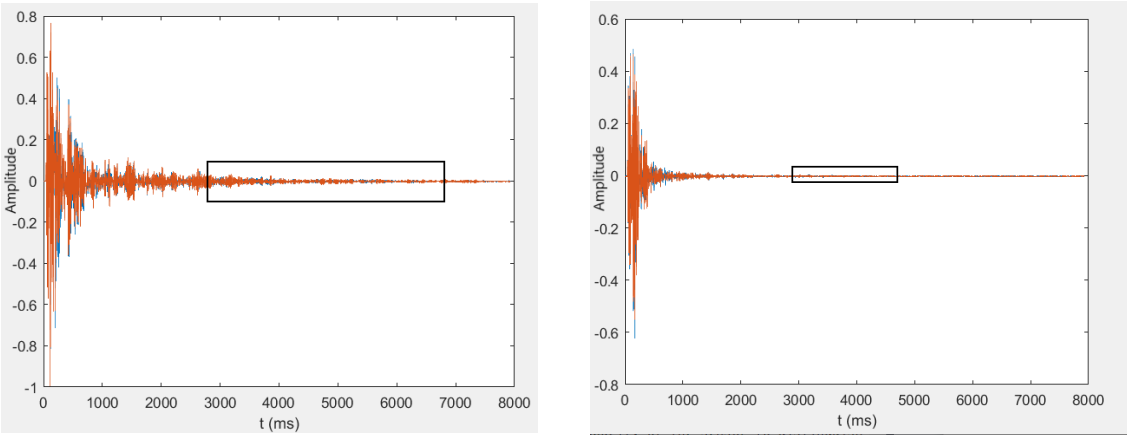

(a) **(b)**

Figure 5.34: Recorded wave for 56% load to compute the CC factors (a) Higher Stress (b)Lower Stress.

The maximum CC factor recorded in the computation was 0.97 and minimum CC factor recorded was 0.93 for the first concrete cube. The little variation in CC factors could be attributed to the noise associated with the loading. Hence it could be proved that no major changes to the micro structure of concrete has been accrued due to the application of 30 load cycles. The calculated Standard deviation observed 0.08.

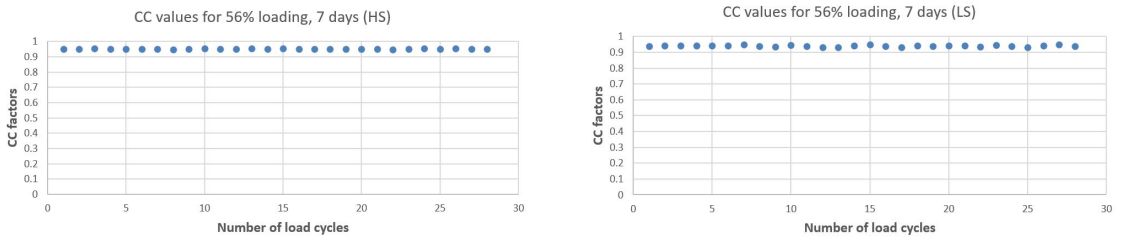

(a) **(b)**

Figure 5.35: Co-relationship Coefficient for 56 percent load,enhanced loading. (a) HS values. (b) LS values.

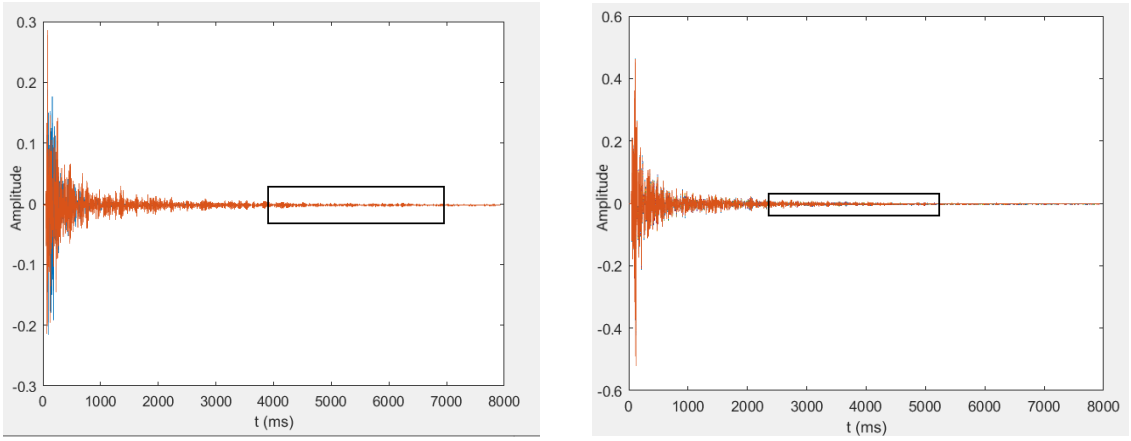

(a) (b)

Figure 5.36: Recorded wave for 56% load to compute the CC factors (a) Higher Stress (b)Lower Stress.

Figure 5.35represents the computed CC factor for the aforementioned loading and figure 5.36represents the boxed section of the wave used to compute the CC factors. The maximum CC factor recorded in the computation was 0.96 and minimum CC factor recorded was 0.945 for the first concrete cube. Hence no variation in CC factors for the second cube were also observed which could indicate some change in the structural medium in terms of micro cracking inside concrete.

CC factor analysis for 60% loading, enhanced loading frequency

The CC factor analysis has been performed for load =60% of the compressive strength of concrete for 30 load cycles.

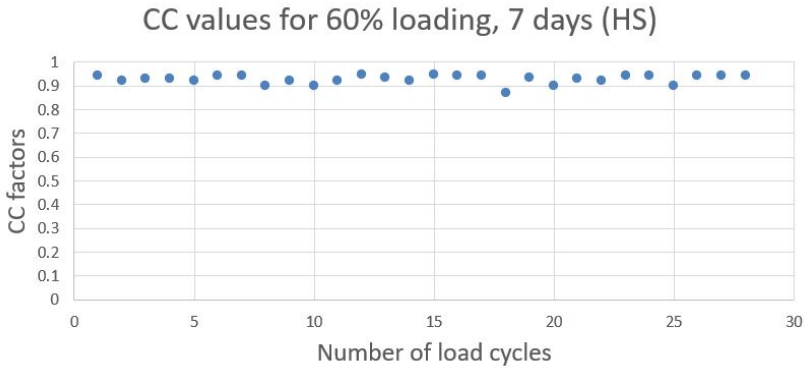

Figure 5.37: Co-relationship Coefficient for 60 percent load,enhanced loading HS values

From the analysis of loading level for 60% load, it was computed that the computed CC factor was greater than 0.88. The maximum recorded CC factor value is 0.95. The standard deviation observed in this case was about 0.01. This standard deviation was larger as compared to previous loading case. But no huge variation in CC factor analysis was seen which can indicate damage inside the concrete cube.

CC factor analysis for 65% loading, enhanced loading frequency

The loading level has been further increased to 65% of the compressive strength in order to get an indication from CC factor analysis about micro cracking inside the concrete. 2 cubes were cyclically loaded with aforementioned loading and the CC factors were recorded for 30 load cycles. Figures 5.38 and 5.40, represents the computed CC factors for 65% loading. It can be seen from the figure 5.38b that for the analysis of first cube, the computed CC factor for the first load cycle is 0.68 in the first load cycle. This value is below the threshold of 0.7 indicating change in structural medium inside concrete.

But interestingly, the recorded CC factor for the higher stress scenario was computed was 0.787. This is because of the difference in the recorded wave forms in the case of Higher and lower Stress analysis.

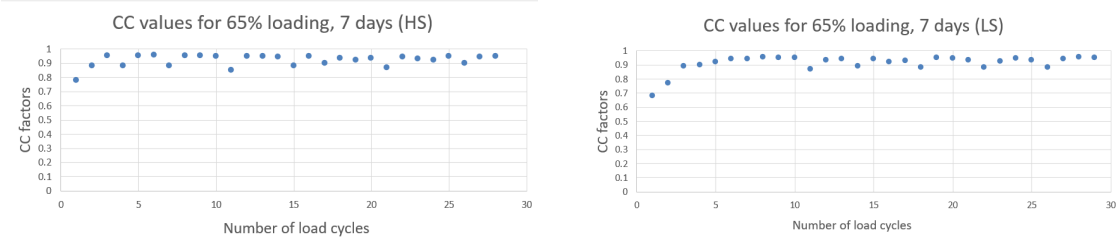

(a) **(b)**

Figure 5.38: Co-relationship Coefficient for 65 percent load,enhanced loading. (a) HS values. (b) LS values.

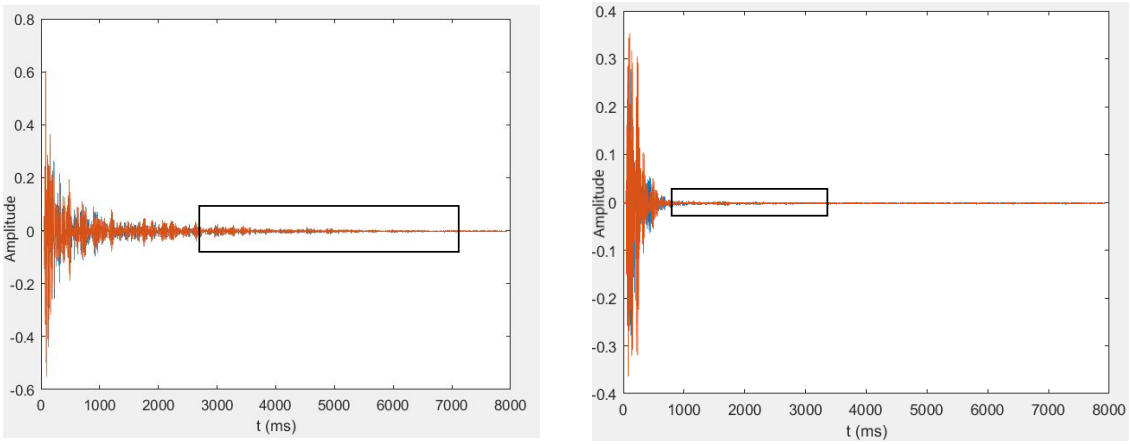

(a) **(b)**

Figure 5.39: Recorded wave for 65% load to compute the CC factors (a) Higher Stress (b)Lower Stress

As mentioned, in figure 5.39, boxed portion represents the recorded wave for the computation of CC factors in the case of 65% loading. It was always observed that Higher Stress analysis resulted into higher amplitude of wave even for the later time windows. This actually gives higher range of window selection to compute the CC factor and hence is more accurate analysis. In case of Lower Stress analysis, as discussed, the amplitude of the wave dies in the late time windows and hence those windows cannot be used to compute the CC factor.

For the analysis of second concrete cube, all the CC factor values were recorded greater than 0.85 as can be seen from the figure 5.40. It is possible that the first cyclically loaded concrete cube might have some imperfections during casting process causing some change in the internal micro structure and hence the recorded value of the CC factor was low.

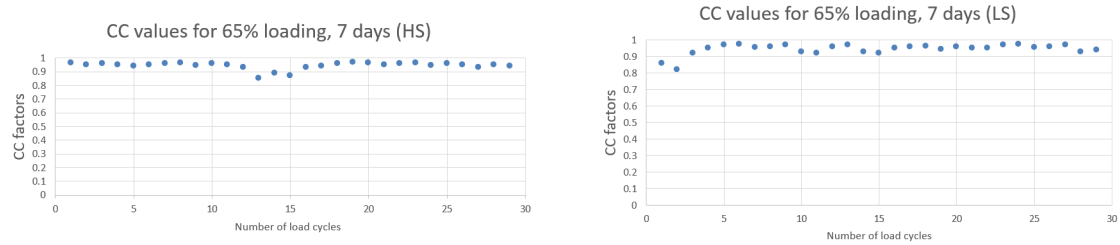

(a) **(b)**

Figure 5.40: Co-relationship Coefficient for 65 percent load,enhanced loading. (a) HS values. (b) LS values.

An interesting observation was the standard deviation incurred among the CC factors for 30 load cycles. The standard deviation recorded between the CC factor values was 0.05, 5 times than 60% loading case. It is understood that as the loading level increases, the noise associated with the loading also increases and hence the standard deviation in computed CC factors can be attributed to the noise associated with the loading and it is also based on the capacity of the sensor to distinguish between the CODA wave and the noise.

CC factor analysis for 70% loading, enhanced loading frequency

It was clear from the Hysteresis curve analysis that under the influence of this loading level, the concrete cube undergoes some plastic deformation and some difference in the mechanical strength of concrete was observed which will be discussed in the later section. At the end of 30 load cycles, surface cracks were observed on the face of concrete cubes. To check the influence of this loading level on CC factor analysis, 2 cubes were cyclically loaded to record and analyse the CODA wave. Analysis of one of the concrete cube was presented in the results section.

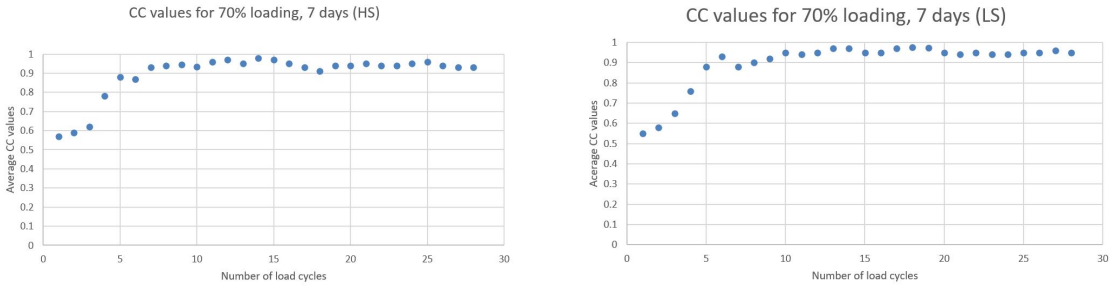

(a) **(b)**

Figure 5.41: Co-relationship Coefficient for 70 percent load,enhanced loading. (a) HS values. (b) LS values.

Figure 5.41 demonstrates the recorded CC factors in the case of 70% loading. It can be observed that the maximum CC factor that was recorded was 0.97 in 14th load cycle in contrast to the lowest CC factor of 0.58 as can be seen from the figure 5.41a. Figure 5.42a and figure 5.42b represents the recorded wave for Higher Stress and Lower Stress analysis respectively. A very high standard deviation of 0.07 was observed in the recorded CC factors. It can be clearly observed that for the first 3 load cycles, the CC factor is lesser than 0.7 and hence those load cycles surely indicate the initiation of micro-cracking inside concrete. It can be observed that after the 4th loading cycle the recorded CC factors are above 0.9, indicating no further damage caused to the further loading cycles.

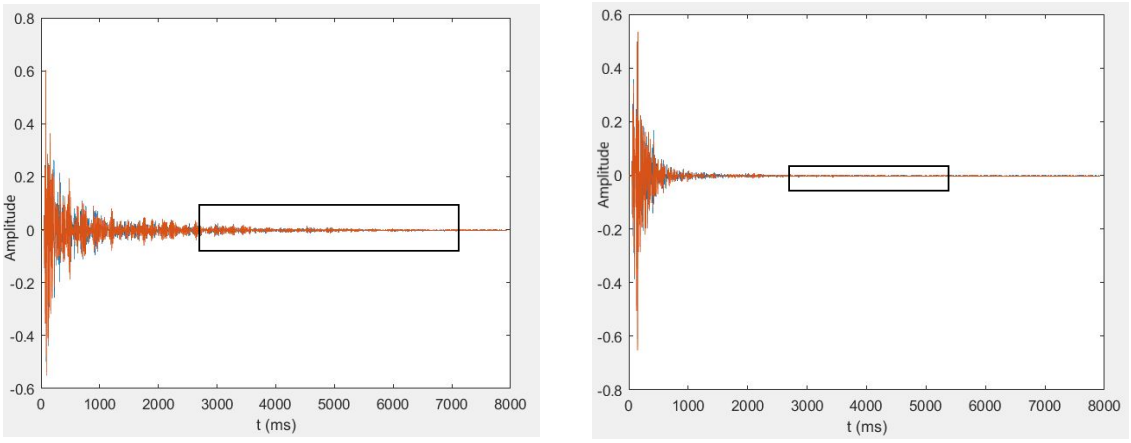

(a) **(b)**

Figure 5.42: Recorded wave for the CC factor analysis of HS and LS for 70% loading.

The reduction in the CC factor can be explained through the axial strain analysis. It can be visualised from the figure 5.21, 5.22, 5.23 that the Incremental strain incurred in the first 3 load cycles is very high as compared to rest all other load cycles. It was also computed through strain analysis that the incremental strain occurrence in first 10 cycles is 83% higher than in the last 20 load cycles. Hence this reduction in CC factor is justified by the increasing incremental strain in first 3 load cycles.

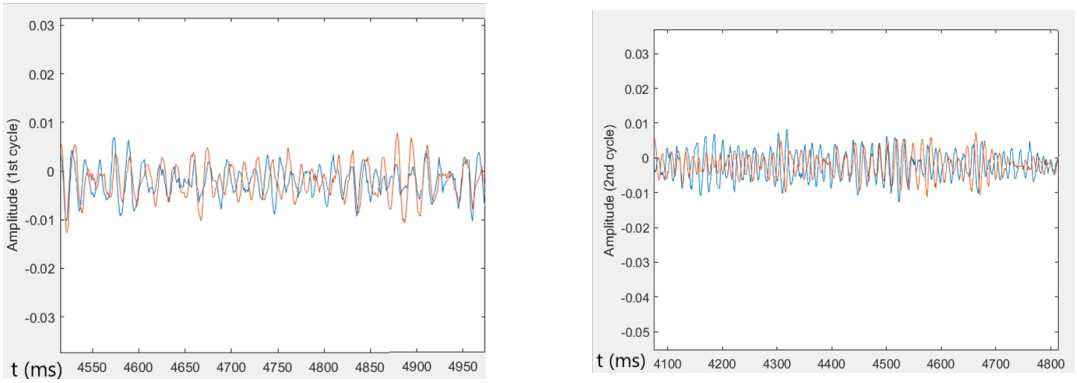

(a) (b)

Figure 5.43: Stretched Wave analysis (a)1st load cycle (b)2nd load cycle.

Figure 5.43 and figure 5.44 shows the stretched wave analysis for first 4 load cycles. In order to visualise the effect of lower CC factors on the stretched wave, a particular late time window was selected and the stretched wave was observed for the first 4 load cycles. It can be seen that when the CC factor is less than 0.7, in the first 3 load cycles, there was very high non-homogeneity among the stretched wave as compared to the preceding recorded wave. But it can also be visualised that as CC factor increases to greater than 0.78, 2 signals almost overlap each other. Hence it can be clearly visualised that non homogeneous nature of waves in the first 3 load cycles caused a reduction in CC factor indicating micro cracking inside concrete cube.

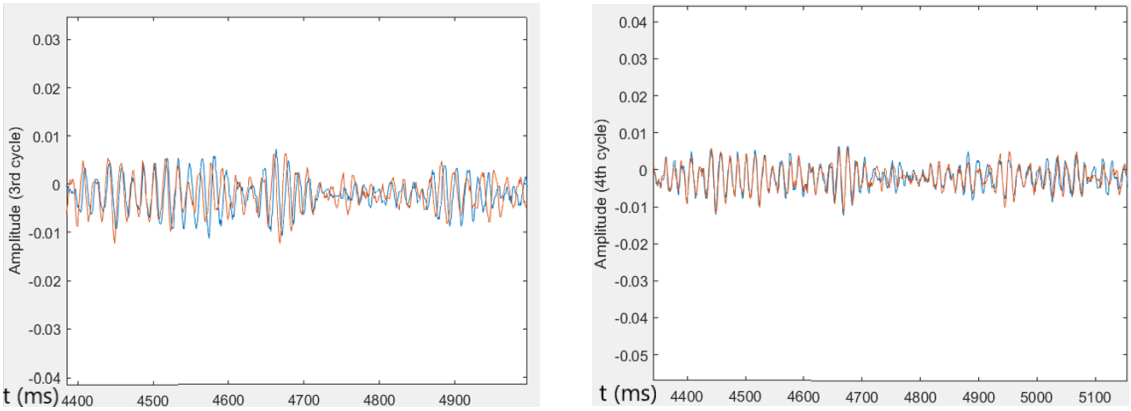

(a) (b)

Figure 5.44: Stretched Wave analysis (a)3^{rd} load cycle (b)4th load cycle.

CC factor analysis for 75% loading, enhanced loading frequency

In order to investigate the effect of further cracking on CC factor analysis, the loading level has been enhanced to 75% of the compressive strength of concrete. 30 load cycles were applied to 3 concrete cubes but the CODA wave recording was performed on one of the concrete cubes. Only 'Higher Stress' values were recorded to compute the CC factor for 30 load cycles. Figure 5.45 shows the CC factor analysis for aforementioned loading case.

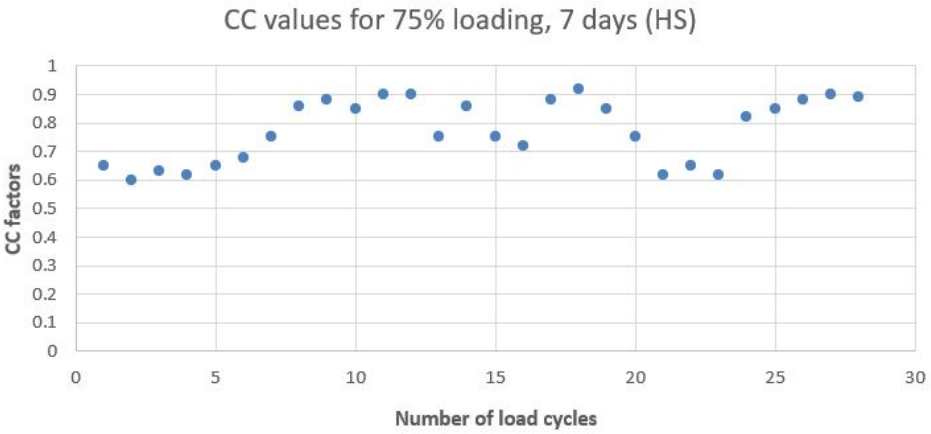

Figure 5.45: Co-relationship Coefficient for 75 percent load, HS value

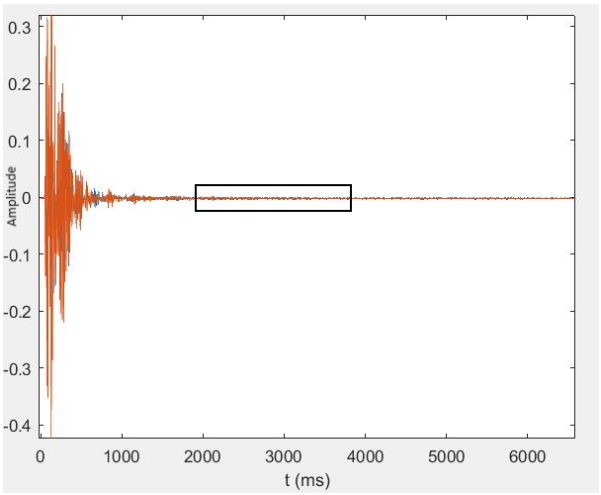

Figure 5.46: Recorded wave to compute the CC factors

Figure 5.46 shows the recorded wave to compute the CC factors. It can be observed that the amplitude of the wave reduces enormously at the late time windows and hence that part of the wave was not used to compute the CC factors. It was observed that the Very high variation among the CC factors was observed for the load cycles as compared to previous loading cases. The maximum CC factor that was computed was 0.9224 for 18th load cycle in contrast with the lowest CC factor 0.6 achieved for the 3^{rd} load cycle. Hence about 34.9% variation was observed in the in overall CC factors for all the load cycles.

As discussed, concrete is in the cracked phase under this loading level. It was deduced from the Axial Strain analysis section that the maximum damage caused to the concrete cube was incurred through the first few load cycles. Also the CC factor analysis corroborate with the axial strain analysis results. As it can be observed from the figure 5.45, for the first 6 load cycles, the value of CC factor is less than

0.7. Hence it can be concluded that major micro-cracks would have formed during first 6 cycles under this loading level.

It can also be observed from the figure 5.45, from the 21-24 load cycles, the recorded CC factor value was less than 0.7. The phenomenon can be seen from load cycle 17 till load cycle 21. A very high reduction and variation of CC factor from 0.9 to 0.6 was observed between those load cycles. This reduction in the CC factor can be justified by the increase in the incremental strain during those load cycles. As it can be seen from the figure 5.26, there was 28% increase in the Incremental strain from 20^{th} load cycle to 21^{st} load cycle. Hence also reduced CC factor was recorded during range of that load cycles. It is also possible that progressive propagation of damage in terms of micro cracks occurs during that particular load cycles. It can also be concluded that due to very high variation in the computed CC factors,as contrast to the case for lower loading levels, each loading cycle causes some change in the structural medium in terms of micro cracking in concrete cube. Hence high variation in CC factors could also be an indicator of structural damage in concrete.

Discussion and recommendations on CC factor analysis
As it can be observed from the figure 5.46 and in some other cases for recording of the wave that the amplitude of the wave reduces a lot in the later part of time windows which in turn gives lower CC values for late time windows. This phenomenon can be observed in the figure 5.37. This issue can be resolved by embedding sensors inside the concrete. Embedded smart aggregates perform best compared to the smart aggregates attached by using acoustic gel. Embedded sensors provide near-perfect coupling with the medium, while gel-attached sensors may be displaced during the course of its service time. While first-arrival assessment is not heavily affected, CWI is definitely affected.

The reduction in the CC factors can be directly linked to the increase in the axial strain caused due to the cyclic loading. It was derived from the axial strain analysis that the damage phases in concrete can be divided into 'Sharp damage increasing phase' and 'Stable Damage phase'. The recorded CC factors less than 0.7 in the case of 70% loading, as can be seen from the figure 5.41, can be directly linked to the axial strain analysis performed in the case of 70% loading (fig.5.22). It can be visualised that average incremental strain occurrence in the first 3 load cycles is equal to 4.71 times the average incremental train occurrence for rest other load cycles. Similarly, in the case of 75% loading, CC factors, less than 0.7 was recorded for first 6 load cycles. As it can be seen from the figure 5.26, there was 28% increase in the Incremental strain from 20^{th} load cycle to 21^{st} load cycle. During those load cycles, it is possible that new micro cracks would have propagated in concrete cube and hence the recorded CC factor was less than 0.7 during those load cycles as can be seen from the figure 5.45.

It was observed in the case of 70% and 75% loading case, variety of surface cracks were observed. As it can be seen from the figure 5.41 and 5.45 that for some load cycles very high CC factor values were observed. Also it was observed that even after major crack has occurred, some next few load cycles have higher correlation coefficients greater than 0.85 were observed. Once the cracks are formed there would be progressive damage in terms of crack opening inside concrete due to the cyclic loading. Cracks will create new interfaces which will change the way the signals propagate, altering their wave-forms. It could be the case that CC factor analysis is more susceptible to the moment of first cracking as compared to the crack propagation inside concrete.

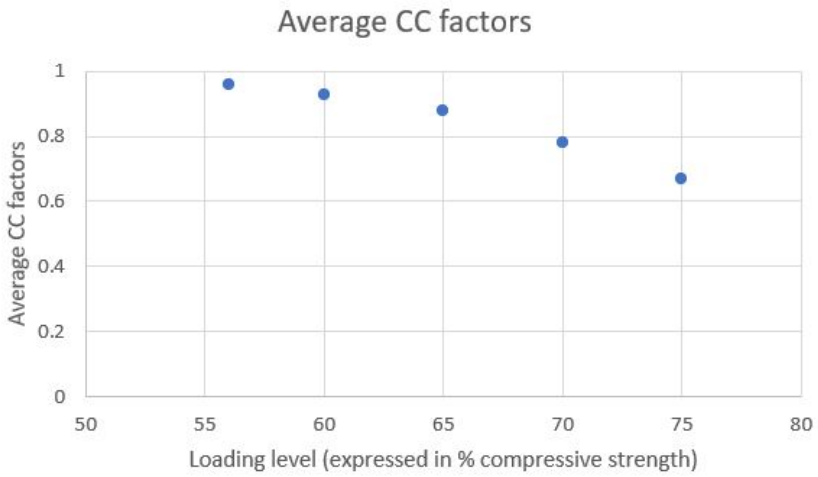

Figure 5.47: Reduction observed in CC factor computation with increasing loading

The reduction in mean CC values with the increasing loading level for all the loading cases has been presented in the figure 5.47. As it can be seen from the figure 5.47, the mean CC value for first 10 load cycles has been calculated for all loading cycles. First 10 load cycles has been selected because very high variation was recorded in the CC factors during first 10 load cycles. The average of 'HS' and 'LS' has been taken and for the loading =75%, average of 'HS' has been computed. The average CC value recorded was 0.96, 0.925, 0.88, 0.779, 0.672 for 56%, 60%, 65%, 70% and 75% of the loading respectively. 19% and 30% reduction in the mean CC value was observed in the case of 70% and 75% loading with respect to 56% loading.

Generally some standard deviation in CC factors could be attributed to the laboratory conditions, variation in temperature, noise associated with loading and exact loading at which the waves are recorded as CC factors are very susceptible to change under a very small variation in aforementioned factors. But all the experiments performed were under the same conditions. Hence it can be attributed that cracking formed will create new interfaces which will change the way the signals propagate, altering their wave forms and hence very high reduction was seen in the recorded CC factor values.

Also from the literature, the occurrence of cycle skipping phenomenon has been studied. While stretching the signal, it is possible that the algorithm miss-picked the wrong epsilon value due to waveform change between recordings, resulting in higher correlation coefficient for an epsilon value which is away from actual epsilon value. This will result in abnormal relative wavespeed change values when compared to other windows of the same signal pair.

In order to investigate the influence of cycle skipping phenomenon in our case, the wave speed change is observed for the time windows which have values which greatly differs from the values in the other windows. But such phenomenon was not observed in the recorded signals. But it is important to realise about such phenomenon as faulty CC values could be computed because of cycle skipping.

5.1.5. Wave Speed analysis

In order to investigate and have indication of damage in concrete, wave speed analysis for various loading level has been performed. In order to comment whether CC factor analysis or wave speed analysis a better indicator of damage assessment in concrete, the computed CC factors shall be compared with the reduction in the wave speed for different load cases. Figure 5.48 shows the plot for the % wave speed reduction for loading = 56% of the compressive strength of concrete. The data presented in the plot consists of higher stress as well as lower stress analysis for 30 load cycles on two concrete cubes.

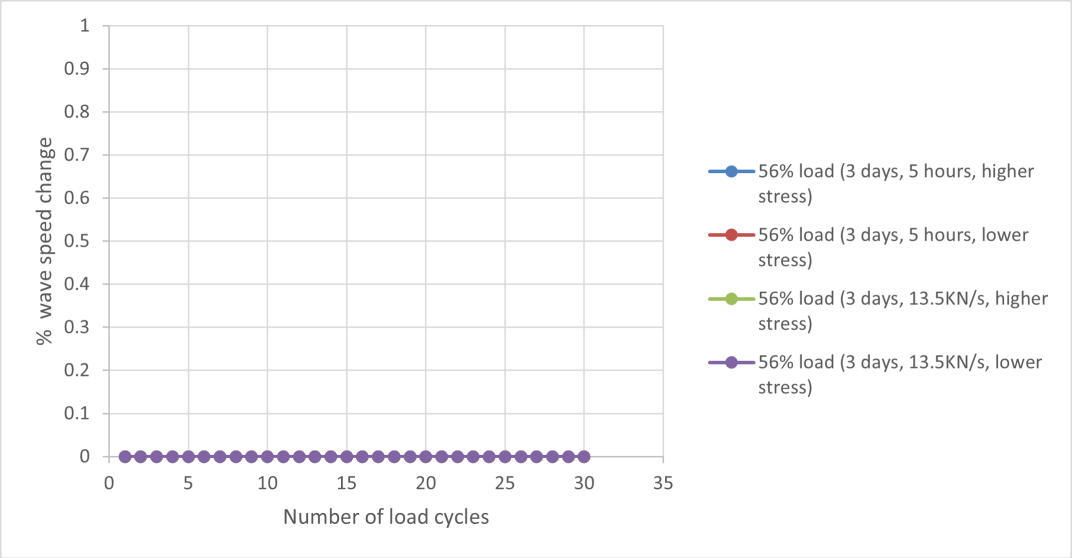

Figure 5.48: Wave speed analysis for 56 percent loading

It can be visualised from the figure 5.48 that there was no reduction in the wave speed that was observed in the course of 30 load cycles. This result was also validated from CC factor analysis as it can be seen in the figure 5.29, 5.31 that very high CC factors were recorded at this particular loading level. A very little variation was also seen among this CC factors. For the higher stress as well as lower stress analysis, wave speed of 4096 m/s was recorded before the start of the first loading cycle and through out 30 load cycles, there was no reduction in the wave speed observed. Hence by this analysis, the result that 56% loading does not cause any damage in concrete is validated.

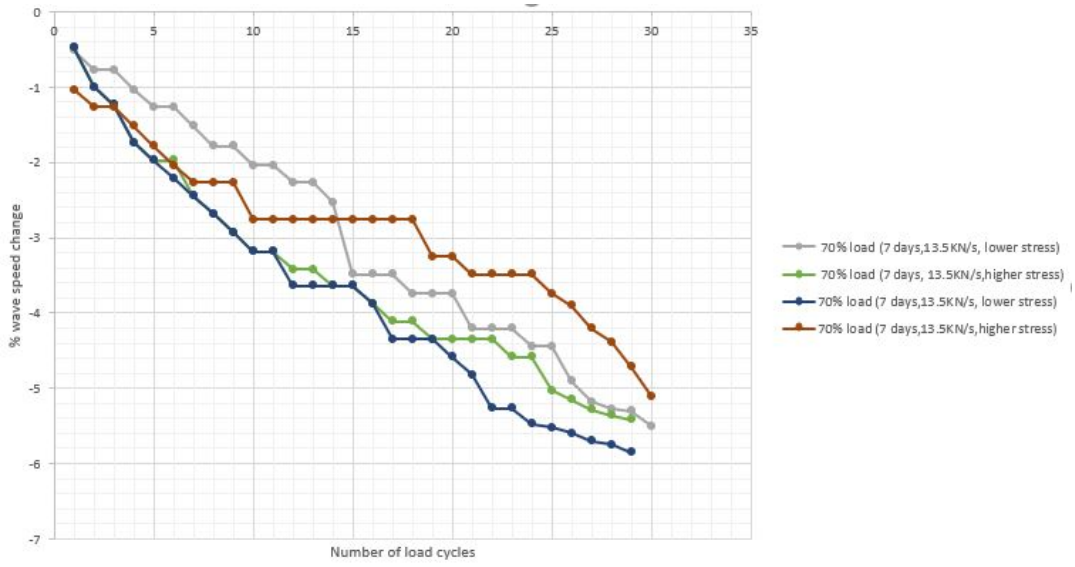

Figure 5.49: Wave speed analysis for 70 percent loading

Figure 5.49 represents wave speed analysis in the case of loading =70% of the compressive strength of concrete. Similarly as in the case of 56% loading, wave speed analysis was performed on 2 concrete cubes. The initial wave speed recorded for 1st cube was 3896 m/s. It can be observed through both the higher and lower stress recording that there was average reduction of 0.7% in the wave speed after the application of 1st load cycle. Hence wave speed analysis gives an indication of micro cracking through the cyclic loading.

The net reduction of about 6% was seen in the wave speed analysis after the application of 30 load cycles. As discussed in previous sections, under this loading level (load =70%) concrete is in cracked state after 30 load cycles have been applied. The reduction in compressive strength of the concrete will be discussed in the next section. Hence 6% reduction in the wave speed is a good indicator of damage in macro scale. For sure, if there is 6% reduction of wave speed than concrete is damaged to such an extent that mechanical properties of concrete will be affected.

When compared with the CC factor analysis, as can be seen from the figure 5.41, first 3 load cycles shows really low CC factors less than 0.7. But it can be observed after 3 load cycles, the CC factor increases and it exceeds 0.8. Hence through the CC factor analysis, it gives an indication that first 3 load cycles has caused some damage in concrete. But as micro cracks once formed, they would propagate through the crack opening under the same cyclic load level. But CC factor analysis fails to indicate the progressive damage propagation in concrete. In contrast to that, a stable decrease in the wave speed is observed which indicates damage propagation phase in concrete cube.

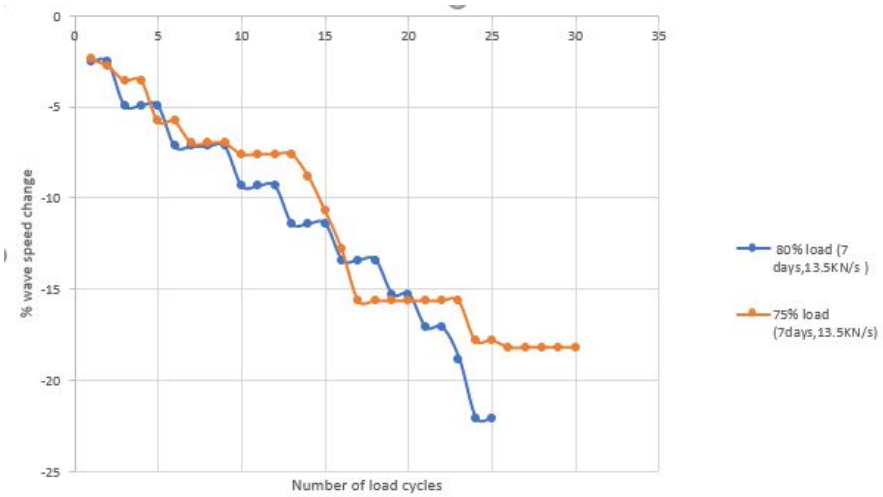

Figure 5.50: Wave speed analysis for 75,80 percent loading

Figure 5.50 demonstrates the wave speed reduction in case of loading = 75% and 80% of the compressive strength of the concrete. In the case of 80% loading only 25 loading cycles applied as very big micro cracks were observed during the initial load cycles. It is to be realised that under this loading level, concrete is already in the cracked state and hence very reduction of about 17% and 22% respectively in wave speed was observed. When compared with the CC factor analysis, as can be seen from the figure 5.45 that there was very high variation in CC factor was seen between the load cycles of 15-22. Also 21, 22 and 23 load cycles recorded CC factors less than 0.7. But as can be seen from the figure 5.50, from load cycle 16-23, no reduction in wave speed was observed.

Hence it can be concluded that the CC factor computation is more sensitive to the moment of cracking rather damage propagation in concrete. Constant reduction in wave speed in case of 70% loading indicating progressive failure in contrast to the higher CC values calculated for the very high CC values for late loading cycles. Hence it is also concluded that wave speed reduction is a good indicator to indicate progressive failure in concrete.

5.2. Influence of cyclic loading on mechanical properties assessment of concrete

To assess the the effect of cyclic loading on early age concrete, the cyclically loaded cubes will placed in the compressive testing machine to check the Compressive Strength.In the case of 56% loaded concrete cubes, with the original load frequency, only 2 concrete cubes with aforementioned loading level were loaded with 30 load cycles. This was because of the time required to perform the cyclic loading procedure. But for rest all other loading levels, cyclic loading process is performed on 3 cubes and average of strength values have been recorded.

5.2.1. Evaluation of compressive strength for concrete subjected to cyclic loading at 3 days age

To investigate the effect of cyclic loading with the load level = 56% of the compressive strength of concrete, 2 concrete cubes were cyclically loaded. Hence after the application of 30 load cycles, the mechanical properties of the concrete are assessed in terms of Compressive Strength of concrete. The concrete compressive strength of 3 unloaded cubes has been computed and then compared with the cyclically loaded samples. For the unloaded samples the average compressive strength achieved is about 33.78 MPa for 3 concrete cubes. For the cyclically loaded two concrete cubes, the compressive strength achieved was 33.615 MPa. A little reduction in the strength can be attributed to heterogeneity in concrete and fact that there is some standard deviation involved with compressive strength computation.

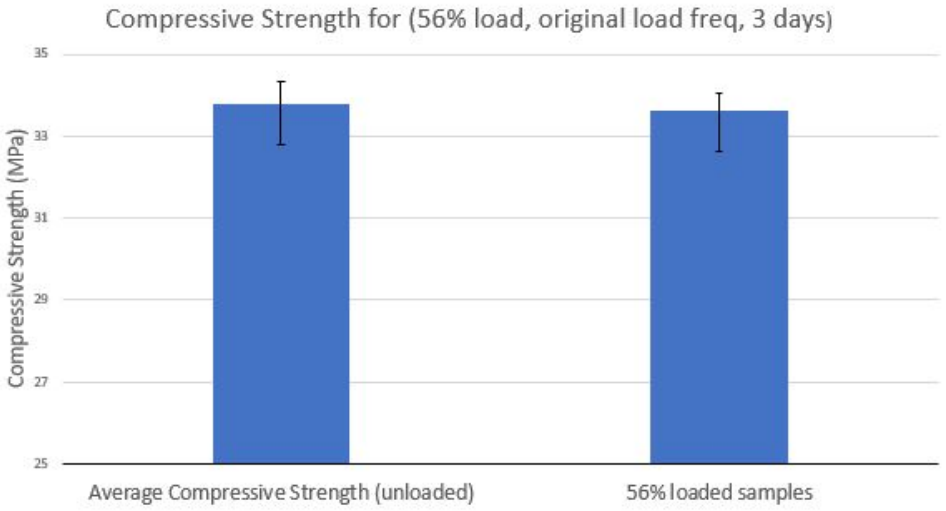

Figure 5.51: Evaluation of Mechanical properties

Hence through the CC factor analysis and comparison of compressive strength for the loaded and unloaded samples, it can be deduced that there is no reduction in mechanical properties of concrete subjected to load =56% of the compressive strength of concrete for 30 load cycles. In order to have reduction in the mechanical properties of concrete, initiation of fracture in the non linear phase should occur during the cyclic loading. As there is no slip or plastic deformation as can be seen from the figure 5.4, it can be concluded that because of the this loading, there is no initiation of micro-cracking inside the concrete which in turn causes reduction in the mechanical properties in concrete.

Visual inspection of the cube has been performed to check the concrete cubes surface. There were no surface cracks that were visualised after the visual inspection. The cube surface is presented in the figures 5.52, 5.53, 5.54.

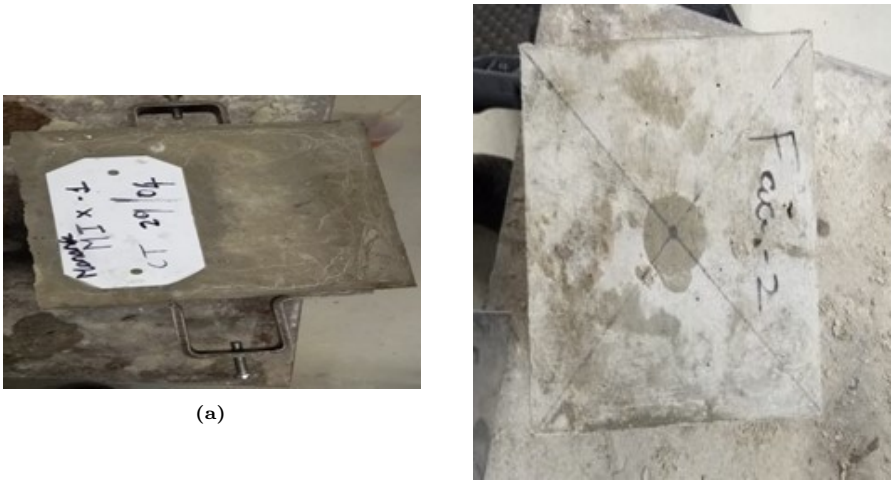

(a) **(b)**

Figure 5.52: Visual inspection of cube after cyclic loading with load level of 56% for 30 load cycles on 3^{rd} day age. (a) Face 1. (b) Face 2.

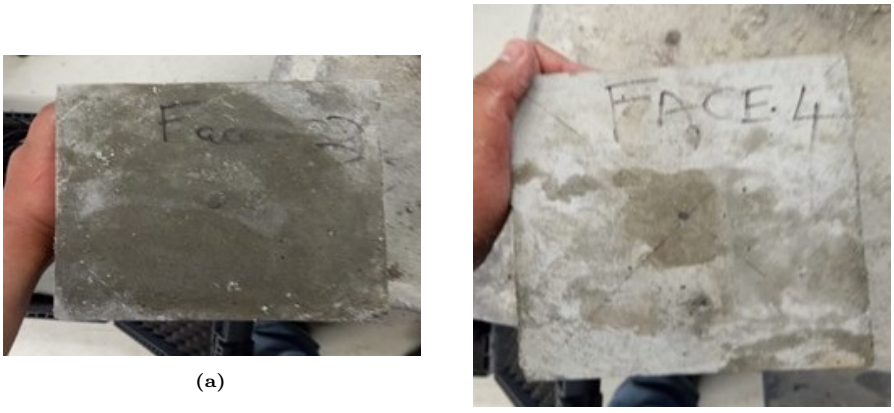

(a) **(b)**

Figure 5.53: Visual inspection of cube after cyclic loading with load level of 56% for 30 load cycles on 3^{rd} day age. (a) Face 3. (b) Face 4.

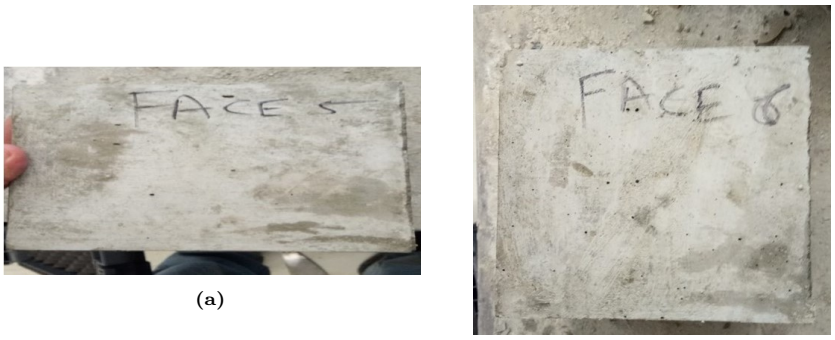

(a) **(b)**

Figure 5.54: Visual inspection of cube after cyclic loading with load level of 56% for 30 load cycles on 3^{rd} day age. (a) Face 5. (b) Face 6.

5.2.2. Assessment of the compressive strength for enhanced loading levels

To investigate the effect of cyclic loading with enhanced load level, from each casting, 3 cubes were cyclically loaded with varying load levels. The load level were increased from 56% till 75% of the compressive strength and the compressive strength has been checked.The average Compressive Strength as can be seen from the figure 5.55 has been computed by averaging all the values of different casting for all the loading levels. The Standard deviation has been taken into account by adding all the variance for the values of casting.

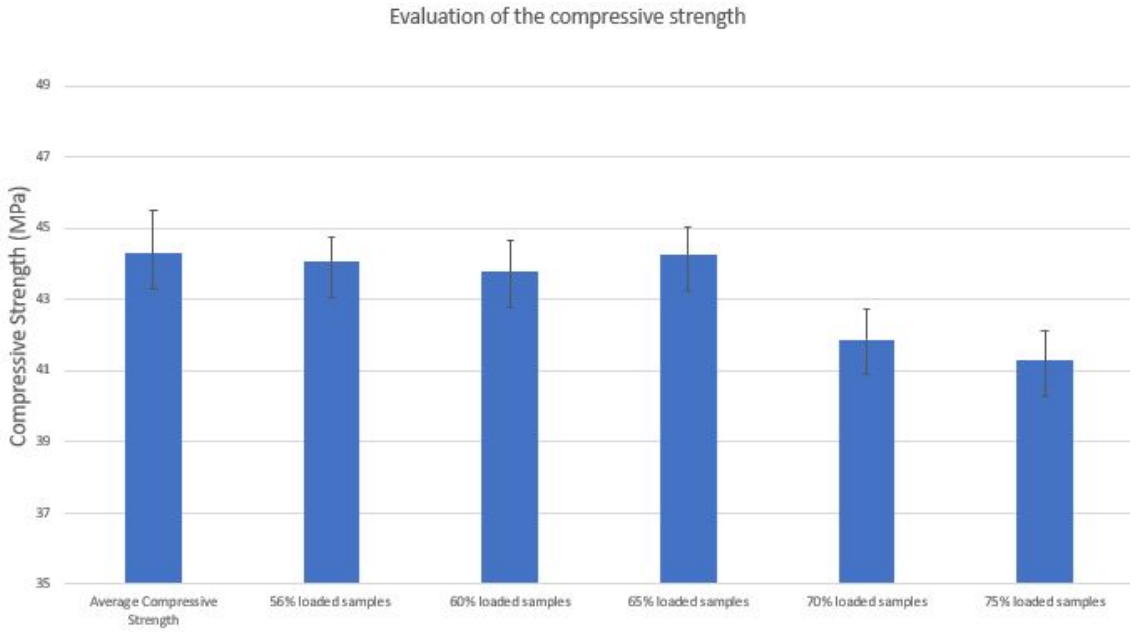

Figure 5.55: Evaluation of Mechanical properties

As can be seen from the figure 5.55, there is no reduction in the compressive strength of concrete when loaded with the load level = 56%, 60% and 65% of the compressive strength of concrete. A bit reduction in the 56% case can be attributed to the heterogeneous nature of concrete. As can be seen in the figure 5.55, when 3 concrete cube samples were loaded with the load level of 70% and 75% of the compressive strength of concrete,there was about 4.1% and 6.8% of reduction in the compressive strength of the concrete. The reduction in the strength can be attributed to the damage caused by the cyclic loading process.

Concrete under uniaxial loading will develop cracks parallel to the direction loaded. These cracks were visualised in the case of loading = 70% and 75% of the compressive strength of concrete. Concrete subjected to uni-axial cyclic loading, with loading level less than 70% for 30 load cycles, the concrete will not undergo any crack propagation. After 70% loading, cracks will begin to increase noticeably. The cracks occurrence can be seen in the picture 5.56

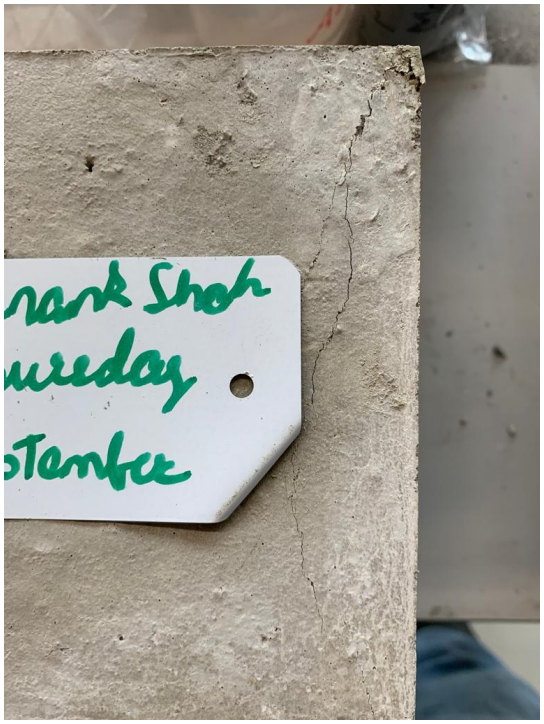

Figure 5.56: Cracking caused due to 70% loading

Considering the standard deviation in the compressive strength of concrete due to heterogeneous nature of concrete, there is some variation in the compressive strength of concrete cubes. One of the reason for the increased compressive strength of concrete is due to the hydration process. The cyclic loading process generally takes about 2.25 hours per concrete cube and the compressive strength of concrete has been computed after the application of cyclic loading on all the 3 cubes. Hence the increased strength for the cyclically loaded samples can be attributed to the continuous hydration for early age concrete cubes that was the case in 65% loading case.

From the analysis of strain results as well as from the verification of the mechanical properties, it can be concluded that for the loading level = 56% and 60%, the deformation caused in concrete is in the elastic phase. For the loading level = 65% of the compressive strength of concrete, the deformation could be in the elastic -plastic phase with some micro-cracks formed inside the concrete cubes. For the load level =70% and above, plastic deformation occurs as visible cracks are observed after the application of 30 load cycles.

There should be some changes in the structural medium when loaded with 65% load as there was some slip observed in the strain axis as well as there was an indication from the CC factor analysis. But it is possible that the cracks are scattered and did not connect together to have effective reduction in the compressive strength. Or it is possible that the micro cracks are of very minute width to have any impact on the compressive strength.

It can also be concluded that increasing the loading frequency from 1.36 KN/s to 13.5 KN/s for the load = 56% of the compressive strength of concrete has no significant impact on compressive strength of concrete cubes. There was very little variation in the computed CC factors for both the load cases and all the CC factors were greater than 0.9. Also this result corroborate with the results of various researchers that suggests that for low cycle fatigue the applied loading level has higher impact as compared to the frequency of loading.

5.2.3. Assessment of Split Tensile Strength for cyclically loaded concrete

It was suspected that performing Split Tensile testing on the loaded specimens, could be a better indicator of the damage assessment due to the concrete being very weak in tension and due to its brittle nature. Hence it was decided to load the concrete cubes under cyclic loading and then measure the Split Tensile Strength. For load = 65%, there was an indication from the CC factor that there could be some micro-cracking inside concrete and probably there is some reduction in Split Tensile Strength due to cyclic loading. Hence, 2 loading level, load =65% and 70% of the compressive strength of concrete has been selected. 30 load cycles has been applied to 3 concrete cubes for each aforementioned loading level. For this cubes CODA wave analysis was not performed.

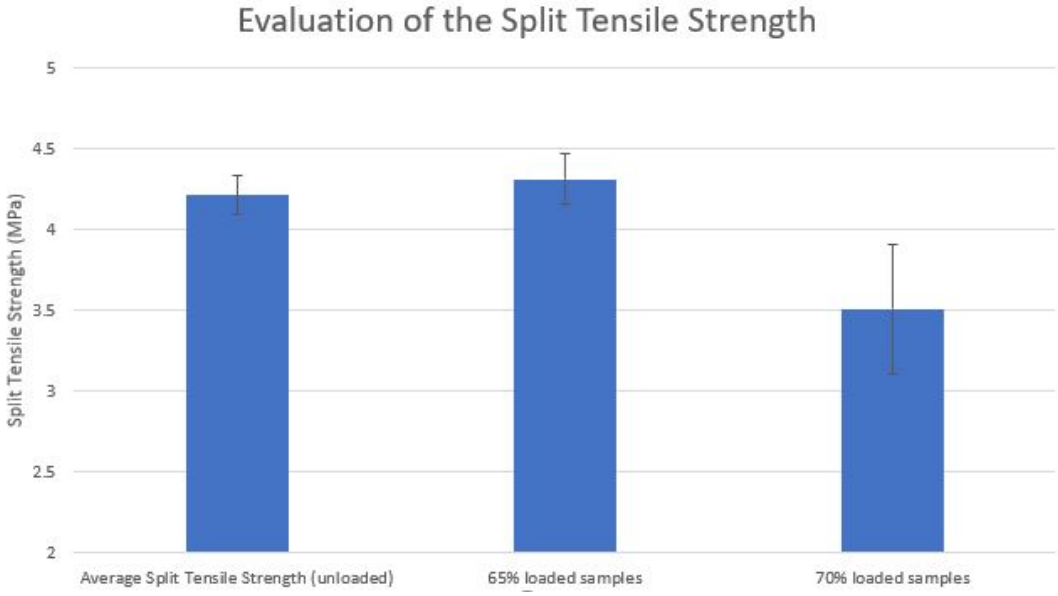

Figure 5.57: Evaluation of the mechanical properties

It can be seen from the figure 5.57 that because of the 65% loading for 30 load cycles, there is no reduction in the Split tensile strength of concrete. Interestingly, the Split Tensile Strength is a bit higher than expected. This could be because of the loading time required to apply cyclic loading and concrete could have gained some strength as it is an early age concrete and the rate of hydration is very high during the early age. About 16.76% reduction in the split tensile strength has been observed in the case of 70% loading case.

The understanding of the mechanism of the split tensile strength is visualised in the figure 5.58. To perform the Split Tensile Strength, 6 concrete cubes were prepared among 3 of them loaded with 65% loading with 30 load cycles and other three with 70% loading. Two strips of nominal thick plywood, free on any imperfections, approximately about 25 mm thick and length is bit longer than the length of cube are used. The bearing strips are placed on the on top and bottom face at the center of the cube as shown in the figure 5.58.The loading was applied without shock and at the nominal rate of 2 $N/(mm^2/min)$ till the failure load and the failure load was computed as the Split Tensile Strength of the cube.

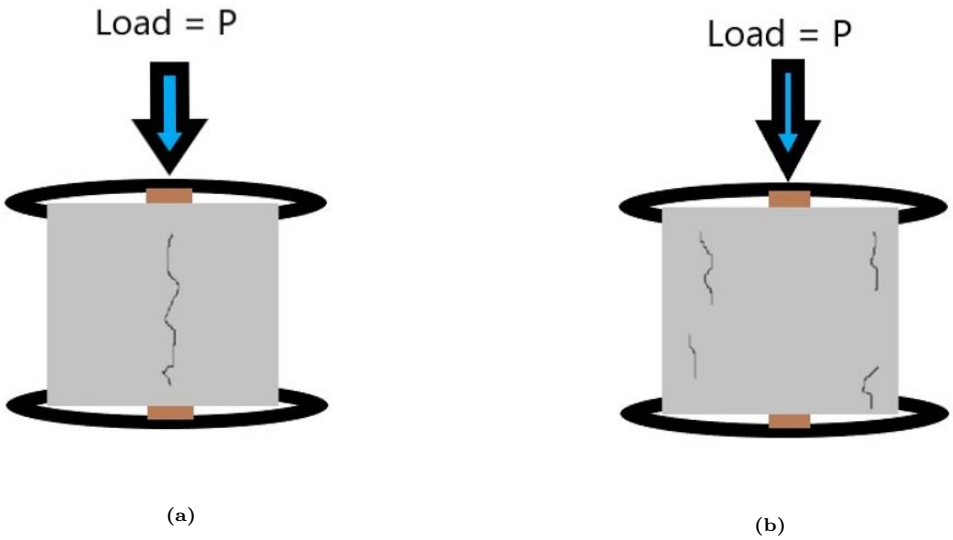

Figure 5.58: Cracking pattern due to cyclic loading. (a) Crack in the direction of loading. (b) Cracks outside the plane of loading.

There could be number of reasons why there was no reduction in Split Tensile Strength observed even though there was an indication from CC factor analysis in case of = 65% loading. It was observed that cracks formed due to cyclic loading are formed in the direction of loading plane. It is evident that cracks formed inside the concrete would tear apart due to the tensile loading which would cause the reduction in the tensile strength in concrete. Hence the location of the cracks inside the concrete cube plays an important role in the reduction of the split tensile strength in concrete.

It could be the case that in the case of 65% loading, as per the indication of CC factor, that there could be an initiation of micro crack by change of structural medium in concrete but that cracks are so minute that they do not cause any reduction in the split tensile strength. Another reason could be the micro cracks formed are not in the direction of the loading plane. The force is transferred from the hydraulic jack to the wooden plank to concrete cube. If the cracks are not within the direction of loading plane, it is possible that there would be no reduction in the splitting tensile strength of concrete as shown in the figure 5.58b. It is also possible that micro cracks are scattered and they do not connect with each other in order to have effective reduction in the split tensile strength.

A very high reduction of 16.76% in split tensile strength has been observed in the case when concrete is loaded with 70% loading for 30 load cycles. It is highly possible that the micro-cracks would have propagated in the direction of loading plane and a big micro-crack could have caused such high reduction in the tensile strength of concrete as can be seen from the figure 5.58a .

5.2.4. Influence of load cycles on strength reduction of concrete

To verify the previous result of maximum damage incurred to the concrete cubes in the first few load cycles, the reduction in concrete compressive strength has been computed for reduced number of load cycles. In order to check the propagation in low cycle fatigue, reduction in concrete compressive strength has been computed.

For the case of cyclic compressive loading = 70 percent of the compressive strength of concrete, it was evident from the high stress, low stress CC factor analysis 5.41 and from the cumulative, Incremental strain analysis 5.22 that maximum occurrence of damage takes place during first few load cycles. The exact number of load cycles varies per concrete cube. But from the analysis it was evident that maximum damage occurrence is incurred in first 10 load cycles.

Hence 3 concrete cubes with the cyclic loading level = 70 percent of the compressive strength were loaded with 10 load cycles each and at the end of the loading process, the compressive strength of the cubes are checked. The results of the reduction in concrete strength for reduced number of load cycles can be seen from table 5.1.

As can be seen from table 5.1 the average compressive strength of 3 cubes during the first casting session was 43.45 MPa and when 3 concrete cubes were cyclically loaded with the load = 70 percent of the compressive strength, the average reduction of 4.17% was observed in the concrete compressive after the application 30 load cycles. To check the reduction in strength due to reduced number of load cycles, in the next casting session, the average compressive strength of 3 concrete cubes was 45.89 MPa. Other 3 concrete cubes were loaded with the load level = 70 percent of the compressive strength, the reduction of 3.51 % in the concrete compressive strength was observed.

Table 5.1: Strength reduction with reduced number of load cycles.

Sr no.	Action	Strength
1	Unloaded samples (3)	43.45MPa(STD.DEV = 0.69)
2	Loaded sample (3) (30 cycles)	41.637MPa (STD.DEV =0.5253) (4.17%)
3	Unloaded samples (3)	43.89MPa (STD.DEV = 0.87)
4	Loaded sample (3) (10 cycles)	42.35MPa (STD.DEV =1.07) (3.51%)

In order to analyse the damage propagation in concrete under the influence of cyclic loading,it is important to understand the initiation process of damage inside concrete. From the literature it was evident that cyclic failure of a plain concrete specimen contains the following several stages:

- Before loading, there exist initial defects and microcracks on the interface between matrix and aggregate, which distribute randomly.
- In the initial loading stage, stress concentration takes place at the tip of interface cracks, which causes cracks to propagate along the weakest direction on the interface.
- These microcracks only propagate mesoscopically with increasing loading, but no macrocracks form. In the last loading stage, where the load is added to its ultimate value, cracks propagate rapidly so that at least a macro-crack through the specimen forms. At this time, the specimen fails.

This paragraph concerns the interpretation of the three stages described above. The material before any loading contains imperfections due to manufacture and different phenomena like shrinkage and swelling.

These structure defects are of random dimensions, orientation and distribution. A given applied load induces a material adaptation to the strain field involving the defects which are perpendicular to the maximum main extension direction and releasing the others. This accounts for stage I. Stage II relates to the slow evolution of the activated defects. The rate of their development and their multiplication, accelerating and inducing in the end an instability. Stage III would not involve any new processes. It should thus be included as part of stage II during which the strain per cycle would keep increasing, however hardly perceptible at the beginning [35].

For the case of cyclic load level = 70% of the compressive strength, it can be observed that the damage proportion due to 30 load cycles has reached only till Stage II. In stage III, as mentioned, the strain occurrence per cycle increases with the increase in the number of load cycles. But as can be seen from figure 5.21 that for the first 30 load cycles, the maximum per cycle strain occurs in the first few load cycles and till the 30 load cycles, the relative strain is lesser as compared to first load cycles.

Hence it is presumed to be safe to assert that maximum damage occurrence is confined to first few load cycles, exact number of load cycles being subjective to the concrete cube. The difference in strength reduction achieved between 30 load cycles and 10 load cycles for load = 70% of the compressive strength is 0.66 percent.

5.3. Crack width analysis and Self Healing potential in concrete

5.3.1. Crack width analysis just after cyclic loading

For the purpose of analysing self healing potential and to visualise the variety of cracks caused due to the cyclic loading, load level = 75 percent of the compressive strength has been chosen. 3 concrete cubes were loaded with the aforementioned loading for 30 load cycles at the 7 days age of concrete. CODA wave analysis was already performed on 75 percent loading case. Strength reduction due 30 load cycles for load = 75 percent loading has already been computed.

In order to determine the extent of the damage caused due to cyclic loading and to analyse the self healing potential due to continuous hydration, concrete cubes, after cyclic loading were divided into 8 different zones based on the crack width measurement. The logic behind the division of zones based on the crack width is to examine the effect of continuous hydration on the crack widths because of 75 percentage loading. After cyclic loading, the concrete cubes were placed in the fog room for the purpose of curing for 7 days. After 7 days of further curing, the crack widths will be analysed again according to the zones divided in order to analyse any reduction in the crack widths due to further hydration induced self healing.

Table 5.2: Crack widths analysis by visual inspection after cyclic loading.

Zone number:	**Observed crack widths**
Zone 1	0.3 mm, 0.2 mm
Zone 2	0.2 mm, 0.05 mm
Zone 3	0.3 mm, 0.08 mm
Zone 4	0.1 mm
Zone 5	0.2 mm
Zone 6	0.1 mm, 0.2 mm
Zone 7	0.08 mm, 0.05 mm
Zone 8	0.2 mm

The crack widths were analysed by the visual inspection. The maximum crack width achieved due to load =75 percent of the compressive strength for 30 load cycles was 0.3 mm. In the literature, the cracking caused due to the cyclic loading can be reviewed and distinguished as: ”physically small cracks” (smaller than 1 mm), ”mechanically small cracks” (smaller than the plastic zone size), ”micro-structurally small cracks” (smaller or comparable to that of the structural unit of the material), and ”chemically small cracks” (cracks whose growth is substantially influenced by the environment).

Through the cyclic loading with the load =75 percent of the compressive strength, it was visually documented that all the surface cracks are were physically small cracks as the crack width was less than 1mm. Although variations in the kinetics of short crack growth exist in different, materials, and appreciable scatter in the kinetics of short crack growth is encountered even under identical experimental conditions, it was visualised and confirmed that the proportionality of the crack-growth rate to the crack length is valid for many materials. This was one of the reason why one primary crack was seen in early

load cycles which increased in crack length due to further load cycles.

(a) **(b)**

Figure 5.59: Crack-width analysis (before hydration) (a) Zone 2 (b) Zone 3

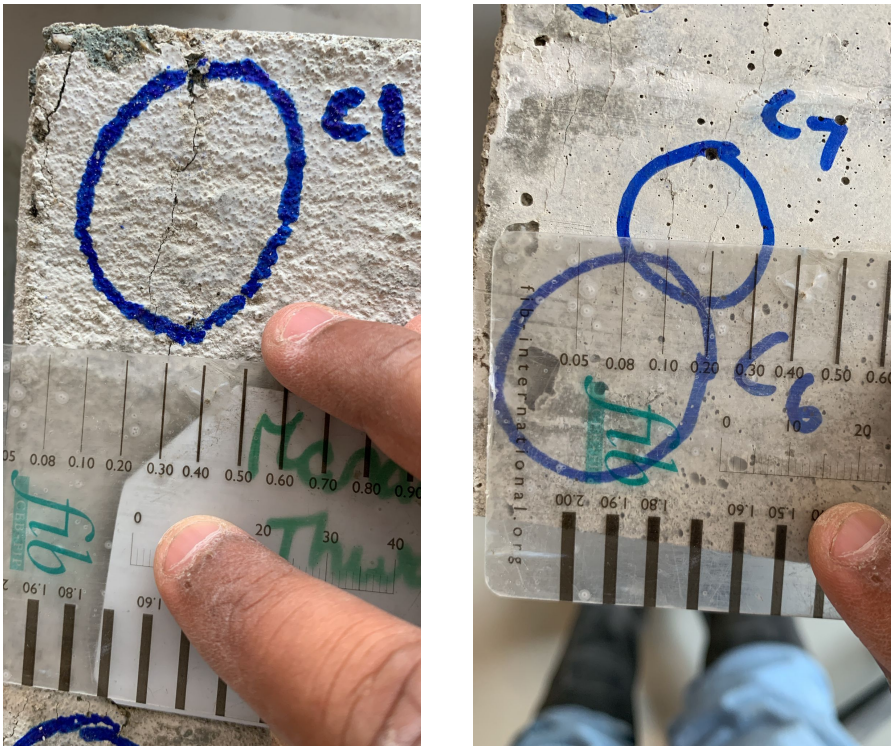

(a) **(b)**

Figure 5.60: Crack-width analysis (before hydration) (a) Zone 1 (b) Zone 7

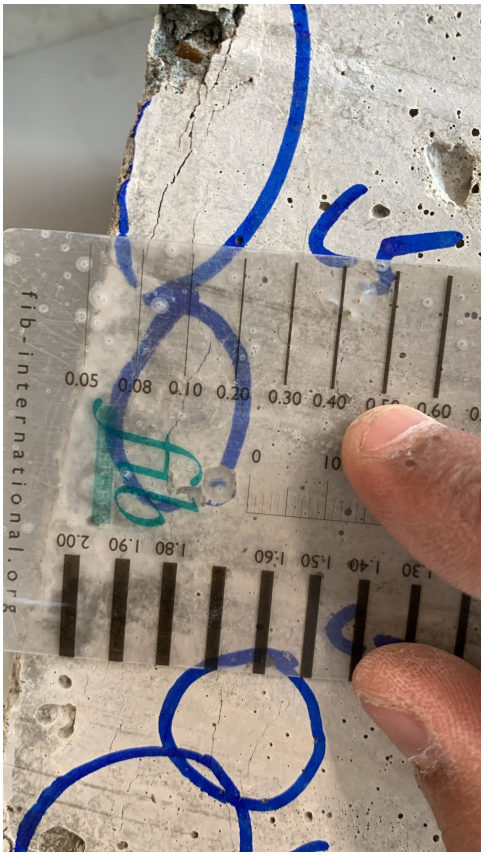

Figure 5.61: Crack-width analysis (before hydration) Zone 5

The cracks caused due to cyclic loading in concrete can be distinguished into three types of cracks: type I crack extends over one grain, a type II crack over two neighboring grains, and a type III crack over three or more neighboring grains on the surface. The evolution of all three types of cracks was visualised through the portable microscope used in the study. During the visual inspection of cubes, type I cracks were visualised the most in number.

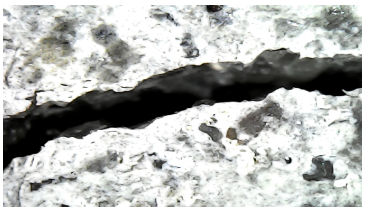

(a) Type I cracks

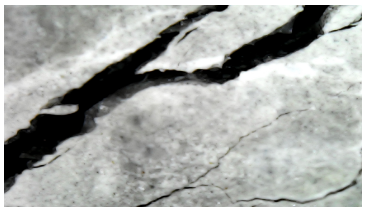

(b) Type II cracks

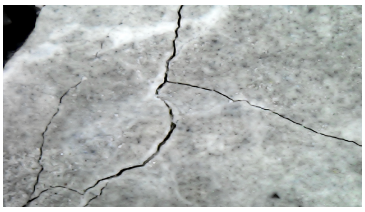

(c) Type III cracks

Figure 5.62: Types of cracks occurrence due to cyclic loading

5.3.2. Crack width analysis after 7 days of continuous hydration

Aforementioned, three concrete cubes after loading with load =75 percent of the compressive strength for 30 load cycles were analysed for crack width classification. After the analysis, the cubes were placed in the fog curing room for 7 days to check the effect on crack width due to continuous hydration and self healing in concrete.

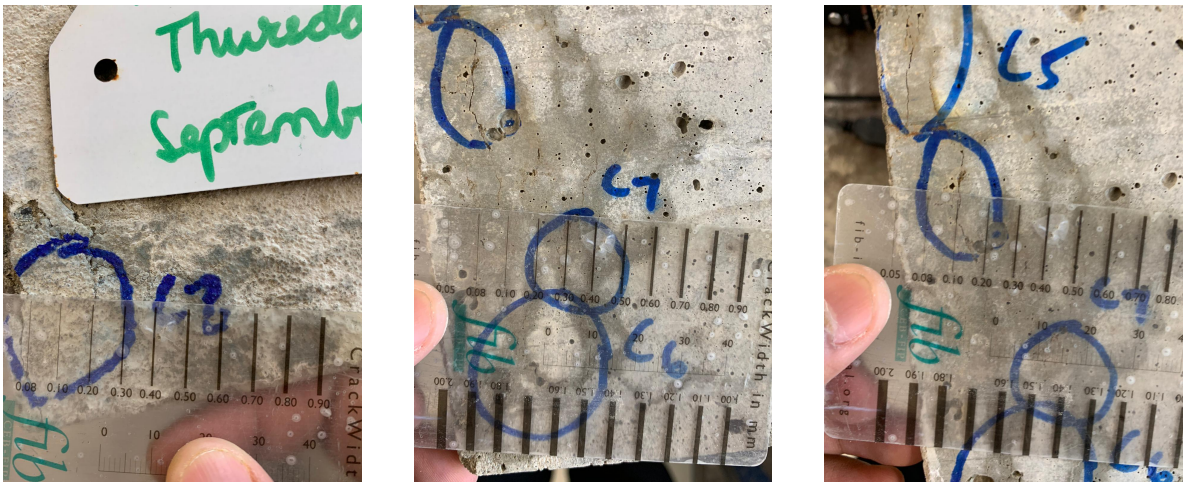

(a) Zone II **(b)** Zone VII **(c)** Zone V

Figure 5.63: Crack-width analysis (after hydration)

(a) Zone III **(b)** Zone III **(c)** Zone VI

Figure 5.64: Crack-width analysis (after hydration)

It was observed that there was no significant reduction in the crackwidths greater 0.1mm. Hence the cracks with the crack widths of 0.3 mm, 0.2 mm, 0.1 mm was not healed at all and there was no reduction in the crack widths due to the formation of healing products due to further hydration induced healing. There could be several reasons behind the failure to form the healing products which will be discussed further. Whereas, in Zone 3 and Zone 7, reduction in the crack width was observed. (5.3) The cracks with the width of 0.08 mm have been reduced to 0.05 mm and cracks with the width of 0.05 mm have been reduced to the width of less than 0.05 mm but exact crack width cannot be calculated because of the least count of the crack width measuring card.

Table 5.3: Crack widths analysis after continuous hydration.

Zone:	Observed crack widths after hydration
Zone 3	0.08 mm $\longrightarrow$ 0.05 mm
Zone 7	0.05 mm $\longrightarrow <$ 0.05 mm

Several studies showed the the possibility of self healing of cracks with the crack width of less than 0.3 mm. After 7 days of hydration for the cubes in fog room, there was not reduction in the crack width observed for the crack width of 0.1 mm. There could be several reasons concerning the failure to heal the cracks over the crack width over 0.1 mm under the fog curing condition.

It was concluded from the research of various researchers that cracks heal with larger crack widths of the range of 0.3 mm under the fully saturated condition. Under this curing condition, the cracks has higher access to water and carbon-dioxide dissolved in the water. As the unhydrated cement powders make contact with water, a chain of reaction called the hydration process starts. Such reaction will convert clinkers contained in the cement powder into cement matrix, which consists of calcium silica hydrate (CSH), calcium hydroxide (CH), and gypsum(3.5,3.6). This are the major self healing products formed in the cracks. Due to fog curing it is possible that interaction of cracks with the moisture is limited as compared fully saturated condition and hence the cracks with the larger crack widths do not heal.

The next reason could be the time of hydration. It is evident from the literature that hydration for a longer time can yield a better self-healing performance inside concrete. In this case, the concrete is cracked at the age of 7 days. After cracking, the concrete cubes are placed in the fog curing room for another 7 days with total age of concrete being 14 days. It is possible that if the cracked concrete cubes are further hydrated under the fog curing conditions than it is possible that the cracks with the greater crack widths could heal or the cracks with the small crack widths (for eg. 0.08mm, 0.05mm) could heal completely.

Another reason for the failure of self healing could be attributed to the material composition of the concrete mixture used for the study. One of the factor could be the usage of water–cement ratio used for the study. With the higher water–cement ratio used for the mixture includes more unreacted cement particles that can be used for further hydration to boost the generation of calcium carbonate. Also, the usage of more CEM III as compared to CEM I could be a factor to enhance the self-healing potential in concrete. CEM III gives higher late strength in concrete and if the concrete is cracked at early age than usage of higher CEM III would have more unhydrated cement particles that could help to seal the micro-cracks.

During the visual inspection, it was investigated that there were some micro cracks with the crack width less than 0.05 mm which was not inspected by naked eyes because of the least count of the measuring card. But those cracks were visualised by the portable microscope just after the cyclic loading and after 7 days of further hydration of the concrete cubes. During the investigation, it was found that some small micro cracks were completely healed. Due to the limitation of the least count of measuring technique, it was not possible to find the exact crack width of the cracks that has been healed completely. Some visuals of the hydration products can be seen in the figure 5.65.

(a) Zone II

(b) Zone VII

(c) Zone V

Figure 5.65: Development of autogeneous self healing products

(a) Zone II

(b) Zone VII

(c) Zone V

Figure 5.66: Development of autogeneous self healing products

There are various solutions used by the researchers to enhance the self healing potential in the concrete. One solution is using Bacteria to precipitate calcite in cracks in concrete. With this method relatively large cracks in reinforced concrete can be filled. The method does not lead to strength improvements of the structure, but by filling the crack, the path to the reinforcement is blocked.
In the second application SHCC materials are studied, which have already a high potential for self healing because of their small crack widths. New additions, like microfibers and SAP's even promote this self healing capacity further.
The third application is for asphalt concrete in which the self healing capacity is enlarged by using encapsulated oil and micro-steel fibres. The latter approach has been proven to work in the laboratory and is applied on real roads in the Netherlands in 2010.

5.4. Effect of continuous hydration on further strength development of cyclically loaded concrete

This section focuses on the Strength development aspect of concrete after loading under fog curing and plastic sealed condition. A series of experiments were performed on the concrete cubes in order to investigate the effect of self-healing potential and effect of hydration on concrete samples.

To analyse the variation in concrete compressive strength, first step was to comprehend the normal concrete strength development in the unloaded stage and under fog curing condition. The values are computed by averaging the results for 3 concrete cubes.
Dark blue line in the figure 5.67 represents the concrete strength development under the aforementioned curing conditions. The average compressive strength achieved at the age of 7 days and 14 days under the fog curing condition is 44.3 MPa and 58.8 MPa. Cyclic loading experiments approximately costs 6-7 hours on average. Hence computation and results are plotted at 7.2 days rather than 7 days.

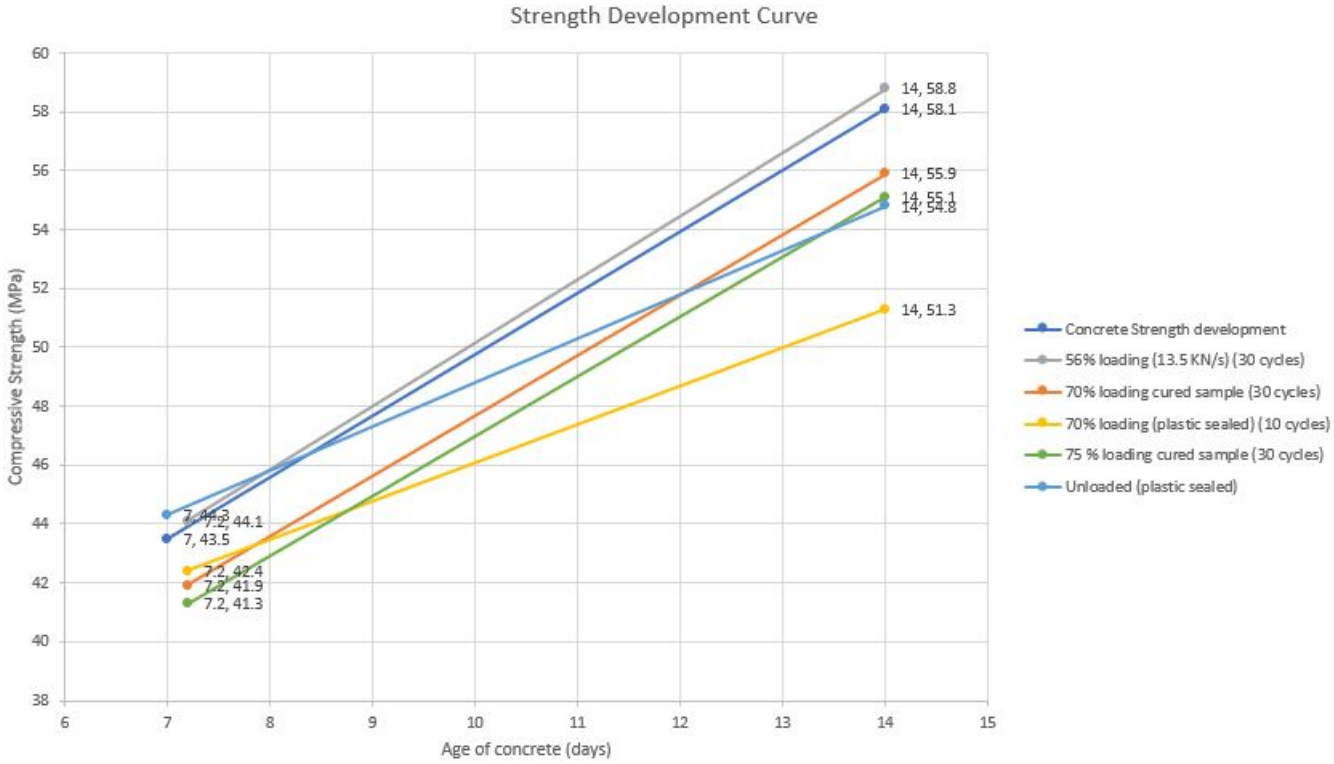

Figure 5.67: Strength Development

Grey line in the figure 5.67 represents the strength development curve for load level= 56% of compressive strength. After the application of 30 load cycles, the compressive strength has been computed on the 7^{th} day age of concrete. To analyse on the strength development of concrete after cyclic loading, 3 concrete cubes, after cyclic loading with aforementioned parameters, were placed under fog curing for another 7 days and the compressive strength was computed henceforth.

It was concluded through the CC factor analysis (ref. 5.31) and computation of strain analysis (ref. 5.10) that there was no reduction in the concrete compressive strength because of the application of 30 load cycles. Also as it can be seen from the figure 5.67, that the cyclically loaded samples reached the concrete compressive strength of 58.8 MPa, very similar to the unloaded concrete. A bit of variation in the strength between the blue and grey line is because of the heterogeneous nature of concrete. Hence it is safe to assume that there is no reduction in the compressive strength at the age of 7 days and the strength develops in the loaded cubes in similar fashion as unloaded cubes. It seems that there is no change in the structural medium because of the application of 30 load cycles.

The next two computations was performed on the load level = 70% of compressive strength of concrete. The orange line represents the 30 load cycles with fog curing condition and the yellow line represents the 10 load cycles with the plastic sealed condition. Plastic sealed condition is implemented in order to restrict any interaction of moisture from the environment. Figure 5.67 shows the comparison of reduction in concrete compressive strength for both the cases.

In order to check the effect of continuous hydration on the strength development of concrete, unloaded concrete cubes (fig 5.68a) along with the loaded concrete cubes (fig 5.68b) were placed in the plastic sealed condition and compression testing has been performed at the age of 7 days and 14 days. Special care was taken with the covering of plastic sheets and it was made sure that all the faces of the cubes were fully covered by plastic in order to avoid any interaction with the outer atmosphere.

(a)

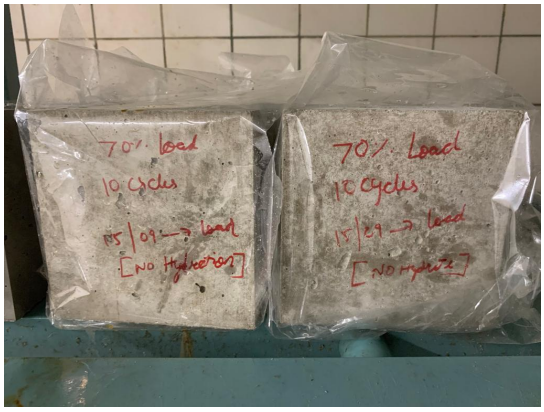

(b)

Figure 5.68: Effect of hydration on strength development of concrete (a) Unloaded samples (b) Loaded samples

It can be visualised from the figure 5.67 that for the age of 7 days there is no reduction in the compressive strength of concrete for the completely plastic sealed condition. The reasoning behind this can be attributed to the internal water content inside the concrete mixture. Many researchers focused on concrete strength development due to internal curing due to high W/C ratio inside the concrete. As per the literature, very little difference was seen in the Degree of Hydration of mortar samples with internal curing, as would be expected at W/C greater than 0.42 [36].

It was also recorded that at the age of 14 days, there was about 5.75% reduction in the compressive strength of concrete for the plastic sealed sample as compared to fog room cured samples. It could be the case that both the sealed and fog room cured samples generated an equal cumulative heat of hydration up to a certain period of time, after which water availability became a limiting factor and hence there was a reduction in the compressive strength of concrete at the age of 14 days. Also it was observed that for the loaded sample with 70% loading for 30 load cycles, when it in plastic sealed condition, there was very high reduction in strength at the age of 14 days. Hence it it was concluded that hydration process of concrete plays very important role in strength development from 7 to 14 days.

In order to analyse any compressive strength recovery due to autogeneous self -healing process, samples with 2 different loading level, load = 70% an 75% of the compressive strength of the concrete has been applied for 30 load cycles and then the compressive strength has been compared with the unloaded samples after 7 days of fog curing. It can be visualised that there was about 4.1% and 6.8% of reduction in the compressive strength for load level = 70% and 75% of compressive strength for 30 load cycles. Similarly, the strength reduction at the age of 14 days that was computed was 3.7% and 5.2% respectively. There was about 0.4% and 1.6% strength recovery that was observed. This recovery could be attributed to the hydration of unhydrated cement particles in concrete. 5.65 and 5.66.

Experimental results indicate that autogenous crack self-healing in cement-based materials has a negligible effect on their ability to achieve mechanical strength recovery. A bit of strength recovery appears to be because of the heterogeneous nature of concrete specimens. Also the exposure condition plays a crucial role in the mechanical strength recovery process. The water submersion condition might be able to achieve the best strength recovery as compared to fog curing conditions. Also mechanical strength recovery seems to be limited to the duration of the hydration and pozzolanic reactions process of cement-based materials, while autogenous crack self-healing could progress even after the hydration process has entirely been completed.

5.5. Resemblance of the research work with the engineering practice

Initially, the major research question was formulated from a real restrengthening project of a bridge in North of the Netherlands. The research question was formulated because of the initial cyclic loading applied to the concrete after 3 days of casting. Hence series of experiments were performed in order to determine long time performance of the cyclically loaded concrete. The β_{cc} factor in the formula to determine the fatigue strength is constant, as discussed in the earlier section, was computed based on the 3^{rd} day strength of concrete due to the first application of loading.

Firstly, cyclic loading level was determined taking into account all the load cases. After computing net compressive stress, the cyclic load was applied for 30 load cycles. It is to be noted that the applied compressive stress includes a number of load cases which are not going to be cyclically applied to the concrete. But to be on the conservative side and for simplification, the total compressive stress was cyclically applied for 30 load cycles. It can be concluded that if the concrete is determined safe under this loading condition than concrete can be deemed safe in actual engineering practice.

From the experimentation it can be clearly concluded that under the 56% loading, which was the maximum compressive stress acting on the early age concrete, for 30 load cycles, the concrete was deemed to be safe. It was clearly indicated through CC factor analysis and wave speed analysis that due to the loading on the 3^{rd} day concrete did not cause any change in micro structure in terms of micro cracking in concrete. Also the further strength development was analysed after the cyclic loading to comment on long term performance of cyclically loaded concrete.

Due to 56% loading, the further strength development was not hindered. Hence it is safe to assert that in the actual engineering practice, it was correct to compute β_{cc} based on the 7^{th} day strength of concrete when the bridge is open for the traffic.

Also the wave speed analysis and CC factor analysis could be used in the real engineering practice to determine the damage in concrete. It was also determined that on the actual construction site, if the concrete is cracked due to cyclic loading, then there is a possibility of self healing of the cracks but the mechanical strength recovery due to the self healing is not possible in the investigated time frame during the study.

Also in real engineering practice, once the concrete is cracked due to cyclic loading, the damage would progressively propagate in concrete as the vehicular loading would not cease to occur. Also, once concrete is in the cracked condition than strength recovery due to self healing is very difficult in real engineering practice. Hence it is recommended that the cyclic loading level should be kept less than 70% of the compressive strength of concrete at t= 7 days (for 30 load cycles), when cyclic loading is applied to early age concrete.

6

Conclusions and recommendations

• One of the main conclusion of this research work is that the cyclic loading with a load level = 56% of the compressive strength of concrete at t=3 days, for 30 load cycles (13.5KN/s frequency), shows no reduction in the mechanical properties of concrete at t=3 and t= 7 days.

• It was also concluded that increasing the loading frequency from 1.36 KN/s to 13.5 KN/s did not affect the mechanical properties of the concrete for the 56% loading case.

• Hence it can be asserted that the $\beta_{cc}(t_0)$factor, which depends on the time when the first cyclic load is applied to the concrete, can be calculated based on the 7^{th} day age of concrete, as 56% loading did not cause any damage to the concrete on the 3^{rd} day.

• Through this study, it was also concluded that when concrete is loaded with 56% cyclic loading, for 30 load cycles at t = 7 days, the further strength development of cyclically loaded concrete is very similar as to the unloaded concrete.

• It was also concluded by comparison of CC factor analysis and wave speed analysis that, the CC factor is more sensitive to the moment of cracking rather than the indication for progressive failure. It was also observed that wave speed analysis is a better indicator of damage propagation in concrete.

• 7% reduction in wave speed indicates damage to concrete in such a manner that mechanical properties of the concrete are affected. It can also be concluded that when the average CC factor reaches the value less than 0.7, than concrete is already in the damaged state.

• Reduction in the mechanical strength of concrete is observed when loading at 70% and 75% of the compressive strength of concrete for 30 load cycles. Maximum damage to the concrete is attributed by the first few load cycles.

• An added value to the research field is that the autogeneous self healing mechanism is possible under the fog curing conditions. Also it was concluded that autogeneous self healing mechanism is not capable to completely self heal the cracks greater than 0.1 mm.

• Even though self healing mechanism is possible under the fog curing conditions, mechanical strength recovery was not observed under the fog curing conditions.

Recommendations

• A huge difference in computed fatigue strength can be achieved if fatigue strength was calculated based on 7^{th} age of concrete as compared to the 3^{rd} age of the concrete. Hence based on the scope of the experiments performed at the laboratory it is suggested that a factor should be included in the fatigue strength formula which takes into account further strength development in concrete.

• As this study was restricted to 30 load cycles, it is important to check the influence of increasing load cycles under the cyclic loading. It would be interesting to observe how many load cycles would lead to failure of a concrete specimen under high cyclic loading level.

• It is recommended to the structural engineers that concrete subjected to a cyclic loading level under 65% of the compressive strength of concrete, for 30 load cycles, would not cause any damage to concrete and hence this kind of loading could be applied in engineering practise in case of time constraints.

• There was a clear indication of micro cracking through the CC factor analysis and hence it is interesting to observe the how the internal micro cracks would propagate inside concrete cube and this phenomenon can be assessed via CT scan or by cutting the concrete cube whenever there is an indication through CC factor analysis .

• It would be interesting to research the effect of embedding sensors inside concrete and its effect on the CC factor analysis. It is expected that the embedded sensors might provide near-perfect coupling with the medium, while gel-attached sensors may be displaced during the course of its service time. Hence a comparative study can be performed between the surface attached sensors and embedded sensors inside concrete to comment on the usability of these sensors in real engineering practice.

• During this study the self healing of cracks is investigated under fog curing conditions but the self healing efficiency of cracks was not determined. Since the study was limited in time of curing, the self healing potential could be bigger. Hence it would be interesting to observe the influence of other parameters like cracking age, curing time and curing conditions on self healing efficiency of concrete.

• In this study, the strength development and strength recovery due to self healing was assessed for 7 days of continuous hydration. Hence the strength development of cyclically loaded concrete up to 28 days should be studied to check if there is some strength recovery for the early age concrete. A clear distinction between the strength recovery due to further hydration and strength recovery due to self healing must be investigated by studying the degree of hydration in concrete.

7

Appendix

mebin

HEIDELBERGCEMENT Group

Gewogen Rijpheid

volgens NEN 5970 — **Datum** 00-01-00

Sterkteklasse	C55/67	**Milieuklasse**	XF4	**Cons.klasse**	F4	**Chlorideklasse**	Cl 0,40
Cementsoort	CEM III/B 42,5 N			**Constante α**	1,0	**Wcf**	0,37
Cementsoort	CEM I 52,5 R			**C-waarde**	1,40	**D-max**	16
				Hulpstof/toevoeging		Superplastificeerder	
Aannemer				**Bouwwerk**			
Plaats				**Opmerking**		uit eerdere metingen	

IJkgrafiek

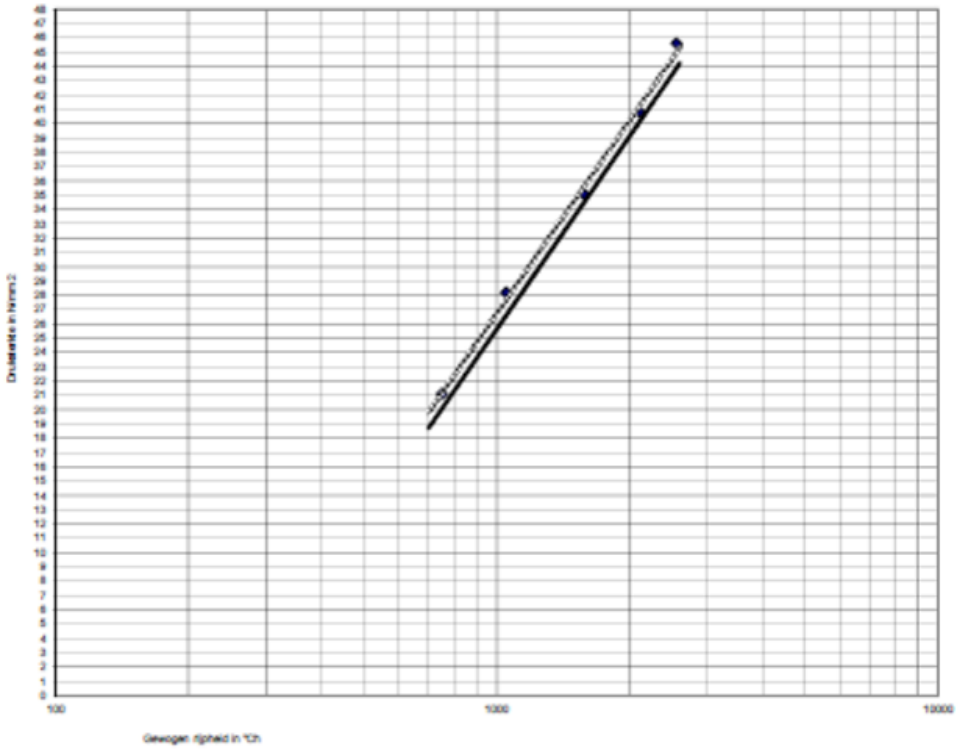

Waarneming	Rijpheid		Druksterkte	
1	750	°Ch	21,1	N/mm²
2	1049	°Ch	28,2	N/mm²
3	1578	°Ch	35,0	N/mm²
4	2105	°Ch	40,8	N/mm²
5	2550	°Ch	45,6	N/mm²

Rijpheid		Druksterkte	
°Ch		0,0	N/mm²

Werkzaamheden ten behoeve van opdrachtgevers worden slechts uitgevoerd op voorwaarde,dat de opdrachtgever afstand doet van ieder recht op aansprakelijkstelling en zich verplicht tot vrijwaring voor iedere aansprakelijkheid jegens derden een en ander behalve indien en voor zover grove schuld en/of opzet wordt aangetoond.

16-5-2018

Versie 02 - april 2012

Figure 7.1: Strength Development curve for the concrete used in the study

CONTROLE BETONSPANNING BGT (KARAK.)

N / A_b	0,00	N/mm²		$\sigma_c \leq 0{,}6\ f_{ck}$	
M / W_o	0,00	N/mm²		f_{ck}	30,00
M / W_b	0,00	N/mm²		f_{cd}	20,00
Spanning bovenzijde $\sigma_{b;b}$	0,00	N/mm²		f_{ctm}	2,90
Spanning onderzijde $\sigma_{b;o}$	0,00	N/mm²		Spannen na	28

* Invloed wapening is niet meegenomen in het bepalen van spanningen

TOETSING BEZWIJKMOMENT $M_{Rd} > ME_d$

Bezwijkmoment M_{Rd}	602	kNm*	Voldoet	N'_b	2134
				y	55
				ε_{pw}	0,57%
				$\Delta\varepsilon_{pw}$	1,52%
				ε_p	2,09%
				σ_p	1528
				$\Delta\sigma_p$	364
				ΔN_p	0
				$\Sigma M =$	0

	laag 1	laag 2	laag 3	laag 4	
ε_s	0,48%	-0,35%	-0,35%	-0,35%	
σ_s	435	-435	-435	-435	N/mm²
N_s	2134	0	0	0	kN

* Gerekend wordt met een horizontaal plastisch traject van de wapening.

Toetsing betondrukzone $X_u < X_{u,max}$

Hoogte betondrukzone X_u	142	mm*	Voldoet	e_{cu3}	0,0035
Maximale betondrukzone $X_{u,max}$ (art 6.1)	181	mm		d_{eff}	338
				f_{yd}	435

* Zonder herverdeling

MIN & MAX - Wapeningsdoorsnede en spanningsbeperking (karak.)

Min. Opp. trekwapening in doorsnede As,min (9.2.1.1)	536	mm²	Voldoet	$A_{s,min\,1}$	536
Max. wapeningdoorsnede As,max (9..2.1.1)	16000	mm²	Voldoet	$A_{s,min\,2}$	5252
$A_{s,tot}$ trekzone	4909	mm²		$A_{ct,BGT}$	252486
Maximale toelaatbare betondrukspaning (art 7.2)	18	N/mm²	Voldoet	K_1	0,6

BEREKENEN SCHEURWIJDTES (FREQ.)

Constructie met voorspanning	Nee	Alleen	Betonstaal	x	148
				$(\varepsilon_{sm}\text{-}\varepsilon_{cm})$	0,001102
				K_4	0,425
Scheurwijdte W_k (7.3.4)	0,27	mm	Voldoet	K_3	3,4
Scheurmoment (M_{cr})	77	kNm*		K_2	0,50
				K_1	0,8

* Invloed wapening is niet meegenomen in het bepalen van M_{cr}

$W_{max} * K_x$	0,36	mm	$\varnothing_{eq}$	25
W_{max}	0,30	mm	$h_{c,eff}$	84
			$A_{c,eff}$	84162
$k_3*c + k_1*k_2*k_4*(\varnothing_{eq}/\rho_{p,eff})$	243	mm	$\rho_{p,eff}$	0,0583
$(50\text{-}0{,}8*f_{ck})*\varnothing_{eq}$	650	mm	$s_{r,max}$	243
$15*\varnothing_{eq}$	375	mm		
Bovengrens $s_{r,max} = 1{,}3 * (h\text{-}x)$	328	mm	σ_s	247
			k_t	Langdurende b

	laag 1	laag 2	laag 3	laag 4			
ε_s	0,124%	-0,10%	-0,10%	-0,10%		α_e	6,09
σ_s	247	-192	-192	-192	N/mm²	E_s	200000
N_s	1214	0	0	0	kN	E_{cm}	32837
						$K_x=(c/c_{nom})$	1,20
	Boven	Onder				$\Sigma M =$	0
ε_c	-0,096%	0,184%				$\Sigma N =$	0
σ_c	-16,46	0,00					

BIJLAGE A

Figure 7.2: Calculated sheet for maximum Compressive Stress acting on concrete

References

[1] Corina-Maria Aldea et al. "Extent of Healing of Cracked Normal Strength Concrete". In: *Journal of Materials in Civil Engineering* 12.1 (2000), pp. 92–96. DOI: 10.1061/(asce)0899-1561(2000)12:1(92).

[2] Rami Alghamri et al. "Preparation and polymeric encapsulation of powder mineral pellets for self-healing cement based materials". English. In: *Construction and Building Materials* 186 (Oct. 2018), pp. 247–262. ISSN: 0950-0618. DOI: 10.1016/j.conbuildmat.2018.07.128.

[3] *BAW Code of Practice: Frost Resistance Tests for Concrete (MFB). Bundesanstalt für Wasserbau.* 2012. URL: :%20https://izw.baw.de/publikationen/merkblaetter/0/BAWCodeofPractice_Frost_%20Resistance_Concrete_MFB_2012.pdf.

[4] Klaas van Breugel. "SELF-HEALING MATERIAL CONCEPTS AS SOLUTION FOR AGING INFRASTRUCTURE". In: (2012).

[5] Klaas van Breugel. *Simulation of hydration and formation of structure in hardening cement- based materials*. Meinema, 1991.

[6] C A Clear. *THE EFFECTS OF AUTOGENOUS HEALING UPON THE LEAKAGE OF WATER THROUGH CRACKS IN CONCRETE*. 2021. URL: https://trid.trb.org/view/266588.

[7] Melchior Deutscher. "Consideration of the Heating of High-Performance Concretes during Cyclic Tests in the Evaluation of Results". In: *Applied Mechanics* 2.4 (2021), pp. 766–780. DOI: 10.3390/applmech2040044.

[8] Carolyn M. Dry. "Design of self-growing, self-sensing, and self-repairing materials for engineering applications</title>". In: *Smart Materials* (2001). DOI: 10.1117/12.424430.

[9] C Edvardsen. "WATER PERMEABILITY AND AUTOGENOUS HEALING OF CRACKS IN CONCRETE". In: *Trid.trb.org* (2021). URL: https://trid.trb.org/view/506056.

[10] Carola Edvardsen. "Water Permeability and Autogenous Healing of Cracks in Concrete". In: *Aci Materials Journal* 96 (1999), pp. 448–454.

[11] C. M. R Fowler. *The solid earth*. 1993.

[12] Xiaofeng Gao, Georg Koval, and Cyrille Chazallon. "A Discrete Element Model for Damage and Fatigue Crack Growth of Quasi-Brittle Materials". In: *Advances in Materials Science and Engineering* 2019 (Feb. 2019), pp. 1–15. DOI: 10.1155/2019/6962394.

[13] Peng Gong et al. "ASR damage detection in concrete from ultrasonic methods". In: *Sensors and Smart Structures Technologies for Civil, Mechanical, and Aerospace Systems 2014* (2014). DOI: 10.1117/12.2045645.

[14] Christoph Hemleben, Michael Spindler, and O. Roger Anderson. "Modern Planktonic Foraminifera". In: (1989). DOI: 10.1007/978-1-4612-3544-6.

[15] Haoliang Huang, Guang Ye, and Denis Damidot. "Characterization and quantification of self-healing behaviors of microcracks due to further hydration in cement paste". In: *Cement and Concrete Research* 52 (2013), pp. 71–81. DOI: 10.1016/j.cemconres.2013.05.003.

[16] Benard Isojeh, Maria El-Zeghayar, and Frank J. Vecchio. "Concrete Damage under Fatigue Loading in Uniaxial Compression". In: *ACI Materials Journal* 114.2 (2017). DOI: 10.14359/51689477.

[17] Stefan Jacobsen and Erik J. Sellevold. "Self healing of high strength concrete after deterioration by freeze/thaw". In: *Cement and Concrete Research* 26.1 (1996), pp. 55–62. DOI: 10.1016/0008-8846(95)00179-4.

[18] HM Jonkers et al. "Application of bacteria as self-healing agent for the development of sustainable concrete". Undefined/Unknown. In: *Ecological Engineering* 36.2 (2010), pp. 230–235. ISSN: 0925-8574. DOI: 10.1016/j.ecoleng.2008.12.036.

[19] C. G. KARAYANNIS. In: *Journal of Earthquake Engineering* 4.4 (2000), p. 479. DOI: 10.1142/s1363246900000217.

[20] Vistasp M Karbhari and Farhad Ansari. *Structural health monitoring of civil infrastructure systems*. Woodhead Pub, 2011.

[21] Victor C Li, Yun Mook Lim, and Yin-Wen Chan. "Feasibility study of a passive smart self-healing cementitious composite". In: *Composites Part B: Engineering* 29.6 (1998), pp. 819–827. DOI: 10.1016/s1359-8368(98)00034-1.

[22] Victor C. Li and En-Hua Yang. "Self Healing in Concrete Materials". In: *Springer Series in Materials Science* (2007), pp. 161–193. DOI: 10.1007/978-1-4020-6250-6_8.

[23] Ernst Niederleithinger et al. "Processing Ultrasonic Data by Coda Wave Interferometry to Monitor Load Tests of Concrete Beams". In: *Sensors* 18.6 (2018), p. 1971. DOI: 10.3390/s18061971.

[24] Karin Olsson and Josef Pettersson. "Fatigue Assessment Methods for Reinforced Concrete Bridges in Eurocode. Comparative study of design methods for railway bridges". In: (2010).

[25] T. Planès and E. Larose. "A review of ultrasonic coda wave interferometry in concrete". In: *Cement and Concrete Research* 53 (2013), pp. 248–255. DOI: 10.1016/j.cemconres.2013.07.009.

[26] Tanvir Qureshi and Abir Al-Tabbaa. "Self-Healing Concrete and Cementitious Materials". In: (2020).

[27] TS Qureshi, Antonis Kanellopoulos, and Abir Al-Tabbaa. "Encapsulation of expansive powder minerals within a concentric glass capsule system for self-healing concrete". In: *Construction and Building Materials* 121 (2016), pp. 629–643.

[28] Bianca J. Reeksting et al. "EMIn-depth profiling of calcite precipitation by environmental bacteria reveals fundamental mechanistic differences with relevance to application". In: (2019). DOI: 10.1101/850883.

[29] Hans-Wolf Reinhardt and Martin Jooss. "Permeability and self-healing of cracked concrete as a function of temperature and crack width". In: *Cement and Concrete Research* 33.7 (2003), pp. 981–985. DOI: 10.1016/s0008-8846(02)01099-2.

[30] Hans-Wolf Reinhardt and Martin Jooss. "Permeability and self-healing of cracked concrete as a function of temperature and crack width". In: *Cement and Concrete Research - CEM CONCR RES* 33 (July 2003), pp. 981–985. DOI: 10.1016/S0008-8846(02)01099-2.

[31] Mustafa Şahmaran et al. "Self-healing of mechanically-loaded self consolidating concretes with high volumes of fly ash". In: *Cement and Concrete Composites* 30.10 (2008), pp. 872–879. DOI: 10.1016/j.cemconcomp.2008.07.001.

[32] Senot Sangadji and Erik Schlangen. "Self Healing of Concrete Structures - Novel Approach Using Porous Network Concrete". In: *Journal of Advanced Concrete Technology* 10.5 (2012), pp. 185–194. DOI: 10.3151/jact.10.185.

[33] Branko Šavija and Erik Schlangen. "Autogeneous healing and chloride ingress in cracked concrete". In: *Heron* 61 (Jan. 2016), pp. 15–32.

[34] E. Schlangen, N. ter Heide, and K. van Breugel. "CRACK HEALING OF EARLY AGE CRACKS IN CONCRETE". In: *Measuring, Monitoring and Modeling Concrete Properties* (), pp. 273–284. DOI: 10.1007/978-1-4020-5104-3_32.

[35] Surendra P. Shah and Stuart E. Swartz. "Fracture of Concrete and Rock". In: (1989). DOI: 10.1007/978-1-4612-3578-1.

[36] Sarwar Jamil Siddiqui et al. "Effect of Curing Water Availability and Composition on Cement Hydration". In: *Aci Materials Journal* 110 (2013), pp. 315–322.

[37] L.P. Singh et al. "Studies on early stage hydration of tricalcium silicate incorporating silica nanoparticles: Part I". In: *Construction and Building Materials* 74 (2015), pp. 278–286. DOI: 10.1016/j.conbuildmat.2014.08.046.

[38] Roel Snieder et al. "Coda Wave Interferometry for Estimating Nonlinear Behavior in Seismic Velocity". In: *Science* 295.5563 (2002), pp. 2253–2255. DOI: 10.1126/science.1070015.

[39] Ahmed Suleiman and Moncef Nehdi. “Effect of autogenous crack self-healing on mechanical strength recovery of cement mortar under various environmental exposure”. In: *Scientific Reports* 11 (Mar. 2021), pp. 1–14. DOI: 10.1038/s41598-021-86596-2.

[40] Surindur Singh Takhar. *The Fatigue behaviour of concrete under lateral confining pressure*. 2021. URL: http://dx.doi.org/10.11575/PRISM/13479.

[41] Kim Van Tittelboom and Nele De Belie. “Self-Healing in Cementitious Materials—A Review”. In: *Materials* 6.6 (2013), pp. 2182–2217. DOI: 10.3390/ma6062182.

[42] R.P. Veerman. “Deflections and Natural Frequencies as Parameters for Structural Health Monitoring: The Effect of Fatigue and Corrosion on the Deflections and the Natural Frequencies of Reinforced Concrete Beams”. In: *Repository.tudelft.nl* (2017).

[43] Kees Wapenaar and Roel Snieder. “From order to disorder to order: A philosophical view on seismic interferometry”. In: *SEG Technical Program Expanded Abstracts 2007* (2007). DOI: 10.1190/1.2793024.

[44] F. H. Wittmann. “Structure of concrete and Crack Formation”. In: *Fracture of Non-Metallic Materials* (1987), pp. 309–340. DOI: 10.1007/978-94-009-4784-9_15.

[45] Yingzi Yang et al. “Autogenous healing of engineered cementitious composites under wet–dry cycles”. In: *Cement and Concrete Research* 39.5 (2009), pp. 382–390. DOI: 10.1016/j.cemconres.2009.01.013.